

**DISSECTION OF DEFENSE RESPONSES OF *skl*, AN ETHYLENE
INSENSITIVE MUTANT OF *MEDICAGO TRUNCATULA***

A Dissertation

by

PEDRO URIBE MEJIA

Submitted to the Office of Graduate Studies of
Texas A&M University
in partial fulfillment of the requirements for the degree of

DOCTOR OF PHILOSOPHY

August 2004

Major Subject: Plant Pathology

**DISSECTION OF DEFENSE RESPONSES OF *skl*, AN ETHYLENE
INSENSITIVE MUTANT OF *MEDICAGO TRUNCATULA***

A Dissertation

by

PEDRO URIBE MEJIA

Submitted to Texas A&M University
in partial fulfillment of the requirements
for the degree of

DOCTOR OF PHILOSOPHY

Approved as to style and content by:

Charles M. Kenerley
(Co-Chair of Committee)

Douglas R. Cook
(Co-Chair of Committee)

James L. Starr
(Member)

Thomas D. McKnight
(Member)

Dennis C. Gross
(Head of Department)

August 2004

Major Subject: Plant Pathology

ABSTRACT

Dissection of Defense Responses of *skl*, an Ethylene Insensitive Mutant of *Medicago truncatula*.

(August 2004)

Pedro Uribe, B.S., Universidad de los Andes

Co-Chairs of Advisory Committee: Dr. Douglas R. Cook
Dr. Charles M. Kenerley

The interactions between *Medicago truncatula* and *Phytophthora medicaginis* were examined using *skl*, a mutant blocked in ethylene perception, and a range of wild accessions of this plant species. *P. medicaginis* infection of *M. truncatula* plants resulted in compatible responses, whereas the mutant genotype was found to be hyper-susceptible to the pathogen. *Phytophthora* reproduction and colonization rates of *Medicago* tissues supported this conclusion. Infection of *skl* with different pathogens reinforced this observation. Ethylene production in infected A17 and *skl* roots showed reduced ethylene evolution in the mutant and suggested that a positive feedback loop, known as autocatalytic ethylene production, amplified the ethylene signal.

To complement the study, expression analyses of defense response genes in this interaction were studied by real time RTPCR of *Phytophthora*-infected and mock-infected roots. The genes analyzed were *PAL*, *CHS*, *IFR*, *ACC oxidase*, *GST*, and *PR10*. The sequences needed for the analysis were found through the scrutiny of the *M. truncatula* EST database employing phylogenetics and bio-informatics tools. In A17 all

the genes studied were up-regulated, although the specific gene expression patterns differed. The comparison of gene expression between A17 and *skl* genotypes allowed the differentiation between ethylene-dependent and ethylene-independent responses. Discrete results showed that *ACC oxidase* homologues were downregulated in the ethylene perception mutant, corroborating the ethylene observations. However, the expression of genes involved in the phenylpropanoid metabolism was increased in *skl* relative to A17, suggestive of an antagonism between the ethylene perception pathway and the regulation of the phenylpropanoid pathway. This result implied that *Medicago* phytoalexins accumulate in the disease interaction, but raised questions about their role in resistance to *Phytophthora* infection.

This study establishes a link between mechanisms that regulate symbiotic infection and the regulation of disease resistance to Oomycete pathogens, especially *P. medicaginis*. The results served to identify a series of *Phytophthora*-induced genes, which remain pathogen-responsive even in the absence of a functional ethylene perception pathway. While it is possible that the products of these genes are involved in resistance to *P. medicaginis*, the present results demonstrate that ethylene perception is required for resistance.

DEDICATION

I dedicate this dissertation to my family whose patience, help and love surrounded me constantly during all these years of research. I specially want to acknowledge the help and support that my wife Leigh Anne gave me, and the constant words of encouragement that I received from my family far away.

ACKNOWLEDGEMENTS

I want to express my sincere gratitude to COLFUTURO, Corporación Colombiana para el Futuro de Colombia, whose scholarship provided me with the initial resources to start this endeavor. Without it, most likely I would not have had the opportunity of learning about plant science in such a respected and traditional place as Texas A&M.

I would like to thank Doug Cook for his support and teaching all these years. Destiny moved him away from Texas A&M for him to reach new goals. The same destiny gave me the opportunity to complement my studies and to test myself in a different environment and to supplement my opinions with the views and feelings from a different place. I would like also to acknowledge the past and present members of the Cook laboratory for their friendship, support, and help.

I would like to thank the members of my committee, Dr. Charles Kenerley, Dr. Thomas McKnight and Dr. James Starr, for their knowledge, help and advice.

TABLE OF CONTENTS

	Page
ABSTRACT.....	iii
DEDICATION.....	v
ACKNOWLEDGEMENTS.....	vi
TABLE OF CONTENTS.....	vii
LIST OF FIGURES	xi
LIST OF TABLES.....	xiv
 CHAPTER	
I INTRODUCTION.....	1
LEGUMES IN HUMAN SURVIVAL AND HOSTS FOR SEVERAL PLANT-MICROBE INTERACTIONS	2
History and Importance	2
Pathogens and Diseases of Legume Crops.....	5
Model Legumes.....	7
<i>PHYTOPHTHORA</i> AS A PLANT PATHOGEN.....	9
The Phylum Oomycota as Important Plant Pathogens.....	9
The Genus <i>Phytophthora</i> and Its Importance in Agriculture.....	10
MOLECULAR BASIS OF VIRULENCE AND PLANT DISEASE RESISTANCE.....	11
METHODS FOR GENE EXPRESSION	22

CHAPTER	Page
II RESISTANCE AND SUSCEPTIBILITY OF <i>MEDICAGO TRUNCATULA</i> NATURAL POPULATIONS TO <i>PHYTOPHTHORA MEDICAGINIS</i>	29
SUMMARY	29
INTRODUCTION.....	30
<i>M. truncatula</i> Pathogen Systems.....	32
<i>Phytophthora</i> crown and root rot	32
<i>Pythium</i> damping off.....	34
Anthracnose.....	34
MATERIALS AND METHODS	36
Plant Material	36
Plant Growth Conditions	36
Seed germination.....	36
Growing conditions	37
Pathogen Growth Conditions	38
Alfalfa crown and root rot, caused by <i>Phytophthora</i> <i>medicaginis</i>	38
<i>Pythium ultimum</i> and <i>P. irregularum</i>	39
Stem and leaf blight, caused by <i>C. trifolii</i>	40
Resistance and Susceptibility of <i>M. truncatula</i> Natural Populations to Infection by <i>P. medicaginis</i>	41
Geographical Location of <i>M. truncatula</i> 's Sources of Resistance and Susceptibility to <i>P. medicaginis</i>	41
Resistance of <i>P. medicaginis</i> Resistant and Susceptible Ecotypes against <i>Pythium</i> sp.....	42
RESULTS.....	43
Resistance and Susceptibility of <i>M. truncatula</i> Natural Populations to Infection by <i>P. medicaginis</i>	43
Geographical Location of <i>M. truncatula</i> 's Sources of Resistance and Susceptibility to <i>P. medicaginis</i>	49
Resistance of <i>P. medicaginis</i> Resistant and Susceptible Ecotypes against <i>Pythium</i> sp.....	51
DISCUSSION	52
III AN ETHYLENE INSENSITIVE MUTANT OF <i>MEDICAGO TRUNCATULA</i> IS HYPER-SUSCEPTIBLE TO <i>PHYTOPHTHORA MEDICAGINIS</i>	59

CHAPTER	Page
SUMMARY	59
INTRODUCTION.....	60
MATERIALS AND METHODS	62
Plant and Pathogen Growth Conditions	62
<i>M. truncatula</i> Infection by <i>P. medicaginis</i> , Soil Experiments	62
<i>M. truncatula</i> Infection by <i>P. medicaginis</i> , Aeroponic Tank Experiments.....	63
Microscopical analysis	64
Ethylene quantification	65
<i>M. truncatula</i> Infection by <i>Pythium</i> sp.....	66
<i>M. truncatula</i> Infection by <i>C. trifolii</i>	66
RESULTS.....	66
<i>M. truncatula</i> Near-Isogenic Line <i>skl</i> Is Hyper-Infected by <i>P.</i> <i>medicaginis</i>	66
Ethylene Quantification of <i>M. truncatula</i> Plants Infected with <i>P.</i> <i>medicaginis</i>	70
Infection of <i>M. truncatula skl</i> with <i>Pythium</i> sp.....	72
<i>M. truncatula skl</i> Mutation Is Not Altered in Resistance to <i>C. trifolii</i> ..	75
DISCUSSION	76
IV TRANSCRIPTION PROFILING OF GENE HOMOLOGUES IN <i>MEDICAGO TRUNCATULA</i>	83
SUMMARY	83
INTRODUCTION.....	84
Pathways for Defense Responses in Plants	89
Real Time PCR Analysis of Gene Expression	92
MATERIALS AND METHODS	93
<i>P. medicaginis</i> Infection of <i>M. truncatula</i>	93
In silica Analysis of Candidate Gene Families	94
Blast search of candidate genes.....	94
In silica inference of gene expression	96
Homologue sequence, alignment and analysis.....	96
RNA Isolation and Reverse Transcription	96
Real Time Reverse Transcription PCR	97
Primer and probe design.....	98
Reaction conditions	99
Methods for data analysis.....	103

CHAPTER	Page
RESULTS.....	105
In silico Analysis of Candidate Gene Families	105
Ethylene biosynthesis pathway homologues.....	105
Plant defense signal transduction homologues.....	106
Stress and detoxifying pathways	108
Phenylpropanoid metabolism homologues	111
PAL homologues.....	111
Chalcone Synthase homologues.....	115
Isoflavone Reductase homologues	116
Real Time PCR Analysis of <i>M. truncatula</i> Homologues.....	121
Choice of internal controls for analysis.....	121
Expression profiling of <i>skl</i> an ethylene insensitive mutant of <i>M. truncatula</i>	125
Expression profiling of <i>ACO</i> homologues.	125
Expression profiling of <i>PR10</i> homologues.	127
Transcriptional analysis of gene members in the phenylpropanoid metabolism.	129
Transcription profiling of <i>GST</i> homologues.	132
DISCUSSION	135
In silico Analysis of Gene Homologues.....	135
Transcription Profiling of Gene Homologues.....	139
Real time PCR.....	139
Gene expression profiling	144
 V SUMMARY	 152
 LITERATURE CITED	 155
 APPENDIX.....	 174
 VITA	 176

LIST OF FIGURES

FIGURE	Page
1	Ethylene signal transduction pathway 16
2	Proposed plant defense responses to pathogens and insects 21
3	<i>M. truncatula</i> ecotypes infected by <i>P. medicaginis</i> 42
4	Disease susceptibility of <i>M. truncatula</i> ecotypes to infection by <i>P. medicaginis</i> 44
5	Disease resistance and susceptibility of selected ecotypes to infection by <i>P. medicaginis</i> 47
6	Geographical location and associated resistance or susceptibility of <i>Medicago truncatula</i> ecotypes exposed to infection by <i>P. medicaginis</i> 51
7	Disease incidence in <i>M. truncatula</i> ecotypes upon infection with <i>P.</i> <i>ultimum</i> and <i>P. irregularum</i> 52
8	Compatible and incompatible responses of <i>M. truncatula</i> ecotypes to infection by <i>C. trifolii</i> 57
9	Disease susceptibility of <i>M. truncatula</i> A17 and near isogen <i>sickle</i> to infection by <i>P. medicaginis</i> 67
10	Total development of <i>P. medicaginis</i> in <i>M. truncatula</i> roots 69
11	Mortality rate of <i>Phytophthora</i> infected and mock-infected <i>M. truncatula</i> plants 69
12	Ethylene evolution in <i>Phytophthora</i> -infected <i>M. truncatula</i> roots. 70
13	<i>Medicago truncatula</i> roots infected with <i>P. medicaginis</i> 71
14	Effect of <i>Phytophthora</i> infection on the development of <i>M. truncatula</i> seedlings 72
15	Disease incidence in <i>M. truncatula</i> upon infection with <i>P. ultimum</i> 73
16	Disease incidence in <i>M. truncatula</i> upon infection with <i>P. irregularum</i> 75

FIGURE	Page
17 Root damage caused by <i>P. medicaginis</i> infection of <i>M. truncatula</i> plants.....	78
18 Root hair deformation caused by <i>P. medicaginis</i> infection of <i>M. truncatula</i> plants	80
19 In silica analysis of ACC oxidase gene expression.....	107
20 In silica analysis of PR10 gene expression	109
21 In silica analysis of GST gene expression.....	112
22 In silica analysis of PAL gene expression.....	114
23 In silica analysis of CHS gene expression	117
24 In silica analysis of IFR gene expression	119
25 In silica analysis of <i>Actin</i> homologue TC85697.	122
26 In silica analysis of <i>His H3</i> , TC85197	123
27 Multiplex of target and reference genes. Subset of results	124
28 Standard curves for amplification of <i>Actin</i> and <i>His H3</i> in multiplex with <i>GAPDH</i>	125
29 Transcription profiling of <i>ACO</i> TC85664.....	127
30 Transcription profiling of <i>ACO</i> TC85507.....	128
31 Transcription profiling of <i>PR10</i> (TC76513)	129
32 Transcription profiling of <i>PAL</i> TC85501	130
33 Transcription profiling of <i>CHS</i> TC76765	131
34 Transcription profiling of <i>CHS</i> TC85138	132
35 Transcription profiling of <i>IFR</i> TC85477.....	133
36 Transcription profiling of <i>GST</i> TC85451	134

FIGURE	Page
37 Transcription profiling of <i>GST</i> TC78052.....	134

LIST OF TABLES

TABLE	Page
1	Change in world population. 2
2	Food production, by region. 3
3	Trends in crop production. 5
4	Resistance or susceptibility to <i>P. medicaginis</i> in <i>Medicago truncatula</i> natural populations. 45
5	Data not included in analyses. 48
6	Infection levels of experimental trays. 50
7	Resistance or susceptibility to <i>C. trifolii</i> in <i>Medicago truncatula</i> natural populations. 56
8	<i>sickle</i> resistance or susceptibility to <i>Pythium</i> sp. 74
9	Disease incidence in <i>M. truncatula</i> A17 and <i>skl</i> plants after infection with <i>C. trifolii</i> 76
10	Index of DNA libraries used in the <i>Medicago truncatula</i> sequencing projects. 85
11	List of gene homologues searched within MTGI. 87
12	Reverse transcription conditions. 97
13	Forward primers used for transcription profiling analysis. 100
14	Probes used in the analysis. 101
15	Reverse primers used in the analysis. 102
16	Concentrations of reagents used for analysis. 103
17	<i>Medicago truncatula</i> PAL homologues. 112

TABLE	Page
18 <i>Medicago truncatula</i> CHS homologues.	113
19 <i>Medicago truncatula</i> IFR homologues.	118

CHAPTER I

INTRODUCTION

The research presented in this dissertation is divided into four chapters. In this chapter, a context for the research is provided by examining legumes as crop species and related aspects of plant-pathogen interactions. In Chapter II, in order to find plant populations that are resistant or susceptible to infection by *P. medicaginis* and *C. trifolii*, the defense responses of natural populations to infection by these pathogens are presented. In Chapter III, the characterization of the interaction between *M. truncatula* and *P. medicaginis* based on the reactions of *sickle*, an ethylene insensitive mutant of *M. truncatula* is further studied using greenhouse and growth chamber experiments. Chapter IV starts with an analysis of genes involved in plant defense responses through the search and study of the *M. truncatula* EST database. This search resulted in the discovery of putative gene homologues that, upon in silico analysis, were suspected of having differential expression subsequent to pathogen challenge. The usefulness of such results is presented in the second part of this chapter, where the genetic responses of *skl* mutant after infection with *P. medicaginis*, based on a subset of the gene homologues previously found are presented, with the purpose of obtaining a framework to explain the breadth of responses affected in *skl* mutation.

This dissertation follows the style and format of Phytopathology.

LEGUMES IN HUMAN SURVIVAL AND HOSTS FOR SEVERAL PLANT-MICROBE INTERACTIONS

History and Importance

The production of food in quantities sufficient to feed a growing human population is one of many challenges that the world faces. According to the Food and Agriculture Organization (FAO), some areas in the world, particularly those countries classified as underdeveloped, are being plagued by disease, others by drought, and many by starvation; furthermore, a large proportion of the human population is living in these developing countries (Table 1). With these statistics in mind, our duty as plant pathologists cannot be limited to plant protection; it has to reach further and address the issue of finding novel ways to provide increased quantities of higher quality foods.

TABLE 1. Change in world population.

<i>Total (Thousands)</i>	1974-1976 Average	1984	1997	1998	1999	2000	2001
World	4,065,143	4,742,039	5,821,129	5,900,184	5,978,721	6,056,710	6,134,138
Developed Countries	1,127,983	1,204,247	1,300,982	1,305,955	1,310,478	1,314,540	1,318,131
Developing Countries	2,937,160	3,537,792	4,520,147	4,594,229	4,668,243	4,742,170	4,816,007
Africa	406,190	523,800	738,677	756,679	774,989	793,626	812,603
Asia	2,345,299	2,771,821	3,524,083	3,573,987	3,623,427	3,672,338	3,720,707
Caribbean	27,162	31,139	36,764	37,159	37,552	37,941	38,327
Central America	78,562	98,401	128,005	130,390	132,765	135,129	137,480
Europe	472,669	489,101	728,901	728,622	728,076	727,304	726,314
N. America Devel.	243,303	265,609	304,557	307,773	310,926	313,987	316,941
N. America Developing	110	115	125	125	126	126	126
Oceania	21,284	23,961	29,328	29,728	30,125	30,520	30,916
South America	216,141	263,390	330,689	335,721	340,735	345,739	350,724
Others	254,423	274,702	0	0	0	0	0

Source: FAO statistics, 2002.

Grains, fruits, and legumes comprise the main categories of plants used for human consumption. Species belonging to each of these groups have received a considerable amount of attention with the intent of improving their nutritional value, quality and palatability. Legume plants are adapted to most areas of the world, and because of early domestication, they have become the major proportion of the daily diet for people in countries located in Asia, Africa and Latin America (6) (Table 2). Legumes are an important source of nutrients, providing essential amino acids such as lysine and threonine, vitamins such as thiamine and niacin, minerals such as iron and calcium, and even energy in the form of starch, making them a central focus in the goal of supplying better quality food for a world in need. Legumes also play a vital role in providing livestock feed in developed countries around the world, where animal protein represents a significant portion of the daily menu (13).

TABLE 2. Food production, by region.

Year 2002	Cereals, Total Production (Mt)	Cereals, Total Yield (Hg/Ha)	Legumes, Total Production (Mt)	Legumes, Total Yield (Hg/Ha)
World	2,031,748,660	292,193	335,247,171	383,085
Africa	118,623,902	158,757	25,191,041	312,899
Asia	986,975,360	226,487	105,917,594	372,099
Caribbean	1,715,372	54,677	375,195	245,507
Central America	33,129,891	236,849	5,415,376	370,783
Developed Countries	841,895,559	356,146	114,098,139	474,817
Developing Countries	1,189,853,100	237,808	221,149,032	349,798
Europe	433,849,818	365,303	21,352,752	524,783
N. America Developed	334,079,376	329,951	88,148,711	317,253
N. Amer. Developing			20	40,000
Oceania	20,056,403	277,558	3,014,324	471,350
South America	103,318,539	226,583	85,832,158	256,495

Source: FAO statistics, 2002

Legumes are extremely important for soil improvement and agricultural productivity due to their capacity to fix atmospheric nitrogen. During the nitrogen fixing process, symbiotic bacteria, living in specialized root-derived organs called nodules, convert atmospheric nitrogen into ammonia. The host legume provides the bacteria with carbohydrates and low oxygen tension, which are critical for nitrogen fixation and bacteria survival. The plant uses the ammonia to produce glutamine, the initial product of nitrogen assimilation, and subsequently to supply other aspects of primary and secondary metabolism with organic nitrogen. Nitrogen fixation is the subject of intense research in the areas of plant pathology, plant breeding and plant physiology. Research on this topic is also of interest to bacteriologists and efforts to improve the understanding and the efficacy of this beneficial interaction are currently underway (188).

During the last 40 years, we have seen the results of a green revolution. Crop yields have improved due to the use of new varieties that were specially selected and bred for larger yields. This improvement has come with boosts in the use of pesticides, irrigation and fertilizers but without affordable crop prices or the desirable increases in cultivated area (Table 3). Because there is a lack of appropriate soils for cultivation, (13), these factors have translated into higher demands for the soils and the plants growing on them to yield. Legume crops can play a vital role to improve this situation. This fact, combined with the knowledge that approximately 30% of the proteins and 50% of the essential amino acids have legume origin, reinforces their importance and provides ample reason to continue research for legume improvement (25).

The untangling of the complex network of interactions leading to nitrogen fixation will allow us to exploit in optimum ways the benefits of this interaction and to make better use of this important family of plants (38). The mechanism by which plants alter their defense responses when exposed to symbiotic organisms, but not when exposed to pathogens, remains unknown; the main objective of this research is to provide a partial answer to this puzzle.

TABLE 3. Trends in crop production.

	1974-1976	1984	2001
Population	4,065,143,333	4,742,039,000	6,134,138,000
Crops total (MT)	1,176,073,938	1,588,126,706	2,020,905,763
Grains (Metric Tons)	1,057,239,695	1,427,970,781	1,751,748,244
Legumes (Metric Tons)	118,834,243	160,155,925	269,157,519
Area Harvested (Ha)	610,318,614	639,627,917	670,358,322
Grains (Ha)	489,943,197	502,998,335	496,498,354
Legumes (Ha)	120,375,417	136,629,582	173,859,968

Source: FAO statistics, 2002.

Pathogens and Diseases of Legume Crops

As with most crops, the list of pathogens and pests affecting legume crops is long and diverse. Nematodes, fungi, bacteria, and viruses all have species which attack legume crops. Bacterial pathogens for example, cause a range of symptoms that vary from seedling blight to stem canker or leaf spots and foliar blights. The main bacterial pathogens of legume species are *Xanthomonas campestris* and *Pseudomonas syringae*. Both can cause high disease losses depending on the type of legume host affected and the virulence of the particular pathovar affecting the crop. At least 20 different pathovars of *X. campestris* have been isolated from legume crops. Fortunately, host

plant resistance, in addition to crop rotation, improved seed production and other management practices have reduced the incidence of the pathogens and their overall threat (6-7).

Root pathogens like *Rhizoctonia*, *Pythium* and *Phytophthora* species can cause crown rots, damping-off and root rots in seedlings, resulting in poor emergence and therefore low crop yields. Another important pathogen, particularly for groundnut species, is *Aspergillus flavus*, which besides attacking seeds and seedlings and causing emergence problems in these species, can contaminate the established plantations with carcinogenic aflatoxins. Because of the extreme danger of aflatoxins, the levels of this compound in peanuts are subject to intense scrutiny and regulation at both the national and international level (6,7). As the seedlings mature, fungi such as *F. oxysporum*, *Aphanomyces euteiches* or *Sclerotinia sclerotiorum* are capable of causing wilts in some of the established plants. Nematodes are also root pathogens, and are perhaps the most significant disease agents affecting legumes. They are almost cosmopolitan, and when associated with fungi, they can create disease complexes and cause extensive damage. They remain difficult to control in the soil and few soil fumigants are certified to control them. Species like *Heterodera goettingianna*, *Meloidogyne incognita* and *M. javanica* are some of the most prevalent (6,7).

Most leaf diseases in legumes are caused by fungi such as *Botrytis*, *Alternaria*, or *Colletotrichum*. Oomycetes, such as *Peronospora pisi* or *P. viciae*, can cause downy mildews under conditions of low temperature and high humidity. Powdery mildews caused by species such as *Erysiphe polygoni* or *E. pisi* and rusts like *Uromyces pisi* are

capable of lowering crop yield by 20% or more if control measures are not taken rapidly (6,7).

Viruses are usually not an extensive problem unless severe vector infestations are present. Potyviruses are the most prevalent; bean common mosaic, bean yellow mosaic and soybean mosaic are of major importance among them. These organisms transmit themselves by means of contaminated seed or insect vectors, usually aphids such as *Aphis gossipi* or *Acyrtosiphon pisum*. Other viruses belonging to groups such as geminiviruses and carlaviruses also affect legume crops and may have different means and vectors for transmission (7).

The relative economic importance of these organisms is usually assessed on a regional basis. Data records of disease loss are available for certain crops and diseases, but few reports exist where an overall, judicious assessment of yield loss is accomplished. Because no reliable data is available to estimate the importance of a disease, this value can be extrapolated from the cost in the use of fungicides, pesticides and soil fumigants applied to the crops. This information alone might not be enough because the pathogens also affect the quality of the crop and thus the price of the yield (6).

Model Legumes

The leguminosae includes many economically important species such as soybean, pea, chickpea, bean and lentil. Some legume crops are used as forage crops, while other species such as peanuts and soybeans are valuable sources of plant oils as

well as food crops (13). The need for understanding nitrogen fixing processes mediated by rhizobacteria has led to the development of genetic models like *Lotus japonicus* and *M. truncatula*.

Both plants have small genomes that make them ideal candidates as model species (38-39, 82, 141). Linkage maps have been developed for both organisms and these maps are providing gene information and markers of agronomically important traits. Comparative genomics is allowing the alignment of genetic maps and the transfer of genetic markers of these model species to the counterparts of agronomically important plants like alfalfa, soybean, beans and peas (34, 198). Colinearity of these maps makes the mapping of these agronomically important traits an achievable task (34).

In a similar way, Expressed Sequence Tags (EST) libraries, constructed from different tissues over a wide range of conditions, are now available in the public domain. Bacterial Artificial Chromosomes (BAC) libraries have also been constructed (126) and have helped in the construction of physical maps for these species and in the cloning of important genes. cDNA microarrays are providing global pictures of the responses of these species to particular stimuli like a pathogen or an environmental condition (188).

Lastly, genetic transformation by different methods is a reality for these species, and it is now possible to overexpress or silence a particular gene to study its effects (23, 94, 182). Eventually, this information will be applied in agronomically important species to increase our knowledge and ultimately to improve crop quality and yield.

PHYTOPHTHORA AS A PLANT PATHOGEN

The Phylum Oomycota as Important Plant Pathogens

The Oomycetes are life forms that belong to the kingdom Chromista. Heterokonta, one of three phyla in this kingdom, contains the class Pseudofungi (Heteromycotina), which is where the subclass Oomycetes is grouped (5).

Characteristic in Oomycetes is the presence of anisokont and heterokont flagella in the zoospores, the asexual reproductive structures of these organisms. Typical as well is a cell wall composition with various types of glucans (β -1,3-glucans, β -1,6-glucans and β -1,4-glucans (cellulose)) (16), similar to that of plants. The Oomycetes life cycle is characterized by a predominantly diploid vegetative stage, interrupted only by haploid stages that occur exclusively inside reproductive structures called gametangia. Mycelium in Oomycetes is coenocytic with few or no septa. Asexual reproduction is possible by the production of asexual reproduction structures called sporangia. Sporangia contain the asexual motile spores called zoospores and they represent the main infective structures of these organisms. Some studies suggest that chemotaxis drives the movement of these infective structures towards suitable hosts (29).

Several important plant pathogens belong to this subclass of organisms. The downy mildews, for example, form an economically important group of obligate parasites of plants. Representative genera of this group of plant parasites include *Bremia*, *Peronospora* and *Sclerospora*. Several species from these groups cause disease symptoms in a wide range of plant species (5). The Phytiaceae family contains the genera *Pythium* and *Phytophthora*, both of which are notable plant pathogens (5).

The Genus *Phytophthora* and Its Importance in Agriculture

Phytophthora species can cause multicyclic foliar and root diseases. This is possible because of the high rate of zoospore production. Under optimum conditions, the inocula of these species can go from barely detectable to high numbers in matter of days to weeks. This inoculum is able to generate secondary infections on the host, giving sense to the term multicyclic. The epidemiology of potato late blight and several other *Phytophthora*-caused diseases such as black pod of cacao (*P. palmivora*) and black shank of tobacco (*P. parasitica*) are good examples of systems that can be described as multicyclic diseases (95).

Potato late blight caused by *P. infestans* is the best known illustration of the terrible potential to cause disasters which these organisms have. The late blight epidemic in Ireland ended with a severe famine that brought this genus of organisms to the forefront of plant pathology research; since then numerous other *Phytophthora* diseases affecting other crops have been studied and classified. In the case of legumes particularly important are the root rot caused by *P. sojae* in soybean and the leaf blight of *P. drechsleri* on pigeon pea. In soybean, plant losses and yield reductions range from 40% in highly tolerant cultivars to total loss in susceptible ones. Disease severity depends on genetic resistance of the cultivar, rainfall, temperature, soil drainage, and management practices (7). For pigeon pea, *Phytophthora* infection is particularly severe in countries like India, where losses of 100% have been reported. The disease is still considered relatively new and precise information on severity and distribution is not

available. Nonetheless, it has been reported in the Dominican Republic, Kenya, Panama and Puerto Rico (156). Alfalfa and other medics are attacked by *P. medicaginis*, causing root rots if poorly drained soils are present. Phytophthora root rot of alfalfa is an important disease in the high plains of Texas and Oklahoma (137), but it is widespread and particularly severe in Australia, where different medics are grown for forage purposes (6-7). In the following section, the molecular basis of virulence and disease resistance, a key concept to deal with these pathogens will be presented.

MOLECULAR BASIS OF VIRULENCE AND PLANT DISEASE RESISTANCE

Resistance and susceptibility against a pathogen is largely divided into two classes. The first is termed horizontal resistance, or general, and it is not directed specifically towards any pathogen. Structural features like cell wall appositions, preformed chemical inhibitors, plant age, and plant developmental status are some examples of this type of resistance. The second type, called vertical resistance, is of a more specific nature and it is directed towards the pathogen. Phytoalexin production and the occurrence of a Hypersensitive Response (HR) in the plant after exposure to the pathogen are some examples of this type of defense response (185). Vertical resistance is caused by the expression of resistance genes in the plant as a consequence of the recognition of the expression of virulence genes by the pathogen. Flor, in 1946, proposed his gene-for-gene theory, in which he stated that for any virulence gene in the pathogen there is a corresponding resistance gene in the plant (67). Usually resistance genes are dominantly inherited (Res), whereas virulence genes are recessively inherited

(vir), but this is not always true. In general, the absence of resistance genes or the expression of the recessive allele in the resistance gene will lead to disease symptoms or compatibility when confronted with the virulence genes of the pathogen (185). Upon expression of the resistance gene, the plant customarily undergoes a fast and localized HR response. Under this response, the cells that are the objects of infection enter into programmed cell death patterns, shown to be mediated by the generation of Reactive Oxygen Species (ROS) in and around the site of infection (129, 144). The HR signals the plant to start producing series of specific kinds of proteins related with pathogenesis that increase the general immune response in the plants (73, 77). For example, in the case of *P. sojae* infection of resistant soybean plants, hypersensitive cell death occurs at the site of infection and synthesis of compounds like callose and the isoflavonoid phytoalexin glyceollin occur in adjacent tissues. Callose formation looks like a general response to injury and not a defense response per se. However, glyceollin production has been shown to be dependent on specific gene activation of the phenylpropanoid metabolism, because the application of α -AminoOxy- β -PhenylPropionic acid (AOPP) or other compounds to inhibit Phenyl alanine Ammonia Liase (*PAL*) expression leads to loss of glyceollin production and development of disease symptoms (145).

Isoflavonoid compounds are also important in symbiotic interactions between plants and microorganisms. In the case of legume plants and *Rhizobium* bacteria, an interaction initiated by flavonoid compounds released by roots of the plant is followed by the specific production of nodulation factors in the bacteria. Nod factor, the compound that is produced by *Rhizobium*, is specifically recognized by receptors in the

plant root. The specificity of the recognition process depends on the chemical modifications present on the chitin backbone of the Nod factor (142). Upon positive recognition, a series of developmental stages transpire that lead to the formation of a new organ, the nodule, which will harbor the nitrogen-fixing bacteria (143).

In the case of *M. truncatula* plants infected with *S. meliloti*, their natural symbiont, a negative feedback pathway involving ethylene mediates Nod factor responsiveness (140). A key mutant used to understand this event is *skl*, a *M. truncatula* ethylene insensitive mutant that has been shown to be a homologue of *A. thaliana* *Ethylene Insensitive 2 (EIN2)*. EIN2 in turn, has homology to the NRAMP divalent cation transporters of eukaryotic systems, suggesting a critical role for metal metabolism in ethylene signal transduction mechanisms (8, 21, 66, 87, 118). Even though the specific mechanism to explain how ethylene regulates nodule number is not clear, research involving *skl* mutation suggest that ethylene is involved in complex mechanisms controlling different levels of the developmental response. In 1997, for example, Penmetsa and Cook (146) proposed that ethylene is the molecule responsible for controlling the extent of infection of roots exposed to *Rhizobium* bacteria. In 2001, Oldroyd et al. (140) showed that A17 *M. truncatula* roots exposed to Nod factor sustained reduced calcium spiking responses in the presence of ethylene, while Nod factor treated *skl* roots continued to have calcium spiking responses similar to Nod factor treated, non ethylene exposed controls. Calcium spiking is one of the earliest responses to Nod factor presence in *Rhizobium* infected roots, possibly creating ion changes in the root hairs that are required for infection thread formation and eventual nodule formation

(140). Previously, Heidstra et al. demonstrated that transcripts of 1-Amino-Cyclopropane-1-Carboxylic acid oxidase (*ACC oxidase*) were negatively correlated with the spatial distribution of nodule development (86). *ACC oxidase* catalyzes the last step in ethylene production, but the specific mechanism of ethylene's involvement in nodulation is not yet known.

In plant-pathogen interactions, the plant hormone ethylene is believed to be involved in plant defense responses. After pathogen infection and subsequent recognition of the pathogen by the host, ethylene is produced by the conversion of S-Adenosyl-L-Methionine (SAM) into ACC. ACC is then converted into ethylene, carbon dioxide and cyanide. Ethylene production generates a molecular and genetic cascade of responses that lead to the induction of host defense-related genes (21, 49, 51, 91, 98, 174).

The dissection of the ethylene signal pathway leading to the expression of host defense-related genes reveals that it starts with a receptor protein that binds ethylene in the presence of copper. Several mutants defective in ethylene perception (i.e. *etr1*, *ers1*, *etr2*, *ein4* and *ers2*) were isolated and cloned from *A. thaliana* (21, 91, 174). The binding of ethylene presumably causes an alteration in the coordination chemistry of copper that results in a conformational change in the ethylene binding site that, in turn, is propagated to the transmitter domain of the EThylene Receptor 1 (ETR1) family dimer pair (21, 91).

The proposed model (21, 33, 91, 174) (Fig. 1) postulates that in the absence of ethylene, the A17 "two-component" receptors, paralogues of the ETR1 family, activate

the regulator Constitutive Triple Response 1 protein (CTR1), which in turn represses the activity of the downstream genes *EIN2* and *Ethylene Insensitive 3 (EIN3)*. Ethylene binding is believed to switch off the receptors, leading to CTR1 inactivation and activation of downstream signaling. Loss of function mutants that affect the binding of ethylene lead to constitutive signaling to CTR1 and confer dominant insensitivity to ethylene. By contrast, mutations in at least three or more receptor family members lead to a lack of activation of CTR1 and therefore a constitutive triple response phenotype. Similarly, loss of function mutants affecting *CTR1* also resulted in a constitutive ethylene-response phenotype, indicating that *CTR1* is a negative regulator of the ethylene response pathway (33, 91, 96, 174). Sequence analysis of *CTR1* shows that it is related to the mammalian RAF kinase family of protein kinases that initiate Mitogen-Activated Protein KINASE cascades (MAP-kinase) of signal transduction. MAP-kinase cascades are often involved in regulation of transcription factor activity (111) (Fig. 1).

EIN2 shows 21% sequence similarity to the eukaryotic NRAMP family of presumptive metal ion transporters and it is required for ethylene signaling between *CTR1* and *EIN3* (8, 21, 174). The mechanism of *EIN2* action remains unknown, but it is possible that it functions directly by regulating a second messenger during the signaling process. Alternatively, *EIN2* could be a metal homeostatic regulator acting indirectly on the ethylene-signaling pathway (8, 33, 98) (Fig. 1). *EIN3* acts genetically downstream of *CTR1* and codes for a transcription factor that initiates a cascade of different responses involving members of a large, plant-specific group of transcription factors called Ethylene Responsive Elements Binding Proteins (EREBP) (171, 174).

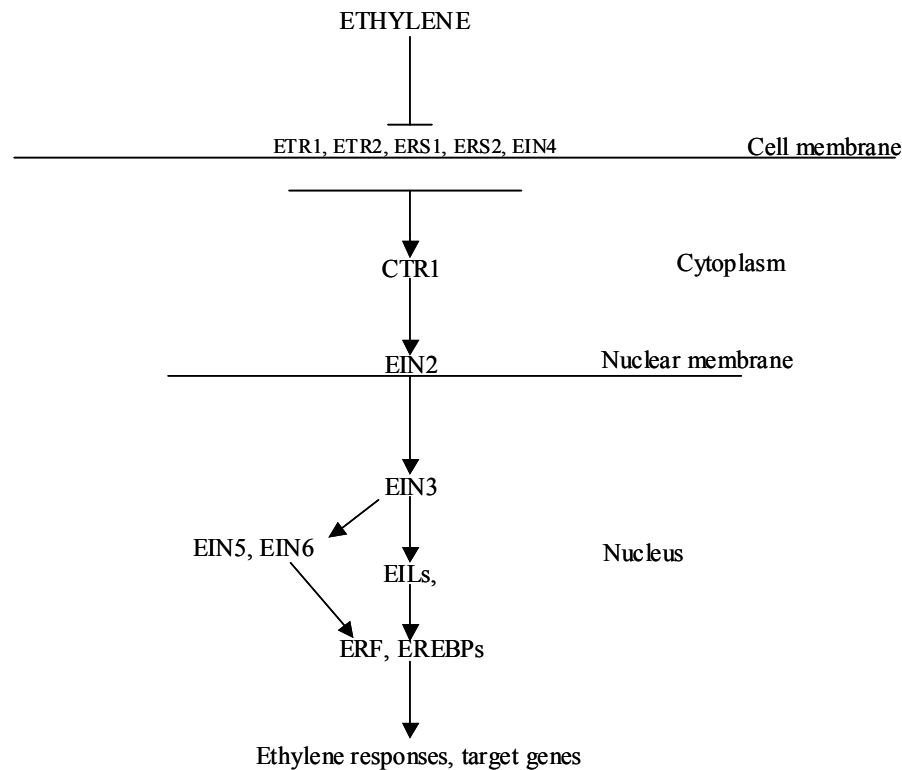


Fig. 1. Ethylene signal transduction pathway. Adapted from Chang C. et al. (33), Stepanova, A.(174) and Ecker, J. (51). Ethylene binding causes the receptors (ETR1, ETR2, EIN4, ERS1, ERS2) to signal to CTR1, which then transduces the signal by loss of repression to EIN2 directly or by means of one or several MAPK. EIN2 is an intra-nuclear protein that in turn signals to different transcription factors such as EIN3 and Ethylene Insensitive Like proteins 1,2,3 (EIL1, 2,3). These proteins accordingly activate or regulate Ethylene Response Factor 1 (ERF1) and other EREBPs that activate or suppress gene induction. The position of EIN2 is not clear. The order of EIN5 and EIN6 is not clear either.

Evidence linking ethylene signaling with defense responses has accumulated in recent years. For example, expression of a dominant negative allele of *A. thaliana* ethylene receptor *ETR1* in transgenic tobacco was correlated with susceptibility to normally non-pathogenic fungi (98). The ethylene signaling pathway appears to interact with the Jasmonic Acid (JA) pathway to generate a defense response that is different and

independent from the Salicylic Acid (SA)-dependent Systemic Acquired Resistance (SAR) pathway (49, 178). Furthermore, a requirement for ethylene during disease resistance was observed in *A. thaliana* plants carrying a defective *ein2* gene. The mutant plants showed increased susceptibility to different strains of the gray mold *Botrytis cinerea*. On the other hand, when the plants were challenged with non-pathogenic strains of *Alternaria brassicola* or *Peronospora parasitica*, no increased susceptibility was observed. These results indicate that ethylene is required for some, but not all, of the defense responses against pathogens (21, 49, 98, 174, 178-179) (Fig. 2).

Among the different plant defense responses, ethylene in conjunction with jasmonic acid (JA) triggers a subset of responses that is important in providing one type of broad-spectrum systemic resistance in plants. This pathway was identified while analyzing the effects of JA to wounds and insect attack. For instance, in injured leaves JA is rapidly and transiently produced in response to pest attack. One of the effects of the rise in JA levels is an upsurge in ethylene production. Other effects include the induction of a different set of defense response genes than those induced by SA. In *A. thaliana*, JA production leads to the induction of the defensin gene *PDF1.2*. This gene encodes an antifungal protein (189). In this same way, another defense protein called thionin is also induced, and furthermore, the same set of genes is activated following induction by ethylene or cell wall oligosaccharide fragments (49, 178). Lipoxygenase, the enzyme responsible for the synthesis of JA and other fatty acid derivatives, is also induced by JA, injury or pathogen attack (17). In this sense, a positive correlation between *LOX* expression and the defense responses of the plants has been observed in

several different plant-pathogen systems. Some examples of this are: *Puccinia graminis tritici* and wheat, *P. coronata* and oats, and *Magnaphorte grisea* and rice (119). The inhibition of ethylene and/or JA production, or reduced sensitivity to both compounds, can negatively affect the initiation of the JA pathway and the downstream responses.

Among the most studied responses of plants to pathogens are the HR and SAR. The HR is an incompatible reaction that occurs at the point of pathogen infection and is distinguished by a localized oxidative burst and cell death (77,104). The HR is believed to control and isolate the pathogen at the point of infection (77,104). In turn, the HR is correlated with SAR (discussed below), although the precise relationship between HR and SAR remains to be determined. Experiments involving *A. thaliana* Defense No Death (*dnd*) mutants suggested that *dnd* mutants fail to produce HR but still show SAR (36, 195). Under the gene-for-gene hypothesis, the plant continually evolves new resistance genes that will allow the establishment of an incompatible interaction between the plant and the pathogen and lead to disease development. Correspondingly, the pathogen evolves new virulence specificities to render susceptible the co-evolving host (43, 67, 104) (Fig. 2). The HR can also be induced during resistance responses to non-host-specific pathogens. It is believed that avirulent pathogens elicit SA accumulation by means of resistance genes, through the action of genes such as Non Defense Resistance 1 (*NDRI*) (31-32) and Enhanced Disease Susceptibility 1 (*EDSI*) (60), which are responsive to induction by different sets of R-genes. The activation of either gene eventually translates into HR and SA accumulation and SAR (49, 75, 89).

SAR is a broadly effective and systemic defense response, dependent on the accumulation of salicylic acid (160). SAR confers protection against many types of pathogens. Upon SA accumulation, Pathogenesis Related proteins (PR) are expressed throughout the plant. Cellulases, chitinases, proteinases, glucanases and antiviral proteins are among the known PR gene products. SAR limits secondary infections and/or spread of the initial pathogen (44, 160). Interestingly, SA accumulation will occur even if the local HR was sufficient to stop the initial infection. In addition to specific PR protein induction, structural and metabolic mechanisms of defense are also activated during SAR. For example, localized cell wall modifications can make the cell wall less pervious to pathogen ingress, while production of toxic secondary metabolites called phytoalexins can act directly to impede pathogen development. SAR can also be triggered by successful infection events, and in this case SA accumulation is also the key element in mounting this associated defense response (49, 160). The signal transduction events that lead to SA accumulation and that trigger SAR are complex and not yet completely understood. Virulent pathogens, for instance, seem to elicit SA production in the plant by means of host regulatory genes such as PhytoAlexin Deficient 4 (*PAD4*) and *EDS* (49, 89). The Constitutive expresser of PR genes 1 gene (*CPRI*) is a negative regulator of both *PAD4* and *EDS*, and has a mutant phenotype that constitutively accumulates SA. SA, in turn, induces the expression of PR genes by means of SA responsive transcription factors. Downstream of SA sits NPR1. Mutations on this gene abolish the expression of some of the PR protein and cause enhanced susceptibility to pathogens (28, 49). This protein was showed to contain several ankyrin motifs, which

are involved in protein-protein interactions (28, 75, 197). It has been proposed that NPR1 protein is targeted to the nucleus as a response to SA accumulation. In the nucleus, it is believed to interact with a subclass of TGA transcription factors, which in turn may intermingle with SA responsive cis-elements of PR genes such as as-1 of PR1 (28, 75, 97, 197). Furthermore, recent literature (50, 58, 105) reports the presence of W-boxes inside the promoter of some PR proteins. The W-box motif interacts with WRKY transcription factors. This family of transcription factors is found only in plants and, in this case, they act as negative regulators of SA dependent gene expression. NPR1 might interact directly or indirectly with these transcription factors (28, 50, 58).

Recently, the Klessig lab (169) identified other mutations that seem to induce PR protein expression responses through signals that are SA dependent but NPR-1 independent or through SA/NPR1 independent pathways. For example, the *ssi1* mutant was shown to suppress *npr1* mutations. Nonetheless, degradation of SA signals abolishes the constitutive expression of PR proteins present in the mutant confirming the need of such signal for its normal expression (168). This last example shows that even though multiple components of this pathway have been characterized (50, 108, 168-169) the complete picture is still not entirely understood. However, multiple genetic analyses have suggested a linear *CPRI-SA-NPRI* pathway that ends with the expression of PR proteins and the acquisition of SAR status (49) (Fig. 2).

In defense responses to pathogens, the signals of SAR seem to interact with those of JA/Ethylene. But the precise relationship between both defense pathways remains obscure. Data suggests that JA/Ethylene and SA accumulation negatively influence each

other (49). Some clarification of this issue came from the characterization of the systemic inducible defense peptides, thionin and defensin, in *A. thaliana*. The study demonstrated that thionin is induced by methyl jasmonate, silver nitrate and *F. oxysporum*, but not by SA (55), which indicates that the JA/Ethylene defense response pathway can be selectively activated.

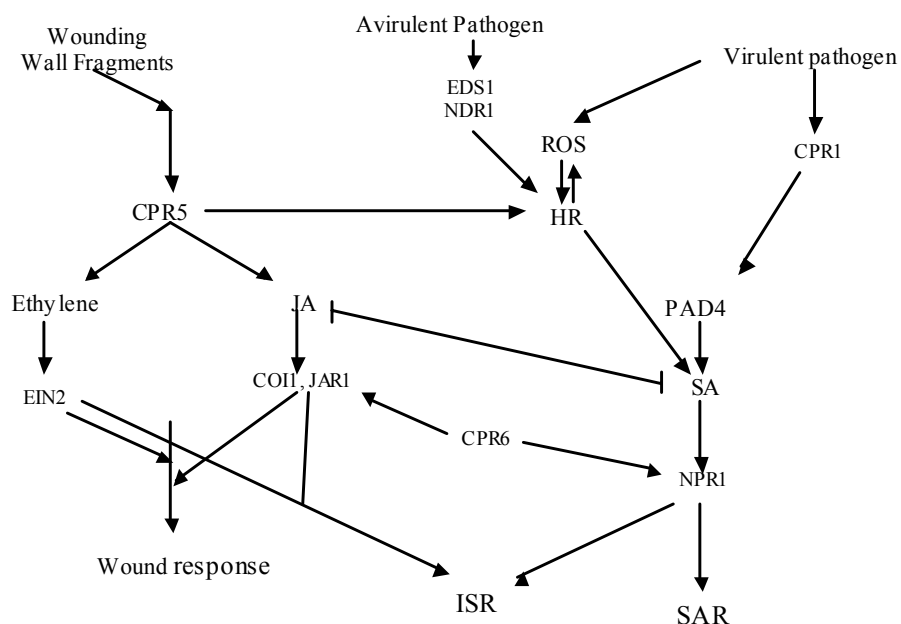


Fig. 2. Proposed plant defense responses to pathogens and insects. Adapted from Dong X. (49), and Glazebrook J (75-76). Multiple genes and connections are missing from the diagram and eventually new genes will need to be included on it. Placement for some of the different genes will change in the near future. The defense responses in plants follow two general pathways, the first dependent on salicylic acid induction and the second dependent on ethylene/jasmonic acid induction. Different plant mutants have been isolated in *A. thaliana* that are defective in defense responses and their analysis has partially helped to position the different candidate proteins in the model. Key proteins in the pathway include COI1 and JAR1 that are specific for JA signaling, while EIN2 seems to be specific for ethylene derived responses related with plant defense. NPR1, on the other hand, is now implicated in SA signaling and in non-SA dependent defense responses. Downstream of these proteins, specific JA or SA-dependent responses are generated, leading to Systemic Acquired Resistance (SAR) Wound Responses or Induced Systemic Resistance (ISR). Upstream of COI1, JAR1, EIN2 and NPR1, several additional proteins have been found, but they remain partially characterized so their importance, position and relevance are currently unclear. Interesting is the proposed link between the production of Reactive Oxygen Species (ROS) and the derived Hypersensitive Response (HR) that has been shown to induce Salicylic Acid dependent responses leading to SAR.

A separate experiment showed that the induction of the PR proteins PR-1-, PR-2 and PR-5 requires SA signaling but not methyl jasmonate or ethylene mediated signaling (77). This results in the induction of SAR-dependent, but not JA/Ethylene dependent, defense responses. In addition, defensin induction in *A. thaliana* was obtained with applications of JA, ethylene, rose bengal, and the non-host pathogen, *A. brassicicola*, but not with SA applications (149). Furthermore, Thomma et al. (178) showed that the induction of PR-3, PR-4, and defensin is dependent on the JA pathway (Fig. 2).

Recently, the characterization of a third pathway named Induced Systemic Resistance (ISR) was started. Root colonization by fluorescent pseudomonads in *Arabidopsis* results in elevated resistance levels against pathogenic bacteria and fungi. The defense mechanism was shown to be dependent on ethylene and JA signals but at the same time independent of SA responses (152, 187). Finally, every day there is more information suggesting that cascades of protein kinases mediate the different defense responses at various levels (196). *MPK4*, for example, is needed for proper JA/ethylene signaling and at the same time inhibits SA signaling. The nature of such phenomenon is not yet completely understood. Another protein kinase characterized is *EDR1* that in a similar way is needed for proper expression of SA signals (19, 70, 151, 194).

METHODS FOR GENE EXPRESSION

Several methods are available to analyze mRNA. Northern hybridizations, nuclease protection assays, in situ hybridizations, reverse transcription PCR, microarrays

and real time reverse transcription PCR are some of the techniques developed to detect and quantify RNA in tissues and samples.

In situ hybridizations, for example, are typically radioactive- or fluorescence-based methods used to localize the expression of a particular transcript. When the probe is incubated in the presence of the tissue where the target gene or transcript is expected to be present, localized hybridization of target and probe molecules will occur. If this happens, photographic or radiological techniques will be able to detect the source of the signal and give positive confirmation of the process (164). An example of this process was done by Ramu et al. (155) to localize and study the expression of *RIP 1*, a nodule-specific peroxidase of *M. truncatula* (37).

Nuclease protection assays are an alternative method for RNA analysis. They are supposed to give excellent sensitivity and are also based on the hybridization of labeled RNA molecules with complementary templates present in an experimental sample. When nucleases are employed to degrade RNA molecules, hybrid RNAs are protected from degradation by their hybrid condition. Gel electrophoresis of digested samples is then used to detect the remaining hybrid molecules. If standards of the samples are used, quantification can be performed (157, 164).

Northern blots are perhaps the most commonly used of all the techniques employed to detect the presence of mRNA. With this technique, it is possible to detect any specific transcript by its hybridization with a radioactively labeled probe. The main advantage of this system is that it is highly specific and sensitive due to the ease of detecting radioactive sources. Problems with the technique include the need of special

equipment to handle radioactive material, the demand of trained personnel and the generation of radioactive waste, which requires the presence of specific facilities and equipment to handle it.

The major drawback of northern hybridizations is the need to repeat the process every time that a new time point is to be analyzed or every time that a new mRNA species is to be detected. In other words, the method causes a slow processing of experimental samples and it is not well suited for experiments involving several time points or different genes. Another potential problem that the sensitivity of this technique can generate is the detection of closely related sequences that could create false signals. Usually the design of the hybridization probe can solve this problem, but, as in the case of very closely related sequences, sometimes this problem cannot be avoided (157).

To move away from the hazardous problems that the handling of radioactivity creates, new detection methods based on colorimetric methods, such as biotin-labeled or fluorescent-labeled probes are currently being implemented. Nonetheless, to detect these novel probes additional detection equipment is needed and because the technology is new and not widespread it is still expensive. The new systems are also facing sensitivity problems that have slowed down their development (164).

Polymerase Chain Reaction (PCR) based methods for quantification of nucleic acids were developed in the early 1990's. PCR is a process that allows the perpetual amplification of any nucleic acid product; it was created during the mid 1980's and multiple variations have been designed since then. A variation of PCR called Reverse Transcription PCR (RT-PCR) allows the generation of complementary copies (cDNA) of

mRNA. A later modification of this technique is Quantitative RTPCR (qRTPCR) that allows the quantification of gene products.

There are two ways to perform qRTPCR. One is called competitive qRTPCR while the second one is called noncompetitive qRTPCR. In both cases, templates previously quantified are used to assess the copy number of the mRNA molecules in the experimental sample. The premise behind qRTPCR is that the quantification process will be valid if the PCR amplification efficiencies of both the standards and the target molecules are the same (69).

Recently, new methods for quantification of nucleic acids were developed. They are based on fluorescent probes that report the presence of nucleic acids by intercalating or specifically hybridizing to them. Two of these techniques are real time PCR and microarrays. Both methodologies have surpassed the developmental phase and are now routinely applied for several purposes. Microarrays, for example, are presenting the transcriptional profiles of organisms based on the expression change of thousands of genes upon exposure to different conditions while real time PCR monitors in real time the increase of a nucleic acid template during the PCR reaction (192). RTPCR has already been shown to be extremely useful to find coordinated gene expression patterns under multiple conditions (166) and even to validate the results of microarray experiments (116).

Microarrays are based on the hybridization of fluorescent-labeled mRNA with the complementary sequences in the array slide (192). The microarray slide is typically a silica surface printed in predetermined patterns with nucleic acids. In the case of *M.*

truncatula microarrays, the slides are printed with specific EST (around 1000) that represent a group of genes coding for most of the physiological and responsive pathways in this species (188). The pattern of printing is repeated in the slide to have data replication. Detection of fluorescent signals allow the generation of images where the presence or absence of a particular RNA species is reported. Because thousands of genes are present at the same time in the array, the displayed results contain an immense amount of data that represents the transcriptional profile of an organism in pre-determined experimental conditions.

Real time PCR has been consistently employed since 1997 to track the changes in concentration of nucleic acids in several systems. It has been successfully applied in research for medicinal purposes (see reviews by Bustin (26-27), Giulleti (74) and McKey (114)) and it has begun to be applied in plant systems. A variation of this technique using reverse transcription was used in this study to quantify and monitor the expression of genes involved in defense responses upon infection of A17 and *skl* roots with *P. medicaginis*. Real time PCR allowed the study of the fate of a relatively high number of genes, providing the details that microarrays or northern hybridizations could not achieve without extensive experimentation.

In the simplest form of real time PCR, nucleic acid intercalating compounds are added to the PCR reaction to monitor the increase of PCR products. Because intercalating compounds bind to any class of nucleic acids, nonspecific amplification of PCR products like primer dimers, pseudogenes or homologous genes to the target sequence can be detected (26, 74). Nonetheless, if abundant template is present and the

specificity of the primer is high, quantification of a particular gene is possible and precise.

To increase the specificity of the reactions and the reliability of the technique, systems that report the specific annealing of fluorescent primers to their complementary templates were developed. The new methods rely on detecting the Fluorescent Resonance Energy Transfer (FRET) that occurs between fluorescent molecules upon excitation with an energy source. The FRET principle states that when a light source is providing photons to the PCR mix, the fluorescent primer or probe inside the reaction tube increases its energy from a resting basal level to the point where it cannot absorb or accept any more energy, losing stability and releasing the excess of energy in different ways, such as heat (friction generated by the kinetic movement of the chemicals), light (fluorescence for example), and usually both (26). Any compound that absorbs energy and releases it using FRET has an optimum wavelength at which it absorbs the maximum of energy and a second one at which emits the maximum of energy. Special light filters inside the detection system are used to provide and screen for these particular wavelengths. When losing the excess of energy in the form of light, the fluorescent molecule typically emits a flash of light in a different wavelength than the one it absorbed. This energy is in turn accepted by a second compound that can act as quencher or as a reporter for the system (190). Two types of fluorescent probes that make use of FRET principles are currently on the market. The first type is called a hybridization probe, while the second type is called a hydrolysis probe. In the case of hydrolysis probes, the reporter molecule and the quencher are located in an amplification

probe. When nonhybridized reporter and quencher molecules are located in close proximity to each other, they do not allow signals to be detected or escape from the system. When hybridization occurs, the enzyme in charge of performing the PCR disintegrates the probe, allowing FRET signals to be detected and quantified by the detection system. This type of assay is called Taqman™ (26, 74).

The amount of fluorescence for all three systems can be correlated with the amount of initial template during the exponential phase of PCR amplification (72, 85) by a mathematical expression of a straight line expressed in logarithmic terms. The mathematical expression uses the change in the fluorescence of the system to correlate the amount of template of the experimental sample with the amplification cycle of the PCR. If the right controls and the optimum amplification conditions have been provided, it is possible to quantify the initial amount of template by extrapolation or direct quantification of the initial sample (72, 85). For this dissertation research, the Taqman™ system was used because it allowed the specific recognition of the particular genes chosen for analysis. In the Appendix, the mathematical considerations needed to perform this technique are presented, while the results of the analyses performed are shown in Chapter IV.

CHAPTER II

RESISTANCE AND SUSCEPTIBILITY OF *MEDICAGO*

TRUNCATULA* NATURAL POPULATIONS TO *PHYTOPHTHORA

MEDICAGINIS

SUMMARY

The *Medicago truncatula* core collection has been screened for resistance and susceptibility to *Phytophthora medicaginis*. The analysis of 96 ecotypes resulted in certain genotypes showing high resistance and certain ones having high susceptibility to the pathogen. Ecotypes such as DZA 222 and DZA 220 were shown to be highly susceptible to *P. medicaginis* infection, whereas the ecotypes GRE 065 and FRA 20031 were found to be resistant. In addition, the resistance and susceptibility of DZA 220, DZA 222, GRE 065 and FRA 20031 to other Oomycetes such as *Pythium ultimum* and *P. irregularum* were also studied. The experimental results were complemented with a preliminary survey of the same collection of 96 ecotypes for disease resistance against *Colletotrichum trifolii*.

This information will provide the beginnings of breeding programs aimed at improving the resistance of commercial varieties of *M. truncatula* to *P. medicaginis*, as well as the map-based cloning of resistance genes. Using comparative genomics or transgenic work, this information can eventually be used to improve other commercially significant legume species also affected by this pathogen.

INTRODUCTION

The past century represented the birth of the green revolution. Many crops were improved through breeding practices, allowing the development of new varieties and hybrids engineered for high yield and the ability to withstand pathogens and pests (24). Plants were selected and backcrossed to refine characteristics such as yield, size, color and taste, in lengthy processes involving the crossings of two or more cultivars and/or ecotypes. Due to the importance of breeding in agriculture, continuous efforts have been made to generate new and improved varieties. In the field of plant pathology, the main task is to find ways to protect the plants from pathogens, and, in the process, provide the grower with excellent yield and quality seed sources. In agricultural settings, the use of high yield varieties is often hampered by the arrival of virulent races of pathogens. When a new strain of a pathogen renders existing cultivars susceptible, the usefulness of the cultivar decreases while the abundance of the pathogen increases correspondingly. The grower is faced with few alternatives, including the application of chemical or biological control agents to reduce the incidence of the disease, the removal of diseased plants with the intent of controlling the pathogen by elimination of infection foci, or finally, the use of new varieties that are resistant to the pathogen (3-4).

The production of new cultivars resistant to evolving pathogens depends on identifying sources for such resistance. A common source of new resistance phenotypes are ecotypes, the wild relatives of cultivated species. The development of resistance genes occurs after selective pressures caused by virulent pathogens reduce the genetic variability of the population under stress. Genetic mutation, outcrossing of susceptible

and resistant individuals within the population, and the arrival of resistant individuals not endemic to the area are the sources for the development of new resistance genes. After a process that involves several generations, the resistant alleles are fixed into the population, and new resistant populations or ecotypes are found (3). The task of plant breeders is to find those genetic sources of resistance and outcross them with existent or commercial cultivars to generate improved crops. With the advent of biotechnology, it is now possible to use genetic transformation and breeding techniques to accelerate the improvement of crops by transferring genes that confer resistance into susceptible cultivars from resistant individuals.

The purpose of genetic models is to expedite the study and understanding of biological processes. The large amount of natural populations collected over the years on model species makes them the perfect resource to find sources of genetic variability. In the case of the model legume *M. truncatula*, an extensive resource of about 400 natural populations, all of them isolated from different regions in the world, is available for research (188). These populations are expected to present different resistance levels to a pathogen, representing an invaluable supply of genetic material for crop improvement. Equally important is the existence of the highly dense genetic maps in model species that has allowed the mapping and cloning of important genes (34). The development of comparative genomics has permitted the transfer of this genetic information from model species into agronomically important species, opening new ways to use the information contained in these natural populations.

In this work, the screening of natural populations of *M. truncatula* for resistance and susceptibility to *Phytophthora medicaginis* was done. This study has the aim of providing insights into the genetic variability of this plant species and offers a glimpse of its usefulness as a source of resistance genes for crop improvement.

***M. truncatula* Pathogen Systems**

Few plant-pathogen interactions have been studied in *M. truncatula*. However, plant-pathogen interactions in the closely related species *M. sativa* (alfalfa) have been widely studied and ample information is available to growers and investigators. Because of the close evolutionary relationship between these two plants, I have hypothesized that many of the pathogens affecting alfalfa will also be capable of producing disease symptoms in *M. truncatula*. Standard assays have been developed to test pathogens in alfalfa (The Standard Tests for Alfalfa Cultivars Handbook), so I used this information to adapt protocols for testing pathogens in *M. truncatula*. The following sections explain the pathogen systems used in this study.

Phytophthora crown and root rot

Also known as alfalfa crown and root rot, this is a root and seedling disease caused by *Phytophthora medicaginis*. This oomycete, under conditions of cold temperatures and high humidity (flooding), develops asexual swimming spores called zoospores. Flooding conditions promote disease development (88, 120, 130-131) by providing a medium for zoospore motility and chemotaxis (29, 57) and by inducing anoxic conditions that interfere with host defenses. Because of the multicyclic

development of this pathogen, it can cause severe epidemics if chemical control or resistant varieties are not used when planting. This pathogen is homothallic and host specific. The pathogen's natural host is *Medicago sativa*, which is a polyploid species, obligatorily outcrossed. The existence of multiple genomes in this species has created a high level of heterozygosity in all the genetic loci of this species and the exploitation of this natural variability has allowed the discovery of natural resistance to most of the problems (120). *Phytophthora* root rot is not an exception; however, resistance to this pathogen is dependent on the density of the pathogen in the soil and on environmental conditions. If flooding occurs frequently, the density of the pathogen will increase and both resistant and susceptible populations will die. This means, as Miller and Maxwell observed in 1984 (120), that both types of plants are capable of becoming infected but the rate of colonization in resistant populations is considerably slower than in susceptible plants (120).

In tetraploid alfalfa, two loci that are incompletely dominant, *Pm1* and *Pm2*, are required for resistance (56). In diploid *M. falcata* plants, resistance to *P. medicaginis* is conditioned by two independently segregating loci, *Pm3* and *Pm4* (83). The nature of the resistance against this pathogen in *M. truncatula* is not well known. Even though breakdown of resistance by this pathogen is not a common situation, these studies of the interaction between *P. medicaginis* and *M. truncatula* can provide new opportunities for unique sources of resistance against this pathogen.

Pythium damping off

Damping off is a disease caused by oomycetes pathogens. *Pythium* species are best known for inciting seedling damping off and pre-emergence rots. Like *Phytophthora*, this organism is filamentous, heterotrophic and similar to true fungi, but more closely related to plants than to true fungi. Several species, including *P. ultimum* and *P. irregularum*, can cause severe losses to alfalfa stands. As in the case of *Phytophthora*, zoospores are the most important infective structures for this pathogen. Control of these species is currently by deployment of resistant individuals, as well as by chemical control (5). However, biological control of these pathogens through the development of suppressive soils has shown some success. These suppressive soils maintain physical characteristics such as pH, iron content and soil type that negatively influence the establishment of pathogenic populations. Under these conditions, the development and colonization of the root interphase by native beneficial populations of bacteria and fungi are favored. Biological control of *Pythium* species is currently investigated using fluorescent pseudomonads and *Streptomyces* bacteria (42, 92) as well by other antagonistic organisms such as fungi of the *Trichoderma* species (191).

Anthracnose

This is a leaf, stem and crown disease caused by the ascomycete *C. trifolii*. It is an important disease of alfalfa that affects growth, forage yield and plant vigor (135, 150). In compatible interactions, this pathogen causes typical anthracnose symptoms characterized by black lesions on the stems and leaves of the plant (133, 183). The pathogen enters the host by means of appressoria and the subsequent development of

penetration pegs. Once inside the epidermis, the fungus colonizes the tissues (136, 150). Upon successful colonization, asexual reproduction structures called acervuli can be visualized on the surface of the infected tissues. In the United States, two different races of the pathogen exist. Race 1 has been detected in all areas where alfalfa is grown, whereas race 2 seems to be confined to the eastern states (136). Specific resistance against these races has been found, but efforts to produce cultivars carrying resistance genes in *M. sativa* have been hampered by the auto-tetraploid and outcrossing nature of alfalfa, causing every cultivar to be genetically heterogeneous. Due to this fact, resistance against a pathogen in alfalfa is expressed in terms of percentage of the population carrying such resistance. Nonetheless, resistance against these races is controlled by two single dominant independent segregating loci, *An1* and *An2* (136). The nature of these genes has not been determined in alfalfa. Model legumes such as *M. truncatula* can potentially facilitate such analyses, either by providing comparative molecular markers that can help with the cloning of the homologues in alfalfa, or by cloning and characterizing the orthologous locus in the *Medicago truncatula*. This pathogen has become a model pathogen for plant-disease interactions, and host transcriptional responses are being characterized by a combination of EST sequencing and transcriptional profiling in *M. truncatula* leaves (188).

MATERIALS AND METHODS

Plant Material

M. truncatula ecotypes isolated from locations in Crete, Greece, Portugal, Spain, France, Algeria and Australia were provided by Dr. Jean Prospero, INRA, France. Seed from cultivar Jemalong A17 and near isogenic *sickle* were obtained from the Cook laboratory (Department of Plant Pathology, UC Davis).

Plant Growth Conditions

Seed germination

Seed were scarified with concentrated sulfuric acid (200 seed/ecotype/cultivar/20 ml H₂SO₄) for 8 minutes inside 50ml falcon tubes, rinsed 5 times with sterile distilled water and left for at least four hours to imbibe water. The seed was then placed in 9 cm Petri dishes containing sterilized moist filter paper, sealed with parafilm, wrapped in aluminum foil and stored inside a 4 °C refrigerator for 2 days to synchronize germination.

After the two days of cold treatment, the dishes containing the seed were transferred to room temperature (usually 20°C), and maintained in the dark to allow germination. After 36 hours at room temperature, a visible radicle of 1½ to 2 cm long had developed in most of the seedlings. This radicle length is long enough to support the seedling if it is transferred into aeroponics tanks. For experiments in soil, a germination time of two days was used.

Growing conditions

The soil used in the experiments was Peter's Professional Potting Soil (Scotts-Sierra Horticultural Products Co.). Individual seedlings were transplanted in pre-shaped potting trays (60 seedlings/tray) or in small pots, 7.5 cm diameter, until well-established. Pathogenicity experiments with *Phytophthora* and *Colletotrichum* were carried out directly in these trays. As the potting soil contained sufficient amounts of macronutrients and micronutrients to support the initial stages of development, slow release fertilizers were added one month after potting. Micronutrients were added at later stages (i.e. at 2 months). Pest control was limited to the control of fungal gnats and whiteflies. For fungal gnats, a biological control formulation based on *Bacillus thuringiensis* (Gnatrol) was added by drenching at the time of potting, with additional applications at one-month intervals. After a two week period of establishment, the plants were maintained with low water regimens. The low humidity in the soil usually helped to keep the levels of fungal gnats under control and it also helped to prevent root rot diseases. To control whiteflies, a detergent-based formulation (Safer Soap) was sufficient to reduce the incidence of the pest. In cases of infestations, contact insecticides such as Avid were combined with the soap as control measures. Preventive measures such as yellow sticky traps that attract insects and help to monitor and reduce the density of the whitefly were also used.

Growing plants inside growth rooms were exposed to 300 $\mu\text{mol}/\text{m}^2/\text{s}$ of light intensity with a photoperiod of 14 h of daylight and 10 h of darkness. The growth room temperature was set to 22°C during the day and 18°C at night. The greenhouse

temperature was maintained below 30°C with the lowest relative humidity possible to prevent sporadic downy mildew outbreaks. In cases of mildew infections, sulfur was burned during the night to control the disease, and the flats and pots spaced to increase the ventilation of the infected area. Lastly, infected tissues were removed.

Pathogen Growth Conditions

Alfalfa crown and root rot, caused by Phytophthora medicaginis

The isolate M2019, used for the experiments, was provided by Dr. Deborah Samac (USDA ARS-Plant Science Research Unit, St. Paul, MN). Zoospores were induced by transferring ten day old cultures growing on V8 agar at 22°C to a 28°C incubator for two days. The cultures were then flooded with 20 ml distilled sterile water and transferred to a 16°C incubator for 12-15 hours (120). Zoospore suspensions were collected and quantified with a hemacytometer. Infection of 2-week-old seedlings was achieved by flooding the experimental trays and evenly spreading the quantified inoculum (1.5×10^5 zoospores/ml) over the soil containing the plants. Negative control treatments were prepared in the same way as the pathogenic treatments, using sterile culture dishes as a mock inoculum source.

Flooding conditions were maintained for two days (120, 130). High soil moisture levels were maintained in the soil, to allow continued disease development. Starting 3-4 days after inoculation and for a period of two weeks, plants were counted and disease symptoms rated daily, using the following standards:

No symptoms, 0; cotyledons affected (chlorosis) or stunting, 1; cotyledons chlorotic/necrotic, monofoliate chlorotic, 2; trifoliate, monofoliate, cotyledons (chlorotic/necrotic), 3; plant totally affected/wilting, 4; plant dead, 5.

The number of resistant plants was expressed as the average severity index (ASI) (10, 153): $ASI = \frac{[(n \text{ class } 5 \text{ seeds}) 5 + (n \text{ class } 4) 4 + (n \text{ class } 3) 3 + (n \text{ class } 2) 2 + (n \text{ class } 1)] * 100}{(N * 5)}$, where N is the total number of seeds expected to germinate from a non-inoculated control (swollen seed – dead seed).

Pythium ultimum and *P. irregularum*

Cultures for both organisms were obtained from Dr. Charles Kenerley, (Department of Plant Pathology and Microbiology at Texas A&M University). Acid-treated and cold-conditioned *M. truncatula* seeds were planted in 3-day-old water-agar dishes previously inoculated with the oomycete under study. The dishes were kept in the dark at 20°C to stimulate seed germination. This temperature is critical to ensure seed germination without induction of a virulent response in the pathogen. After 48 hours of darkness, the dishes were transferred to a photoperiod of 14 h light and 10 h dark, with a reduced temperature of 18 °C. The thickness and concentration of the water-agar was crucial for this experiment. A17 seeds have normal tropisms and will grow towards gravity and light. *skl* mutants are unable to efficiently penetrate typical agar concentrations (2% or so), so a maximum 1% agar was used in all the experiments.

The rating system followed the recommendations of the Standard Tests for Alfalfa cultivars (9-10, 15), as listed below: Resistant (1), healthy seedling; primary root

free of necrosis; slight discoloration may be present. Resistant (2), infected seedling; primary root tip necrotic but firm. Moderately susceptible (3), infected seedling; primary root tip soft and rotted. Susceptible, dead seedling (4), germinated seed with emerged radicle rotted. Highly susceptible (5), dead seed; no germination at all, seed rotted.

The number of resistant plants was expressed as the average severity index (ASI), calculated as Powell et al. and Altier et al. (10, 153): $ASI = \frac{((n \text{ class 5 seeds} - N \text{ dead seeds in germination control}) 5 + (n \text{ class 4}) 4 + (n \text{ class 3}) 3 + (n \text{ class 2}) 2 + (n \text{ class 1})) * 100}{(N * 5)}$, where N is the total number of seeds expected to germinate from a non-inoculated control (swollen seed – dead seed).

Stem and leaf blight, caused by C. trifolii

The pathogen was generously provided by Dr. Nichole O'Neill, USDA-ARS, Bellville MD. The isolate 2sp2 belongs to the race 1 of the pathogen. Suspensions of conidia were prepared by flooding 7-day-old *C. trifolii* culture dishes (1/2 strength oatmeal agar) with sterile water (132, 134-136). The conidia were quantified and adjusted to 1×10^6 CFU/ml and then sprayed to runoff on the leaves of 2-week-old seedlings (± 3 ml/plant). Inoculated plants (60 plants/tray) were kept under humidomes to maintain conditions of high humidity (95-100%) for 2 days to assure efficient germination of the fungal propagules (132, 136). Disease symptoms were rated and scored starting on the seventh day after inoculation as follows:

75-100 % survival, resistant.	RR
50 - 75 % survival, moderately resistant.	R
25 - 50 % survival, moderately susceptible.	S
0 - 25 % susceptible.	SS

Resistance and Susceptibility of *M. truncatula* Natural Populations to Infection by *P. medicaginis*

The experimental design consisted of planting four different *M. truncatula* ecotypes and two controls (A17 and *skl*) in single trays. Ten seedlings per ecotype/genotype, totaling 60 seedlings/tray were used in each experiment. To comprise the full collection of ecotypes surveyed a total of 24 trays were used. Each of the genotypes tested was planted in randomized positions along the tray.

Nonetheless, a predetermined pattern for planting the seedlings of each ecotype was used to facilitate the screening and the generation of infection patterns (Fig. 3). Two weeks after planting, the trays were flooded and inoculated with a suspension of *P. medicaginis* zoospores following the protocols previously presented. Disease symptoms were rated as described. The consistency of the results was checked by replicated experiments of resistant and susceptible ecotypes.

Geographical Location of *M. truncatula*'s Sources of Resistance and Susceptibility to *P. medicaginis*

To determine if geographical origins were correlated with resistance of an ecotype, the points of origin and their corresponding resistance to the pathogen were plotted on a map. Each ecotype was color-coded according to its corresponding score using the following system: resistant (0-40% disease) green, moderately resistant (41-60% disease) yellow, moderately susceptible (61-80% disease) orange, and susceptible (81-100% disease) red.

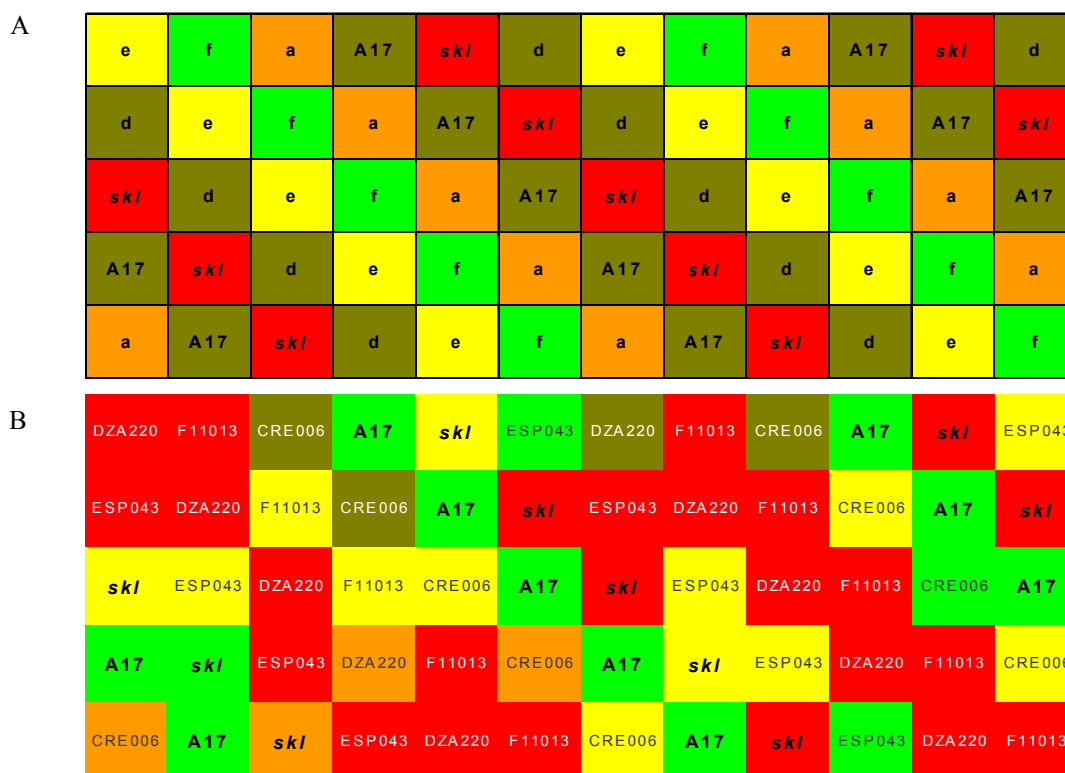


Fig. 3. *M. truncatula* ecotypes infected by *P. medicaginis*. A. Each square represents an experimental individual, planted in a pre-determined pattern that locks the position of seedling in the tray, generating a blueprint after infection that could look similar to what it is shown in this example. The letters inside each of the squares represents the ecotype/genotype planted in that place. After infection, resistant individuals were rated dark green, green or yellow, while susceptible/dead plants were rated with orange and red. B. An example is shown of experimental data, based on a template such as the one in Fig. 3-A.

Resistance of *P. medicaginis* Resistant and Susceptible Ecotypes against *Pythium* sp.

To preliminarily characterize the responses of some of the ecotypes susceptible or resistant to *P. medicaginis*, and gauge their response to other Oomycetes, 15 seeds each of four *M. truncatula* natural populations were exposed to *Pythium ultimum* or *P. irregularum* infection in replicated experiments. Infection protocol and seedling set up followed the methods previously presented. The *P. ultimum* experiment was replicated

three times while the *P. irregularum* experiment was replicated two times. The populations studied were A17, *skl*, FRA20031, GRE065, DZA220 and DZA222.

RESULTS

Resistance and Susceptibility of *M. truncatula* Natural Populations to Infection by *P. medicaginis*

The 96 populations were screened for resistance or susceptibility against *P. medicaginis*, a range of responses varying from almost total immunity to *P. medicaginis* infection to complete lack of resistance to the pathogen (Table 4, Fig. 4) was found. The ecotypes showing the extreme responses, i.e. highly resistant like GRE065 and A17 or highly susceptible like DZA222 and DZA220, were tested in two additional but independently performed experiments for consistency of results; the results of both trials were in agreement with what was previously observed (Fig. 5).

To test if the developmental status of the plant had an effect on its resistance to the pathogen, correlation analysis between the severity indexes of the ecotypes against their corresponding developmental status was performed. For the analysis, the size of the plant represented the independent variable, whereas severity of infection was the dependent variable. The statistical analysis showed that DZA220 had a correlation coefficient of -0.149, FRA20031 had 0.328, A17, 0.091, *skl*, 0.003 and GRE065 had -0.705. The observed results suggest that there is independence between parameters. The complete results of the analyses are shown in Table 4. At the time of infection, all the plants belonging to DZA222, had the same developmental status, showing full expansion

of first trifoliolate and full development of second trifoliolate (category 4 in the chart). This developmental status was considered slightly above the average of the rest of the ecotypes but within the normal ranges observed during the experiment (i.e. full expansion of first trifoliolate with barely distinguishable second trifoliolate (between 3 and 4 on the scale)).

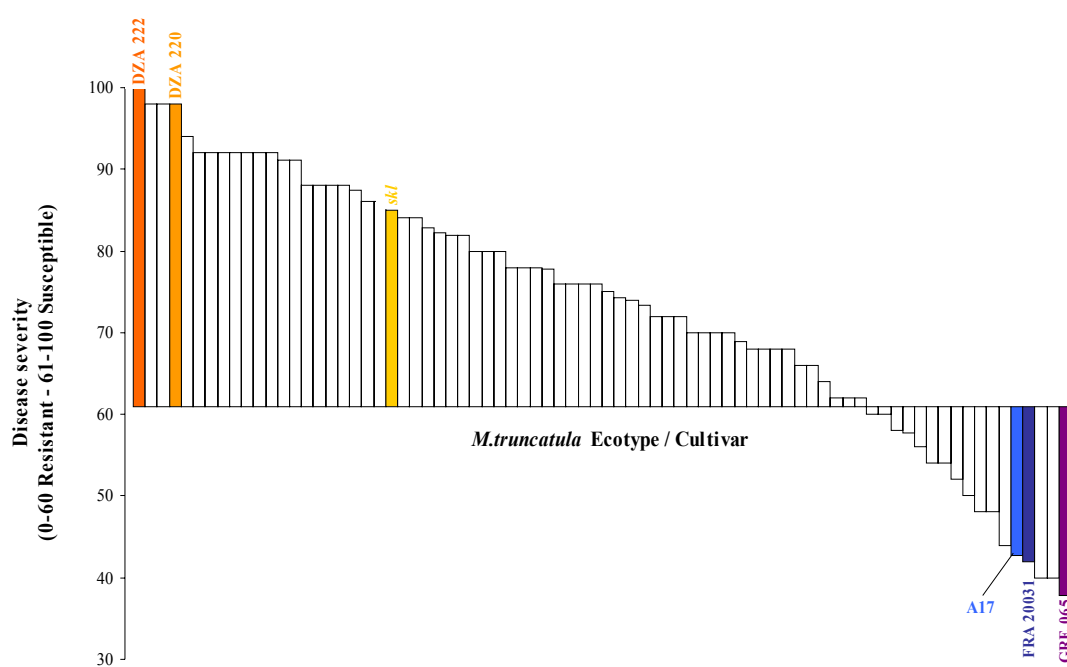


Fig. 4. Disease susceptibility of *M. truncatula* ecotypes to infection by *P. medicaginis*. Data representation of the results presented in Table 4. Disease susceptibility for each ecotype was calculated as the weighed average of 10 infected plants, measured according to the formula created by Powell et al. (153).

Consequently the impossibility of performing the correlation analysis on this ecotype was not a deterrent to include it in the results. In addition, preliminary experiments demonstrated that genotype A17 has a moderately high resistance against *P. medicaginis* whereas the *skl* mutation was found to be susceptible to the pathogen (see Chapter III).

TABLE 4. Resistance or susceptibility to *P. medicaginis* in *Medicago truncatula* natural populations.

Tray	Ecotype/ Cultivar (d)	Severity (a)	Size (b)	Correlation (c)
14	GRE 065	37.78	3.33	-0.71
16	FRA 20047	40.00	2.56	0.00
20	FRA 20086	40.00	3.90	0.55
15	FRA 20031	42.00	3.30	0.33
	A17	42.68	4.15	0.09
9	PRT 180	44.00	3.20	0.52
15	ESP 095	48.00	3.50	0.18
18	FRA 20061	48.00	3.90	0.12
20	FRA 20081	50.00	3.78	-0.03
24	DZA 236	52.00	3.00	0.00
9	MOGUL	54.00	3.40	-0.15
19	ESP 101	54.00	3.20	-0.07
16	GRE 098	56.00	2.60	0.24
10	GRE 052	57.78	2.78	0.44
10	FRA 34042	58.00	3.10	0.68
18	ESP 099A	60.00	4.50	0.21
24	DZA 241	60.00	3.00	-0.63
11	DZA 046	62.00	3.33	-0.46
13	SEPHI	62.00	3.00	-0.55
15	DZA 061	62.00	3.40	-0.10
9	GRE 043	64.00	2.80	0.32
13	DZA 058	66.00	3.22	0.16
22	FRA 20089	66.00	3.40	-0.33
11	FRA 20009	68.00	3.78	-0.26
12	DZA 055	68.00	3.00	0.16
13	ESP 074	68.00	3.11	-0.12
19	FRA 20069	68.00	2.78	0.31
12	FRA 20015	68.89	3.25	-0.13
3	CRE 006	70.00	2.40	0.00
10	ESP 045	70.00	3.70	-0.25
10	PARABINGA	70.00	2.89	0.00
22	ESP 140	70.00	3.30	0.48
2	PRT 176	72.00	2.67	0.43
11	ESP 048	72.00	3.67	0.32
13	GRE 064	72.00	2.67	0.04
21	FRA 20087	73.33	3.22	0.25
9	DZA 045	74.00	3.10	-0.30
24	ESP 158	74.29	2.86	-0.36
24	ESP 159	75.00	2.50	-0.56
6	CRE 009	76.00	2.56	0.24
7	PRT 179	76.00	3.70	-0.52
14	FRA 20025	76.00	3.67	-0.26
17	FRA 20048	76.00	5.22	0.40
16	DZA 105	77.78	2.78	0.20
3	FRA 11007	78.00	3.11	0.52
6	FRA83005	78.00	2.89	0.76

TABLE 4: cont

Tray	Ecotype/ Cultivar	Severity (a)	Size (b)	Correlation (c)
22	DZA 230	78.00	3.20	-0.20
2	FRA 11005	80.00	3.00	0.19
16	ESP 096	80.00	3.37	-0.24
17	FRA 20058	80.00	6.10	0.47
15	GRE 093	82.00	3.30	-0.11
18	DZA 213	82.00	3.30	0.27
6	PRT 178	82.22	2.89	-0.77
7	FRA 11012	82.86	3.00	-0.53
17	ESP 098A	84.00	5.00	0.10
18	DZA 210	84.00	3.40	0.32
	skt	85.03	4.03	0.00
2	CALLIPH	86.00	3.78	-0.44
22	ESP 105	86.00	3.33	-0.70
3	DZA 016	87.50	3.13	-0.45
6	DZA 027	88.00	2.22	0.38
11	GRE 063	88.00	3.33	-0.35
12	PARAGGIO	88.00	2.89	-0.16
14	ESP 080	88.00	3.89	-0.09
2	GRE 020	91.11	3.00	-0.52
12	ESP 050	91.11	3.50	-0.35
3	ESP 039	92.00	2.89	-0.38
7	ESP 041	92.00	3.78	-0.23
7	GRE 040	92.00	3.33	-0.22
14	DZA 059	92.00	5.50	0.00
19	DZA 219	92.00	2.89	-0.07
19	ESP 100	92.00	2.78	0.40
21	ESP 104	92.00	3.22	0.03
20	ESP 103	94.00	3.78	0.36
17	DZA 202	98.00	5.56	-0.24
20	DZA 220	98.00	3.45	-0.15
21	DZA 221	98.00	3.56	-0.20
21	DZA 222	100.00	4.00	error

(a) Disease severity data of the plants was calculated as the weighted average of the total number of plants per ecotype used in the experiment according to the formula derived by Powell et al. (153). Numerical Key: No symptoms: 0-20, Cotyledons affected or stunting: 21-40, Cotyledons and monofoliolate affected: 41-60, Trifoliolate, monofoliolate and cotyledons affected: 61-80, Plant totally affected or wilting: 81-99, Plant dead: 100.

(b) Size of the plants is the average developmental stage of the experimental plants at the moment of infection. Numerical key: cotyledons opened: 1, cotyledons + unifoliolate opened: 2, cotyledons + unifoliolate opened + 1st trifoliolate not expanded: 3, cotyledons + unifoliolate + 1st trifoliolate expanded: 4, cotyledons + unifoliolate + 1st trifoliolate expanded + 2nd trifoliolate not expanded: 5, cotyledons + unifoliolate + 1st and 2nd trifoliolate expanded: 6, cotyledons + unifoliolate + 1st and 2nd trifoliolate exp + 3rd trifoliolate not expanded: 7.

(c) Correlation analysis: Positive correlation; large values of plant size are associated with large values of severity. Negative correlation; small values of plant size are correlated with large values of disease severity.

(d) Ecotypes are coded by region of origin. FRA=France, PRT=Portugal, ESP=Spain, CRE=Crete, GRE=Greece, DZA=Algeria. Not coded entries equal to commercial cultivars, A17= Jemalong A17.

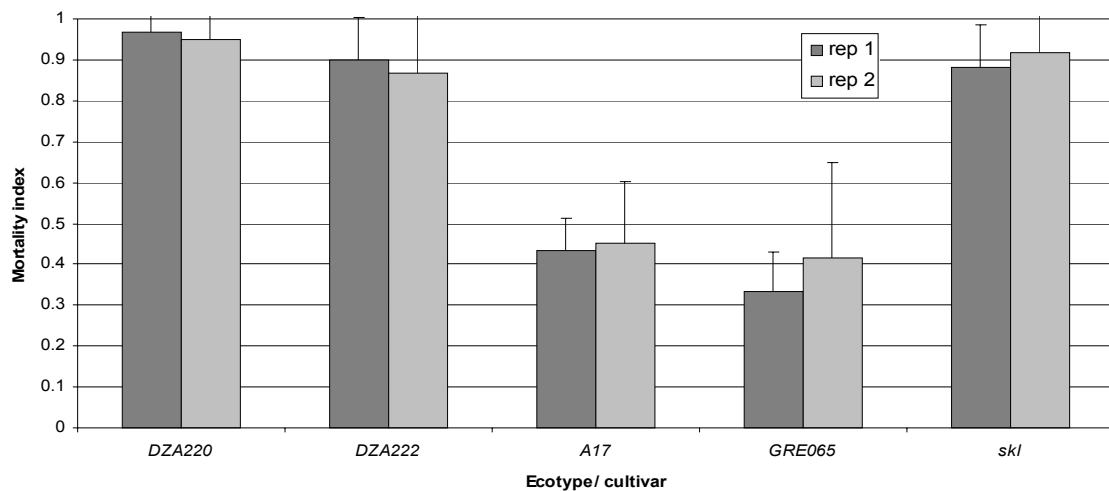


Fig. 5. Disease resistance and susceptibility of selected ecotypes to infection by *P. medicaginis*. Results of experiments involving the ecotypes showing the highest susceptibility and highest resistance to *P. medicaginis*. 12 plants per ecotype, plus the controls A17 and the *Medicago truncatula* mutant *sickle* were planted in flats and rated according to the protocols used, in two simultaneous but independent experiments.

The reactions of A17 and *skl* were used as internal standards to assess the infection levels in each of the experimental trays. To correct the experimental variation within the trays, the average disease index and the corresponding standard deviation of all the experimental trays was calculated (Table 6). In the same way, SDI for each individual trial was calculated. Because *skl* is hypersusceptible to *P. medicaginis*, trays where the SDI deviated less than 1.3 sd from the experimental average SDI found for *skl* were discarded. Correspondingly, because A17 is resistant to infection, experimental data deviating more than 1.3 sd from the A17 average severity index found in the experiment were discarded also. Based on these parameters, data from trays no. 4, 5, 8 and 23 was discarded (Table 5).

TABLE 5. Data not included in analyses.

Tray	Ecotype/ Cultivar	Severity	Size	Correlation	Cause
	BORUNG				
1	CRE 005	N/A	N/A	N/A	Germination problems
	DZA 012				
	ESP 031				
	CRE 007	90	3.2	0	
4	CYPRUS	98.00	3.50	0.25	Too much infection in controls
	GRE 033	84.00	3.20	-0.55	
	PRT 177	80.00	2.89	0.20	
	DZA 022	100.00	3.60	N/A	
5	ESP 040	84.00	3.90	0.16	Too much infection in controls
	FRA 11008	90.00	3.60	-0.16	
	GRE 037	91.11	3.44	-0.43	
	DZA 033	94.00	3.50	0.14	
8	ESP 043	86.00	3.80	0.51	Too much infection in controls
	FRA 11013	98.00	3.80	-0.13	
	HARBINGER	98.00	4.20	-0.44	
	DZA 231	72.000	3.100	-0.527	
23	DZA 233	74.000	3.110	0.036	Too little infection in controls
	ESP 155	66.000	4.000	0.203	
	ESP 156	42.500	3.860	0.404	

(a) Disease severity data of the plants was calculated as the weighted average of the total number of plants per ecotype used in the experiment according to the formula derived by Powell et al. Numerical Key: No symptoms: 0-20, Cotyledons affected or stunting: 21-40, Cotyledons and unifoliate affected: 41-60, Trifoliate, unifoliate and cotyledons affected: 61-80, Plant totally affected or wilting: 81-99, Plant dead: 100.

(b) Size of the plants is the average developmental stage of the experimental plants at the moment of infection. Numerical key: cotyledons opened: 1, cotyledons + unifoliate opened: 2, cotyledons + unifoliate opened + 1st trifoliate not expanded: 3, cotyledons + unifoliate + 1st trifoliate expanded: 4, cotyledons + unifoliate + 1st trifoliate expanded + 2nd trifoliate not expanded: 5, cotyledons + unifoliate + 1st and 2nd trifoliate expanded: 6, cotyledons + unifoliate + 1st and 2nd trifoliate exp + 3rd trifoliate not expanded: 7.

(c) Correlation analysis: Positive correlation; large values of plant size are associated with large values of severity. Negative correlation; small values of plant size are correlated with large values of disease severity.

(d) Ecotypes are coded by region of origin. FRA=France, PRT=Portugal, ESP=Spain, CRE=Crete, GRE=Greece, DZA=Algeria. Not coded entries equal to commercial cultivars, A17= Jemalong A17.

The ecotypes DZA222 (DSI=100), DZA221 (DSI=98) and ESP104 (DSI=92) growing on tray 21 were almost completely annihilated by the pathogen. The fourth ecotype, FRA20087, assayed in this tray had a SDI of 73.33, still higher than the SDI

observed for the internal controls growing in the tray. The SDI values observed for tray 21 suggest susceptibility to the pathogen. Replicated experiments involving DZA222 yielded the same high susceptibility to *P. medicaginis* (Fig. 5). Interestingly, a close look at Table 6 suggests that data from tray 21 should have been similarly discarded. In that tray, the SDI for A17 was 8 and for *skl* was 60. Both of these averages were below the expected averages and out of the cut off ranges employed, suggesting underinfection of the experimental plants, but clearly the observed results suggest that the ecotypes growing on the tray were not affected by the lack of infection found for both controls (*skl* and A17) and therefore they were not discarded.

Geographical Location of *M. truncatula*'s Sources of Resistance and Susceptibility to *P. medicaginis*

The ecotypes used in the previous experiment are accompanied by extensive documentation, including information regarding the precise geographical location of their origin. In cases where resistance against *P. medicaginis* represents adaptive variation, one might expect to find geographical pockets of resistant ecotypes. To test this hypothesis, the geographical origin of each ecotype was plotted on a map.

As shown in Fig. 6, a cluster of resistant ecotypes was identified in the French island of Corsica, whereas a cluster of susceptible ecotypes was identified in Algeria. Interestingly, the African populations seem to change from moderately resistant for those located near the Mediterranean coast, almost at the same longitude of Corsica, to susceptible, the farther they are found from this location.

TABLE 6. Infection levels of experimental trays.

Tray number	A17			<i>sickle</i>		
	Average Tray DSI	Std. dev	Distance from Average ^a	Average Tray DSI	Std. dev	Distance from Average ^b
EXP	50.57	25.11		87.62	11.01	
1	66.90		16.32	93.57		5.95
2	64.00		13.43	100.00		12.38
3	74.00		23.43	91.43		3.81
4	84.44		33.87	100.00		12.38
5	84.00		33.43	100.00		12.38
6	77.78		27.20	91.11		3.49
7	72.00		21.43	100.00		12.38
8	88.00		37.43	97.78		10.16
9	18.00		-32.57	74.00		-13.62
10	42.00		-8.57	86.00		-1.62
11	50.00		-0.57	86.00		-1.62
12	48.89		-1.69	82.00		-5.62
13	36.00		-14.57	86.00		-1.62
14	82.00		31.43	100.00		12.38
15	48.00		-2.57	87.50		-0.12
16	54.00		3.43	95.56		7.94
17	66.00		15.43	98.00		10.38
18	16.00		-34.57	74.00		-13.62
19	18.00		-32.57	76.00		-11.62
20	28.00		-22.57	88.00		0.38
21	8.00		-42.57	60.00		-27.62
22	24.00		-26.57	88.00		0.38
23	26.00		-24.57	72.00		-15.62
24	37.78		-12.80	76.00		-11.62
	Upper limit to accept (1.3 sd):		32.648	Lower limit to accept (1.3 sd):		-14.318

a. The cut off value used to accept or reject experimental data in a particular tray was calculated as 1.3 times the standard deviation of the index found for A17 in all the experimental trays. Trays where the measured distance from average (Average DSI tray – Average DSI exp) was higher than the cut off value were rejected.

b. The cut off value used to accept or reject experimental data in a particular tray was calculated as -1.3 times the standard deviation of the disease severity index found for *sickle* in all the experimental trays. Trays where the measured distance from average (Average DSI tray – Average DSI exp) was smaller than the cut off value were rejected.

The absence of geographical information for the continental French populations precluded mapping of these individuals. Nonetheless, a look at Table 4 shows a

distribution of responses similar to what was found for Spain (Fig. 6), suggesting a mix of resistant and susceptible populations, with the majority rated as moderately susceptible or susceptible.

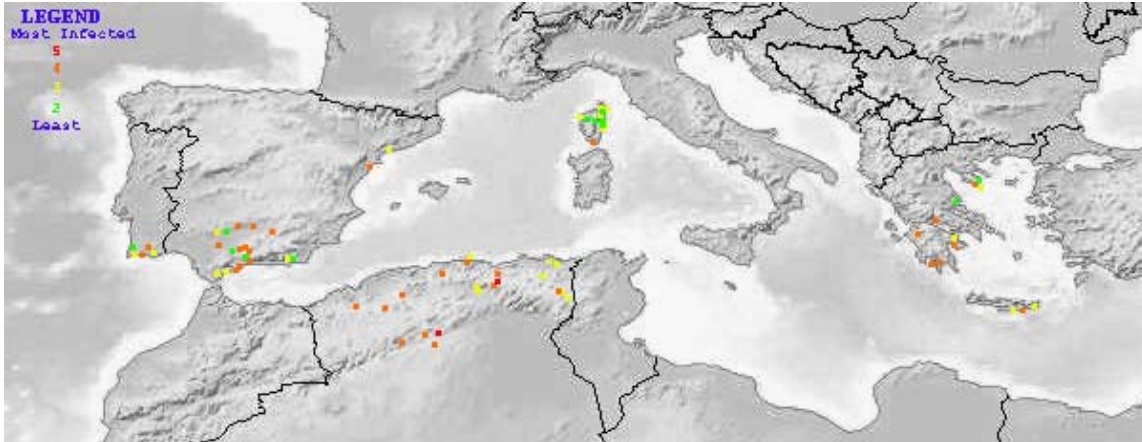


Fig. 6. Geographical location and associated resistance or susceptibility of *Medicago truncatula* ecotypes exposed to infection by *P. medicaginis*.

Resistance of *P. medicaginis* Resistant and Susceptible Ecotypes against *Pythium* sp.

The cultivar A17-jemalong, the A17 strain used in the experiments was found resistant to *P. irregularum* with an average disease index around 1.8. The remaining ecotypes tested, DZA220, DZA222, GRE065, and FRA20031 displayed similar responses with disease indexes close to 2.8, making them moderately susceptible to this pathogen. Interestingly, the near-isogenic to A17, *skl*, was found to be more susceptible than A17 to this pathogen, with similar disease levels than the rest of the tested ecotypes Fig. 7.

P. ultimum infection of ecotypes showed a similar trend. A17 was the most resistant, followed by *skl* and then the rest of the ecotypes with very similar responses.

Despite this similar response, all of the ecotypes were found to be susceptible to this pathogen and DZA222 apparently is the most susceptible to infection by this pathogen

Fig. 7.

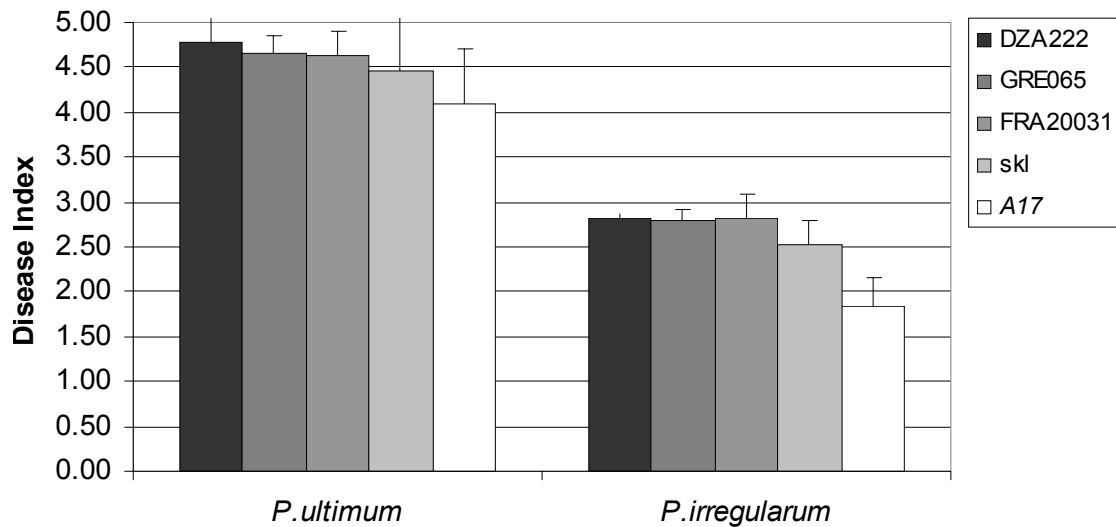


Fig. 7. Disease incidence in *M. truncatula* ecotypes upon infection with *P. ultimum* and *P. irregularum*. Data shown is the result of replicated experiments. Each experiment consisted of 3 agar-dishes inoculated with the pathogen and planted with 15 seeds of each of the ecotypes under research. Data was analyzed according to the protocols presented.

DISCUSSION

The study of plant-pathogen interactions in wild germplasm can facilitate cultivar improvement by both classical and molecular approaches to breeding. With this purpose in mind, the responses of *M. truncatula* natural populations were evaluated in detail for *P. medicaginis*. A subset of ecotypes was further evaluated for their responses to the oomycetes, *P. ultimum* and *P. irregularum*. *P. medicaginis* is an important pathogen of

alfalfa and *Pythium* species are major seed pathogens of a wide range of plants. Based on these analyses, the potential resistant ecotypes to these pathogens were defined.

The response of *M. truncatula* ecotypes to *P. medicaginis* was examined in greatest detail. To reduce the chance of artificially labeling well developed plants as resistant ecotypes and small or poorly developed plants as susceptible, correlation analysis between the developmental stage of the plant at the moment of infection and its corresponding disease index after infection were performed. This was an important point because in aeroponics assays it was observed that A17 plants infected with *P. medicaginis* developed secondary roots to replace the loss of infected roots. This secondary defense response correlated with the extent of plant development and could skew the experimental results. The results of the cases where the correlation between the two parameters was high (-.95 or more), suggesting that well-developed plants correlated with low disease levels, were discarded. Experimental results were also removed from analysis when their correlation showed that small, poorly developed plants could statistically be linked with high levels of disease.

To normalize disease ratings between assays, the *M. truncatula* mutant *skl* was used as a positive control for infection. *skl* is impaired in its defense response to Oomycete pathogens. Near isogenic A17 was used as the resistant cultivar control. In some cases, the disease severity ratings observed for both control genotypes differ from what was expected. Localized differences in the flooding levels of the experimental trays during the inoculation stages of the experiment and changes in the viability of the quantified inoculum prior to infection could explain these results. Particular trays

yielded quite low infection rates, while other trays resulted in almost total plant death (Table 6). To minimize that experimental variation, any tray departing more than 1.3 standard deviation units from the average disease rating was removed from the analysis. This was accomplished by comparing the disease ratings of each individual tray to the experimental average disease rating of all the trays using the formula presented by Altier and Thies (9).

An interesting experimental result of this analysis was obtained in tray number 21 (Table 6). In this tray the average disease index for A17 and *skl* was lower than the observed average of all the trays suggesting under-infection of the experimental plants. Nonetheless, the ecotypes growing in this tray were almost completely killed by the pathogen clearly showing susceptibility to *P. medicaginis* (Table 4). The disease symptoms observed for these ecotypes (i.e. DZA222, DZA221, ESP104 and FRA20087) did not suggest contamination with any other pathogen. The developmental status and correlation coefficients for these ecotypes similarly did not imply any problems affecting the plants or skewing of the results (Table 4). Furthermore, replicated experiments involving DZA222 and *P. medicaginis* showed again the high susceptibility of this ecotype to the pathogen (Fig. 5), further reinforcing the conviction that genetic susceptibility to the pathogen in these ecotypes was behind the results. If the results in this tray were to be rejected, the reason for the rejection would have been the low infection level of controls. A look at Tables 5 and 6 shows that the expected patterns for rejection of data holds in the remaining cases (i.e. too much infection in controls correlates with high SDI in the ecotypes growing in the trays and vice versa). In this

case, the pattern is totally the opposite. The ecotype data for tray 21 did not correlate with the low infection of the controls and the rejection of this data would imply the faulty not labeling of a negative result as negative, a parameter that these analyses were not intended for. In statistical terms, I could have configured a hypotheses error of the β type.

A positive outcome of the findings of these screens is that breeding programs and studies aiming to find the genetic basis for disease resistance against *P. medicaginis* can be initiated using the resistant and susceptible ecotypes identified here. Of particular interest was the identification of putative geographical centers of resistance and susceptibility (Fig. 5). Ecotypes isolated from Corsica appear to be more resistant to infection than, for example, ecotypes isolated from Algeria, which showed the highest susceptibility to this pathogen. Further experiments involving nearest neighbor analysis should clarify this hypothesis. Determining the genetic basis of these resistance phenotypes and monitoring the frequency and distribution of functionally defined alleles would allow a population level study of these *Medicago-Phytophthora* interactions. Preliminary experimentation has also been done to test the responses of a subset of ecotypes to infection by *Pythium* species. In the case of *P. ultimum*, the results suggest that this pathogen is extremely virulent to *M. truncatula*. Conversely, the *P. irregularum* results suggest that moderate resistance to this pathogen is present in the ecotypes. It is possible that part of the observed results can be explained on the basis of the host developmental status. In this research, the development of *P. irregularum* was slower than *P. ultimum*, allowing longer development of the seedlings used in the experiment.

Another possibility is that *P. irregularum* is more pathogenic to this species if the plant is in an earlier developmental stage (non germinated seed instead of 4mm root length seedling) when exposed to the pathogen.

TABLE 7. Resistance or susceptibility to *C. trifolii* in *Medicago truncatula* natural populations.

	CULTIVAR/ ECOTYPE	<i>Colletotrichum</i>	
		Resistant	Susceptible
1	DZA 046	RR	
2	DZA 061		SS
3	DZA 105		SS
4	DZA 220		SS
5	DZA 221		SS
6	DZA 222		SS
7	ESP 040		SS
8	ESP 098A		SS
9	FRA 20047		SS
10	FRA 20061		SS
11	GRE 040		SS
12	GRE 064		SS
13	GRE 093	RR	

Preliminary screen for resistance and susceptibility of *M. truncatula* natural populations to *C. trifolii*. Experiments with *C. trifolii* race 1, pathovar 2sp2 consisted in applying to run off (≈ 3 ml) a spore suspension (7.2×10^5 /ml) of the pathogen to trays containing 60-2 week old *M. truncatula* plants. The same 96 ecotypes assayed for resistance and susceptibility against *P. medicaginis* were used in here. Ecotypes for which no information is provided, resulted in no significant difference in their response with A17. SS: susceptible, RR: resistant.

Not included in the results section was the initial characterization of the responses of *M. truncatula* ecotypes to infection by *C. trifolii*. Preliminary experimentation showed the incompatible response of A17 and *skl* to this pathogen. To clarify if the observed resistance was due to plant genetics, instead of issues such as inoculum viability, unfavorable environmental conditions for the development of the pathogen, or a combination of the two, a small-scale survey using only one plant per ecotype was set up. The results of the experiment were exciting in the sense that

compatible responses in some of the ecotypes were observed. Genotypes like DZA222, ESP040 and GRE040 were completely killed by the pathogen. However, DZA046, GRE093 and A17 were shown to be resistant. Because the experiment was only an initial survey, further experimentation is needed to confirm these results (Fig. 8, Table 7).



Fig. 8. Compatible and incompatible responses of *M. truncatula* ecotypes to infection by *C. trifolii*. Two week old *M. truncatula* plants were sprayed to run off (± 3 ml) with a suspension of *C. trifolii* conidia (1×10^6 conidia/ml), inoculated plants were kept inside humidomes for two days. The photograph shows a subset of the observed disease symptoms two weeks after inoculation.

These studies involving *M. truncatula* ecotypes need to be complemented by repeating the screenings with *C. trifolii*. Previously Samac and collaborators (135) finished the screening of the U.S. *Medicago* core collection for resistance and susceptibility to *Phoma medicaginis*. Currently, several more screenings of this same type have been started, and the analysis of the responses of *M. truncatula* natural

populations to important pathogens and pests, like the nematode *Meloidogyne incognita*, the fastidious bacterium *Xylella fastidiosa*, the parasitic plant *Cuscuta trifolii* (dodder) and the economically important pest *Hypera postica* (alfalfa weevil) are on their way (D.R. Cook, personal communication). Similar screenings involving aphids and other fungal pathogens are currently being done (188).

CHAPTER III
AN ETHYLENE INSENSITIVE MUTANT OF *MEDICAGO*
TRUNCATULA* IS HYPER-SUSCEPTIBLE TO *PHYTOPHTHORA
MEDICAGINIS

SUMMARY

In recent years, studies of the legume-*Rhizobium* interaction have expanded to include the analysis of plant mutants defective in symbiotic development. Such studies provide the basis for understanding developmental and regulatory pathways involved in nitrogen fixation interactions. One such mutant is the *Medicago truncatula* hyper-nodulation mutant *sickle* (*skl*), which shows increased infection by *Sinhorhizobium meliloti*, the natural nitrogen fixing symbiont of this plant. The *skl* mutation is recessive and confers insensitivity to the plant hormone ethylene.

Here it is shown that *skl* also displays an increased susceptibility to infection by pathogenic organisms, particularly oomycetes. The coincidence of these phenotypes in *skl* mutation (i.e. symbiosis, disease susceptibility and ethylene insensitivity) creates an opportunity to study the commonalities between genetic control of infection by symbiotic and pathogenic microorganisms, in particular those dependent on the perception of the plant hormone ethylene.

INTRODUCTION

Several Ethyl MethaneSulfonate (EMS) mutagenized populations of *M. truncatula* cultivar A17 have been screened for their symbiotic interaction with nitrogen fixing microorganisms, specifically the symbiotic bacteria *S. meliloti* (38). From these screenings, two sets of mutant plants were initially identified and are being studied. The first subset showed a phenotype characterized by a lack of development of nitrogen fixing root nodules, whereas the second subset showed a higher than usual number of nodules on inoculated roots. From the first group mutations such as *Does not Make Infections1 (dmi1)*, *dmi2* and *dmi3* have been characterized and recently cloned (11, 30, 54, 121).

From the second subset of plants, two mutants, *Super Numeric Nodules (sunn)* and *SicKLe (skl)*, were identified (146,148). Phenotypic and physiological analysis of *skl* plants demonstrated that they are pleiotropic for delayed petal and leaf senescence. In addition, *skl* showed decreased abscission of seedpods and leaves, and was hyperinfected by symbiotic bacteria, allowing approximately 10 times the normal number of persistent infections in the plant. As a consequence, *skl* plants showed an increased number of symbiotic nodules. Genetic analysis of the *sickle* mutation demonstrated that these phenotypes are conferred by a single, recessive gene (150).

Sickle seedlings exposed to ethylene failed to produce the typical triple response observed in A17 plants. The triple response is an ethylene dependent response characterized by decreased elongation of hypocotyls and roots, and an exaggerated apical hook in response to exogenous ethylene (174). Exposure of A17 or *skl* plants to

either ACC or ethylene gas showed that nodulation of A17 was effectively blocked by both compounds, whereas the nodulation of the mutant *skl* was insensitive to these treatments. ACC is the immediate precursor of ethylene and *skl* insensitivity to this compound was observed even at the high dose of 300 μ M ACC (10x higher than the ED₅₀, for A17 plants) (146). Overall, these data supported the hypothesis of *skl* involvement in ethylene perception or transduction of ethylene-derived plant signals. Cloning of *skl* mutation was recently achieved and it was shown to have homology to the *A. thaliana* *EIN2* gene (manuscript under preparation). Therefore, *skl* has been hypothesized to act in the ethylene perception pathway in a similar way as the *Arabidopsis thaliana* mutant *ein2* (Dr. D. Cook personal communication). On the other hand, *sun*n plants showed a similar increase in the number of symbiotic nodules, with root insensitivity to the hormone ethylene. Despite the similarities between both mutations, genetic analysis suggested that *skl* and *sun*n correspond to different unlinked loci and furthermore, define separate genetic pathways that control nodule number and organogenesis processes upon infection with *S. meliloti* in *M. truncatula* (148).

To study the commonalities between genetic control of infection by symbiotic and pathogenic microorganisms, seedlings of three of these mutants (*dmi1*, *skl* and *sun*n) were exposed to zoospores or mycelia of *Phytophthora medicaginis*. The results showed that *skl* mutant was more susceptible than A17 to infection by this pathogen. On the other hand, the responses of *dmi1* and *sun*n were not different from the infected A17 control, the genotype A17 (results not shown). Parallel analysis indicated that *skl* mutants were not altered in their gross response to arbuscular mycorrhizal fungi (Dr.

Maria Harrison, personal communication). *skl* was also unaltered in its response to the nematode pathogen *Meloidogyne incognita* (Dr. H. Zhu, personal communication) and to the fungal pathogens *Fusarium oxisporum* and *Rhizoctonia solani* (data not shown). Taken together, the data suggest that ethylene signaling is a common feature of defense against oomycete pathogens and regulation of infection by *Sinorhizobium meliloti*.

MATERIALS AND METHODS

Plant and Pathogen Growth Conditions

M. truncatula seed scarification and germination, preparation of aeroponic tanks and soil trays and growing conditions for experimental plants followed the protocols presented by Cook et al. (37). *P. medicaginis* cultures were grown as presented in Chapter II to induce zoospore production. The inoculum was quantified using hemacytometers and adjusted to 1.5×10^5 zoospores/ml. *P. ultimum* and *P. irregularum* were grown initially on corn meal agar at 23°C. 5-day-old colonized corn-meal agar pegs were then transferred to water-agar dishes (0.8 %). 3-day-old infected water-agar dishes were used as source of infection for experiments involving *P. ultimum*, and 5-day-old dishes were used with *P. irregularum*. Conidia of *C. trifolii* were prepared as previously presented in Chapter II.

***M. truncatula* Infection by *P. medicaginis*, Soil Experiments**

Inoculation of *M. truncatula* plants with *P. medicaginis* was performed by flooding 2-week-old plants growing in trays with water and evenly distributing the quantified

inoculum in the flooded tray. To achieve this, the inoculum was diluted in 1 L of water and then evenly distributed on the soil contained in the tray. To assure zoospore germination and pathogen localization of the host, flooding conditions were maintained for 2 days (120,130).

Soil experiments to characterize *P. medicaginis* infection of the *skl* mutation were conducted in 50 cm x 30 cm trays, planted with 60 seeds of either *skl* or A17. Four inoculated replicates were analyzed for each genotype, and two replicates were subject to mock inoculation. *P. medicaginis* zoospores were used to flood-inoculate trays at 12 days post germination, when the plants had opened the first trifoliolate. Disease symptoms were recorded at 0, 6, 8, 10, 12, 14, 16, 18 and 24 days post-inoculation.

***M. truncatula* Infection by *P. medicaginis*, Aeroponic Tank Experiments**

To grow the plants for microscopic analysis and to collect roots for ethylene production experiments, 72 L Rubbermaid trash cans were adapted into aeroponic tanks, as described by Gallusci et al. (71). A Defensor mist generator (aeroponic generator) non-sonicating model 505S Air Humidifier-Atomizer (AxAir Ltd. Pfaffikon, Switzerland) was used to create misting conditions to nourish the roots. The aeroponic tank was washed thoroughly with soap, and rinsed with deionized sterile water. NaOCl (20%) was used to treat every component of the tank for at least 30 minutes, followed by at least three additional rinses with sterile water. If pathogens were previously used in the tank, an extended overnight treatment period was used. In those cases, the misting

motor would be left on overnight to sterilize itself thoroughly. A similar timeframe, using sterile water, was used to rinse the motor and tank after bleaching it. To grow the plants inside the tanks, the nutrient medium established by Lullien et al. (113) was used. All the stocks solutions were prepared and autoclaved separately for 20 min at 115°C, with 20 in Hg.

M. truncatula seedlings growing aeroponically were carefully removed from the tanks and organized into group of 10 seedlings. The roots of the seedlings were subsequently submerged in a *P. medicaginis* inoculum solution (1.5×10^5 zoospores/ml) for 2 h and returned to the tank. Non-inoculated controls were prepared by soaking control plants in a liquid solution that resulted from flooding non-inoculated V8 agar dishes with sterile water to mimic the conditions for *P. medicaginis* zoospore production. At specific times groups of plants were removed from the tank for analysis. The time 0 was defined as the moment at which the plants were moved back to the tank after being exposed to the pathogen.

Microscopical analysis

Seedlings of *skl* and A17 used for microscopy were grown aeroponically (37). *M. truncatula* plants, when growing inside aeroponic tanks, develop faster than in soil and previous experiments have shown that opening of the first trifoliolate occurs four days earlier than in soil (S. Ramu, personal communication). Therefore, *P. medicaginis* zoospore inoculation of experimental plants was performed when the seedlings were 8-days-old. The evaluation times were 0, 2, 4, 6, 12, 24, 48, 72, 96 and 120 hours after inoculation. At the scheduled times, 10 plants/genotype were retrieved and fixed in

2.5% glutaraldehyde and stored in 0.1% PIPES buffer pH 7.2 at 4°C for analysis. Individual samples were examined with a dissecting microscope (model SZH 10 Olympus, Tokyo, Japan) and (or) with an Axioskop compound microscope (Zeiss, Jena, Germany).

Quantification of *P. medicaginis* reproductive structures developing over a region defined as the first four cm of root tissue measuring from the tip of the root was performed by counting the number of sporangiophores, oospores or chlamydozoospores developing on the infected roots.

Ethylene quantification

The plants used for ethylene quantification were grown inside aeroponic tanks. *P. medicaginis* zoospore infection of *M. truncatula* plants was achieved as described. Infected and control roots were cut below the hypocotyl and placed inside glass vials. The vials were sealed with serum-stoppered caps. Ethylene quantification was performed on samples taken at 0, 2, 6, 12, 24, 32 and 48 hours after inoculation. Each sample consisted of three individual plant roots, replicated three times. An incubation period of 3 h was provided for each sample. For analysis of ethylene evolution, the protocol of Finlayson et al. was followed (64). Briefly, 1 ml of sample was collected and analyzed using a 10SPlus gas chromatograph (Photovac, Markham, Ontario, Canada) equipped with a photo ionization detector. Control vials, without roots, were sampled at each time point to correct for background ethylene. After each measurement, the weight of the samples was taken. Ethylene production was expressed in terms of nM of ethylene per gram, per hour.

***M. truncatula* Infection by *Pythium* sp.**

In the case of *Pythium ultimum* and *P. irregularum* experiments, seeds (acid treated and cold conditioned) were evenly distributed in the colonized water-agar dishes in experiments replicated three times. During two days, the dishes were kept at 18°C in the dark to stimulate germination, and subsequently moved to a growth chamber set to 14 h light and 10 h darkness, with a constant temperature of 18°C. Disease rating was assessed using the protocols described in Chapter II on the fifth day after inoculation.

M. truncatula* Infection by *C. trifolii

Experiments with *C. trifolii* race 1, pathovar 2sp2 consisted of applying to runoff a spore suspension of the pathogen (7.2×10^5 /ml) to trays containing 60 2-week-old *M. truncatula* plants. Three replicates per genotype (A17 and *skl*) plus a non-inoculated control were used. Infected and control trays were covered during the 48 h after inoculation to keep the relative humidity inside the trays close to 100%. Plants were watered daily as needed and data was collected at seven and 14 days after inoculation. Infection was assessed as previously presented in Chapter II.

RESULTS***M. truncatula* Near-Isogenic Line *skl* Is Hyper-Infected by *P. medicaginis***

Infection of *M. truncatula* plants with *P. medicaginis* resulted in responses that differed with the plant genotype. Symptoms in A17 plants started as chlorosis of the cotyledons, followed by chlorosis of the monofoliate, then the trifoliate, general

chlorosis and wilting and, finally, death of the plant. However, symptom development in *skl* genotype progressed considerably faster than in A17 leading almost invariably to death. Most of the plants went from the initial stage of cotyledon chlorosis almost directly into general chlorosis and wilting.

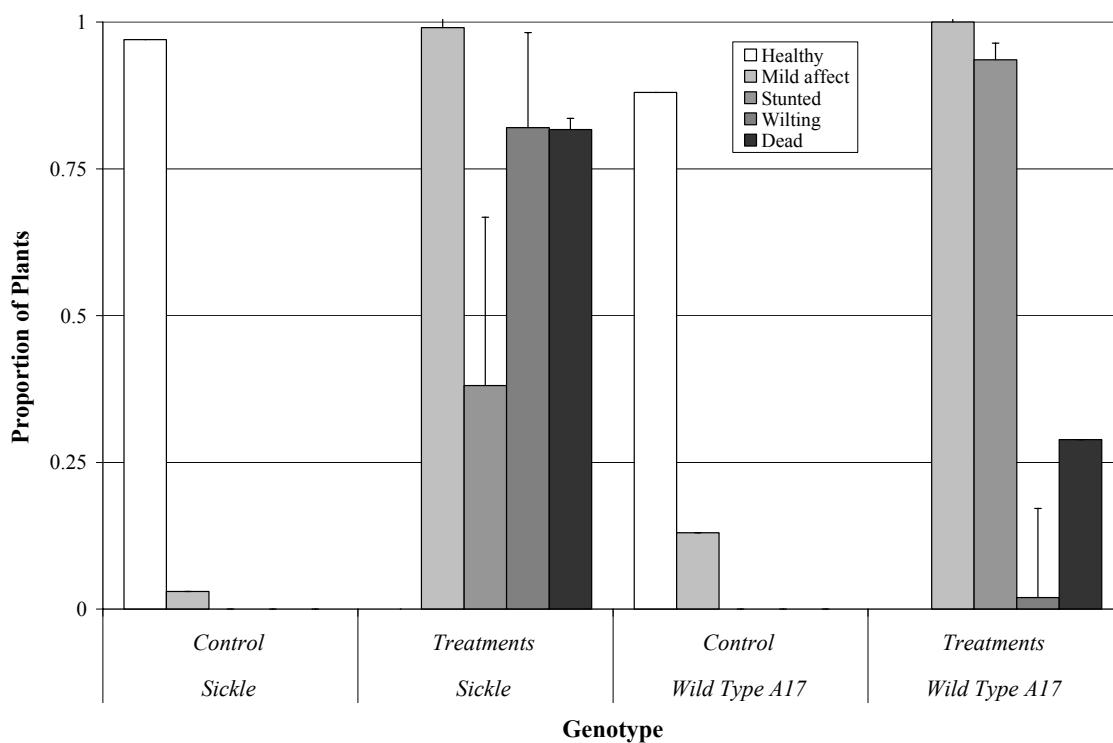


Fig. 9. Disease susceptibility of *M. truncatula* A17 and near isogen *sickle* to infection by *P. medicaginis*. Four days after inoculation and for a period of two weeks, infected plants were rated daily for symptom development. The graph shows the proportion of plants that developed particular symptoms at any time during the duration of the experiment.

The time frame for symptom development was different. In A17 plants, trifoliolate chlorosis and(or) general plant chlorosis occurred ten days after inoculation, while *skl* plants were wilting by the sixth day of the experiment. By the tenth day of

experimentation about 50% of the *skl* plants were dead (Fig. 9 and Fig. 10). A17 plants were killed around 30% of the time, while 80% of *skl* plants were dead by the end of the experiment (Fig. 9). Control plants remained healthy for the duration of the experiment (Fig. 9).

To obtain information about pathogen colonization and reproduction, and to get independent confirmation of the results, *P. medicaginis* infected and non-infected A17 and *skl* plants were analyzed microscopically. Collected data showed extensive and massive colonization of root tissues. A number of reproductive structures, mainly sporangiophores, were easily recognized. The results showed reproduction of the pathogen appearing at 48 h post-inoculation. At this time point, it was already possible to differentiate between the two genotypes. The results showed that *P. medicaginis* reproduction in *skl* plants was significantly higher than in A17. At 48 h after inoculation, almost six times more reproduction was observed in *skl* than in A17 (Fig. 11). At 72 h after inoculation, pathogen reproduction in A17 seemed to be progressing faster than in *skl* plants, but still *Phytophthora* reproduction in *skl* plants was higher than in A17 (Fig. 11). At 96 hours, the production of new pathogen reproductive structures seemed to have slowed down in both ecotypes, but at 120 hours post-inoculation additional reproduction was seen in both ecotypes (Fig. 10). At the end of the experiment, almost 600 reproductive structures could be seen developing in *skl* plants, versus 300 quantified in A17 (Fig. 11). Mortality rates for *skl* and A17 were 70% and 20 %, respectively (Fig. 10).

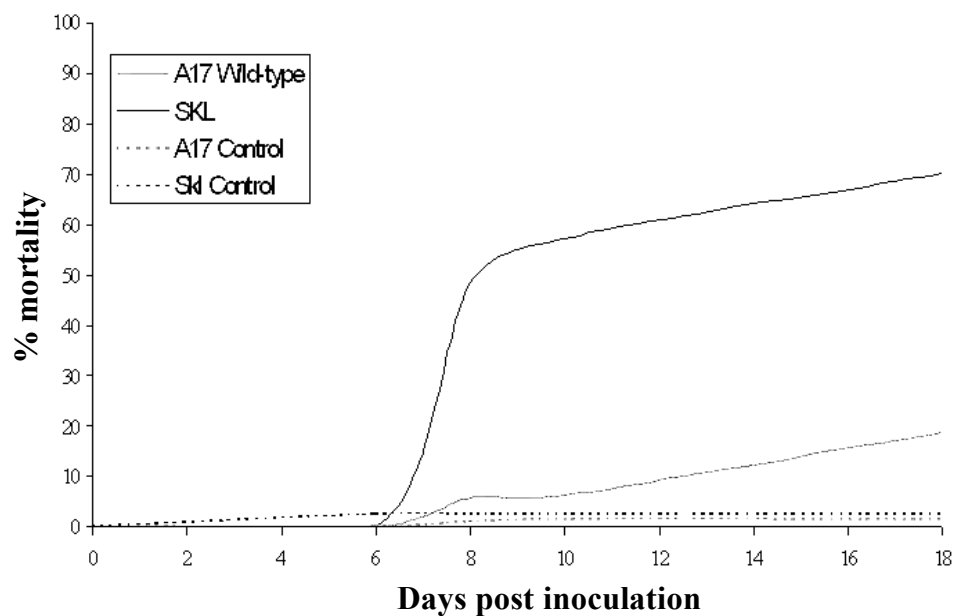


Fig. 10. Mortality rate of *Phytophthora* infected and mock-infected *M. truncatula* plants.

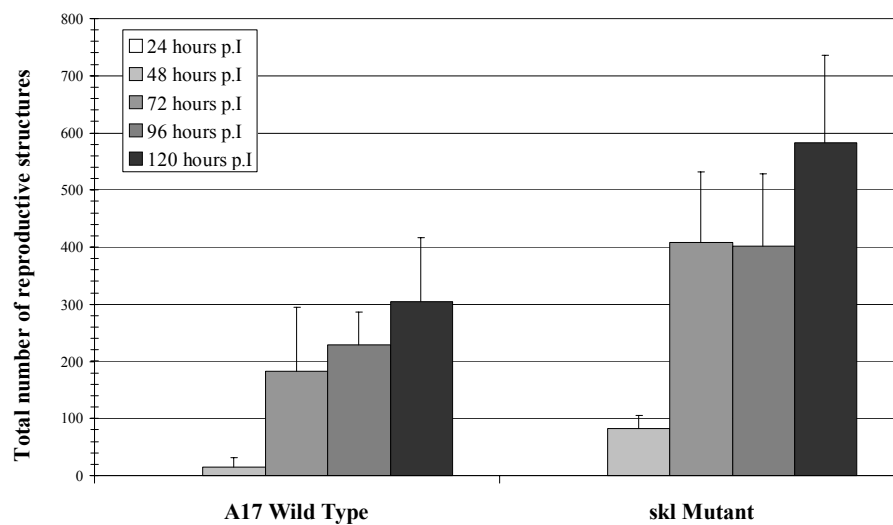


Fig. 11. Total development of *P. medicaginis* in *M. truncatula* roots. Ten plants per ecotype per time point were microscopically examined to detect the absence or presence of oomycetal reproduction structures. Data presented is the average number of oospores, sporangiospores or chlamidospores observed in infected roots.

Ethylene Quantification of *M. truncatula* Plants Infected with *P. medicaginis*

Because *skl* plants are ethylene insensitive, an experiment was set up to determine if *skl* insensitivity to ethylene was also affecting ethylene production as a response to pathogen infection. Results of two independently performed experiments showed a bimodal pattern of ethylene evolution (Fig. 12). For A17 plants, the highest rate of ethylene evolution occurred at 32 hours after inoculation; an additional small peak of ethylene production was also observed around 6 hours after inoculation. *M. truncatula skl* plants also produced ethylene at a slower rate than in A17, but at a higher rate than the non-inoculated controls (Fig. 12).

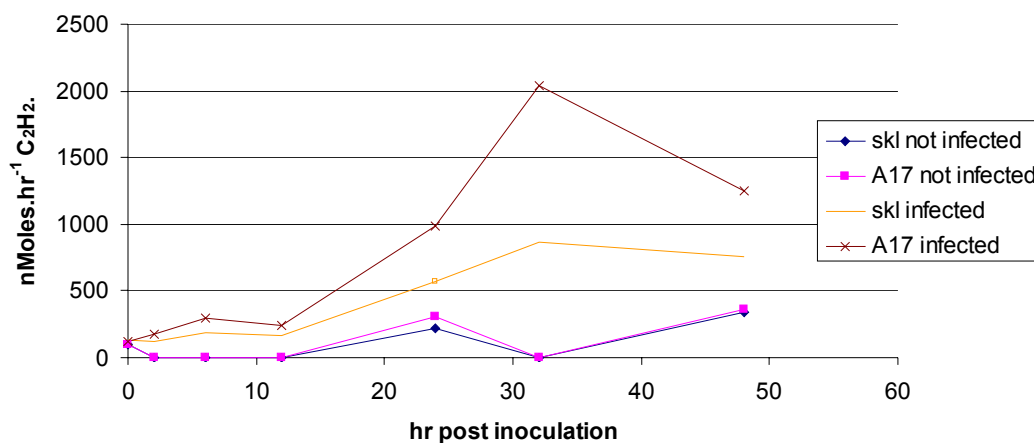


Fig. 12. Ethylene evolution in *Phytophthora*-infected *M. truncatula* roots. Data was obtained by gas chromatography using the protocol presented by Finlayson et al. Data shown is the average of three roots per time point. Each time point was replicated three times. The experiment was performed twice.

Visual inspection of infected A17 plants 48 hours after inoculation showed intense root tip curvature in response to ethylene production (Fig. 13), a response not

observed in *skl* plants (Fig. 13). These results were later positively correlated with gene expression analysis of ethylene-forming enzyme *ACC oxidase* over the same time course experiment (see Chapter IV).

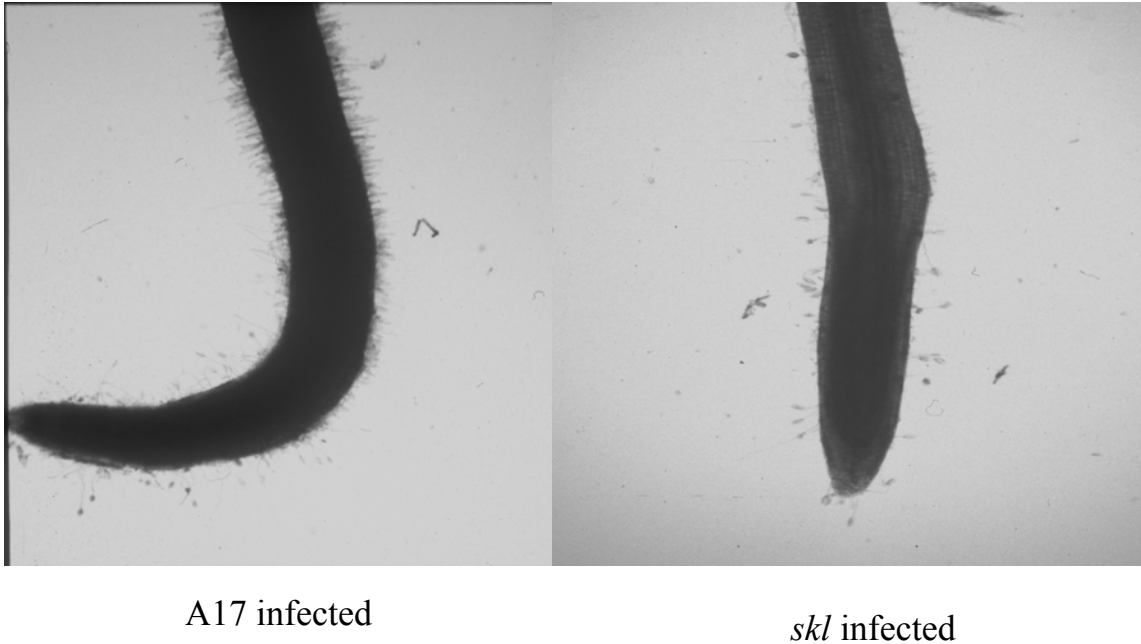


Fig. 13. *Medicago truncatula* roots infected with *P. medicaginis*. The microphotographs show the different physiological response of A17 and mutant plants 48 h after inoculation.

In addition, the effect of *P. medicaginis* inoculation on plant development was calculated by comparing the fresh weight of 10 inoculated plants against the initial weight of 10 non-inoculated control plants over a 36 h time course experiment. The results showed that *skl* stops developing after inoculation. A17 plants continued growing for at least one day before the pathogen-induced stress slowed growth (Fig. 14).

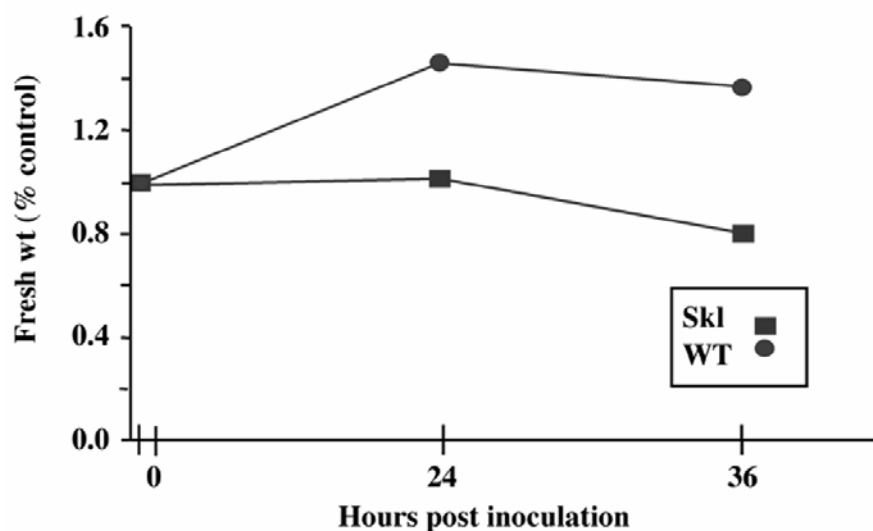


Fig. 14. Effect of *Phytophthora* infection on the development of *M. truncatula* seedlings. Data is the fresh weight of 10 inoculated plants against the initial weight of 10 non-inoculated control plants.

Infection of *M. truncatula skl* with *Pythium* sp.

The results of *P. ultimum* infection showed that this pathogen caused severe symptoms in *M. truncatula* seedlings. Observations of infected seedlings five days after inoculation demonstrated that 74% of the infected *M. truncatula skl* seedlings that germinated were completely macerated, and the remaining seedlings were severely affected and stunted. On the other hand, 68% of germinated A17 seeds were severely affected and stunted, while the remaining 32% of the seeds were dead and macerated. Non-inoculated controls showed between 92% and 100% germination and developed normally, free of infection.

Quantification of disease severity resulted in A17 plants with disease severity indexes (DSI) of 4.2, whereas *skl* plants were more severely infected, with DSI of 4.5 (Fig. 15). The statistical analysis of the two independently performed experiments

showed that in first instance the observed results were not statistically significant (Table 8). In this experiment, a sample size of 20 seeds per plate was used. The repetition of the experiment using a larger sample size (50 seeds/plate) gave statistically significant results that support the hypothesis of different disease susceptibility between A17 and *skl* seeds when infection by *P. ultimum* (Fig. 15 and Table 8).

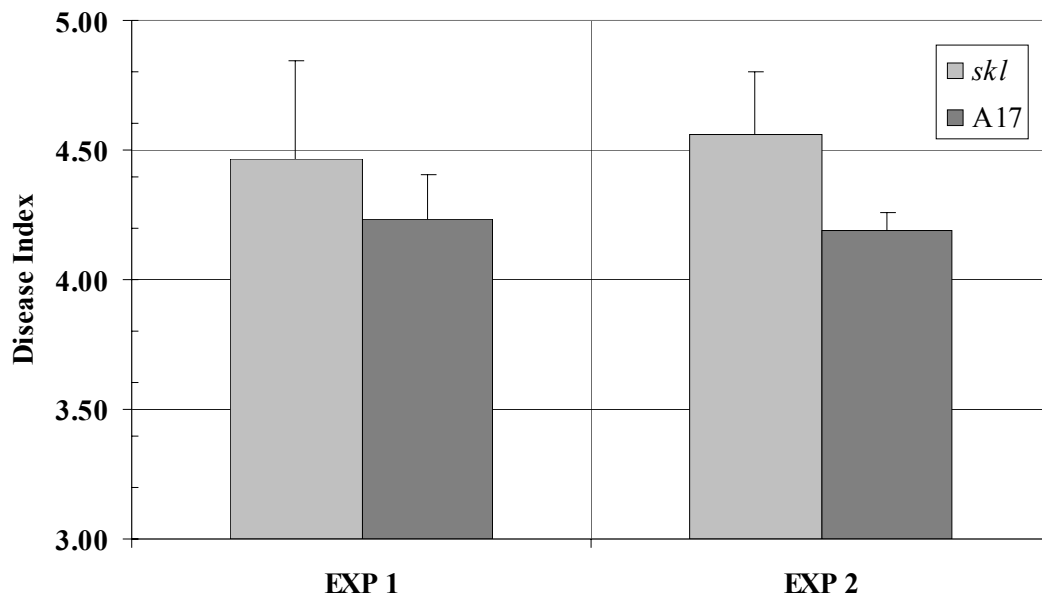


Fig. 15. Disease incidence in *M. truncatula* upon infection with *P. ultimum*. 50 seeds per genotype were planted on three day old, *Pythium* colonized water-agar dishes. Each experiment was replicated three times.

In the case of *P. irregulare* infection of *M. truncatula* seeds, the observations of diseased seedlings five days after inoculation showed that A17 seeds were able to germinate and to grow continuously. Mutant *skl* seeds also germinated, but several ulcer-type lesions covered the individual roots. The root tips of *skl* seedlings were dead

and swollen in most cases (data not shown). These results suggest that genotype A17 is moderately resistant to this pathogen.

TABLE 8. *sickle* resistance or susceptibility to *Pythium* sp.

		No. seeds	Average		P(T<=t)	$\alpha = 5\%$
			<i>skl</i>	A17		
<i>P. ultimum</i>	EXP 1 ^a	20	4.47	4.23	0.1923	No reject
	EXP 2 ^b	49	4.56	4.19	0.0313	Reject Ho
<i>P. irregularum</i>	EXP 1 ^a	21	2.93	2.26	0.0568	No reject
	EXP 2 ^b	51	2.88	2.01	0.0024	Reject Ho

Hypotheses tests using T student statistics were used to test the Ho hypothesis that *skl* and A17 are infected in the same way by *Pythium* sp. For the analysis an α of 5% with two degrees of freedom was used to find the rejection value and the associated probability. Data shown is the result of two independent experiments. a. Experiments labeled 1 were the result of three experimental replicates using 20 seeds. b. Experiments labeled 2 were the result of three experimental replicates using 50 seeds.

Quantification of disease severity indicated that A17 has a DSI of 2.14 when infected with this pathogen. *M. truncatula skl* seeds also showed a greater susceptibility to this pathogen with a DSI of 2.9 (Fig. 16). As in the case with *P. ultimum* infection of *M. truncatula* seeds, the results of statistical analysis of *P. irregularum* infection of A17 and *skl* seeds yielded results that in first instance were not statistically significant at the 95% confidence interval used. The repetition of the experiment using a larger sample size resulted in statistically significant differences between the average DSI for both genotypes (Fig. 16 and Table 8).

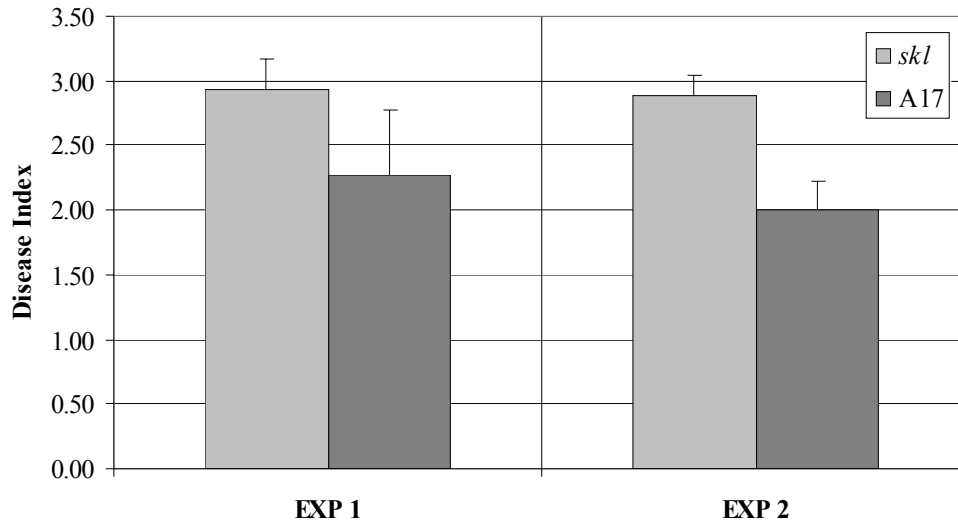


Fig. 16. Disease incidence in *M. truncatula* upon infection with *P. irregularum*. 50 seeds per ecotype were planted *Pythium* colonized water-agar dishes. Each experiment was replicated three times.

M. truncatula skl* Mutation Is Not Altered in Resistance to *C. trifolii

Data analysis (Table 9) showed that *M. truncatula skl* plants were not more susceptible than A17 when inoculated with this pathogen. Furthermore, both genotypes seemed highly resistant to infection. In the few cases where successful infections were observed, disease progression never occurred. To confirm pathogen colonization of the tissues, samples were taken to the plant diagnosis laboratory at Texas A&M University. Microscopical observation of infected leaves confirmed the presence of acervuli bearing the typical bi-celled conidia produced by this pathogen. The primary symptom observed in the plants consisted of localized necrotic spots on cotyledons and leaves. The spots were reminiscent of hypersensitive responses and localized cell death events.

TABLE 9. Disease incidence in *M. truncatula* A17 and *skl* plants after infection with *C. trifolii*.

		No. Plants	Cotyledons		Stem		Monofoliolate		Trifoliolate		Dead plants
			Spots	Chlorosis	Spots	Chlorosis	Spots	Chlorosis	Spots	Chlorosis	
A17	Control	58	0	5	0	0	1	0	5	0	0
	1	48	12	0	0	0	4	0	6	0	0
	2	46	0	0	0	0	0	0	2	0	0
	3	52	0	0	0	0	0	0	5	0	0
	Total	204	12	5	0	0	5	0	18	0	0
<i>skl</i>	Control	60	1	1	0	0	11	0	4	0	0
	1	58	0	0	0	0	5	0	10	0	0
	2	59	0	0	0	0	0	0	1	0	0
	3	58	1	1	0	0	0	0	2	0	0
	Total	235	2	2	0	0	16	0	17	0	0

A spore suspension of *C. trifolii* race 1, pathovar 2sp2 (7.2×10^5 /ml) was applied until runoff (± 3 ml) to the leaves of 60 two week old *M. truncatula* seedlings. Three replicates per genotype plus non-inoculated controls comprised the experimental set up. After inoculation the relative humidity inside the trays was kept around 100% for 48h. Plants were watered daily as needed and data was collected seven days after inoculation. Data presented corresponds to number of plants showing particular symptoms.

DISCUSSION

The understanding of plant-microbe interactions in model legumes has increased as a result of the development of tools for genetic and proteomic analysis (188). To understand the mechanisms of development of nitrogen fixing nodules in legume plants, several studies involving nodulation mutants have been published (11, 30, 54, 121-122, 146,148). These studies suggest that upon infection of symbiotic bacteria, the host responds with defense responses. In the case of *M. truncatula* plants exposed to *S. meliloti*, a mutation called *skl* that acts in the nitrogen fixation symbiotic program has been shown to control the number of bacterial infections leading to nitrogen fixation (140, 146). To understand *skl* mutation and gauge the breadth of its responses, *skl* mutant plants were exposed to pathogenic microorganisms.

The finding that *skl* is affected in its defense responses towards pathogens and also in its responses to symbiotic bacteria opens a window of opportunity to study the similarities between genetic control of infection by symbiotic and pathogenic

microorganisms. Because *skl* is a mutation that affects a gene in the ethylene signal transduction pathway, this research further supports the long known role of ethylene in plant defense responses towards pathogens (49-50, 55, 98, 149, 179). The results of this study suggest that *skl* can be used to classify defense responses of *M. truncatula* into ethylene-dependent and ethylene-independent categories. Although the role of ethylene perception in regulating infection by oomycetes and nitrogen fixing bacteria is clearly established, it remains uncertain if the downstream responses are also related.

The initial experiments with *P. medicaginis* were surprising not only because of *skl* hyper-infection, but also because of the speed of infection. The initial intention of the experiments was to follow disease symptoms over a three-week period, however, 10 days after inoculation maximum disease severity was recorded. The observed results have conclusively shown that the pathogen was able to complete its life cycle in *M. truncatula* plants. Microscopic observations of *skl* and A17 infected roots showed an increase in pathogen colonization in the mutant plant as expressed by the number of reproductive structures formed by the pathogen. The results also showed a faster progression of disease symptoms in *skl*-infected plants compared to A17 plants.

Microscopic examination of infected roots revealed the ease and speed at which *P. medicaginis* colonized the root surface in *skl* plants. In addition to the observed differences in pathogen reproduction and speed of colonization, subtle, un-quantified responses also appeared in A17 but not in *skl* plants. For example, it was observed that A17 plants that survived pathogen challenge developed secondary root growth. Development of secondary roots after pathogen inoculation was not observed in *skl* (Fig.

17). Similarly, A17 roots acquired patchy dark brown color 72 hours after inoculation, reminiscent of hypersensitive cell death events in the infected roots (Fig. 17). Vital stains could be used to test this hypothesis. Alternatively, methods to quantify and localize sources of production of reactive oxygen species (ROS) could have been used to further explore this possibility. In *Rhizobium–Medicago* interactions, ROS production has been observed during nodule development (37, 155) and involvement of ROS in defense responses to pathogens has been shown elsewhere (77, 104, 172). Another interesting parallel was the root hair deformation caused by *Phytophthora* infection (Fig. 18).

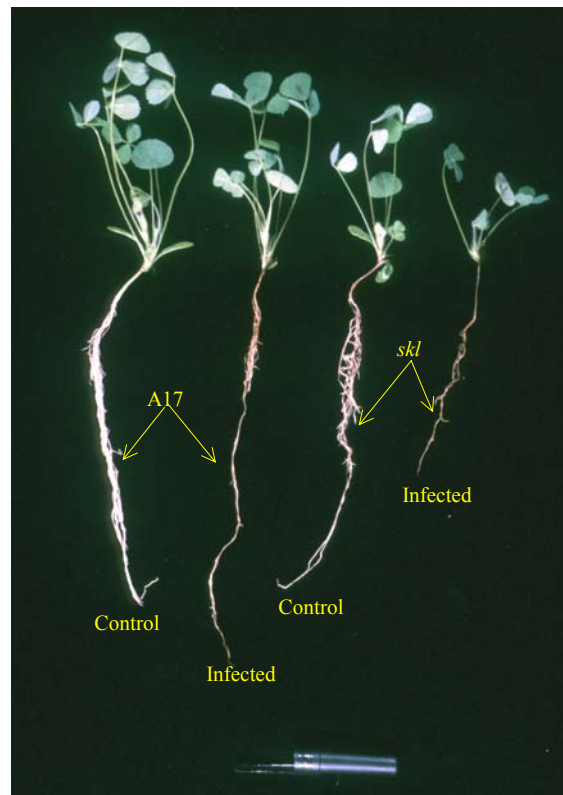


Fig. 17. Root damage caused by *P. medicaginis* infection of *M. truncatula* plants.

Root hair deformation is one of the earliest responses to rhizobial infection in legume plants and provides a point of entry for bacterial infection and subsequent nodule development (19, 143, 176). A third response comparable to *Rhizobium* inoculation of *M. truncatula* is the involvement of ethylene in the control of the defense response. In A17 *M. truncatula* seedlings, the use of ACC, the immediate precursor of ethylene, after infection with *S. meliloti* resulted in decreases in the number of symbiotic nodules, supporting a role of ethylene in controlling the persistence of symbiotic infections in this plant species. Exposure of *skl* seedlings to ACC did not result in reductions in nodule formation even at the high dose of 300 μ M (146). In a similar sense, an increase in the number of infections leading to nodule formation was observed in Aminoethoxy Vinyl Glycine (AVG)-treated hypo-nodulating pea plants (*Sym16*) exposed to *Rhizobium leguminosarum* bv. *Viciae* (78), AVG is an ethylene inhibitor. *Vicia sativa* and *Lotus japonicus* roots growing under light conditions produced high amounts of ethylene that correlated with arrestment of nodule formation in both species. Addition of AVG to the growing media restored their normal nodule development (186). *Phytophthora* infection of *M. truncatula* plants also resulted in ethylene production as shown in Fig. 12. Ethylene evolution in infected plants started with a small induction six hours after inoculation, followed by a second stronger burst 32 hours after inoculation. Although A17 plants showed the largest response, *skl* mutants also produced ethylene but in a lesser proportion.



Fig. 18. Root hair deformation caused by *P. medicaginis* infection of *M. truncatula* plants.

The recent identification of *skl* as a homologue of *A. thaliana* *EIN2* suggests that functional homology between both genes should be expected. *skl* mutation has the genetic background of A17 and has been backcrossed at least four times with its parental genotype to create a near isogenic line. The results presented here have shown that ethylene insensitivity in *skl* mutants translates into increased susceptibility when exposed to *P. medicaginis* and therefore provide the basis to prove such functional homology between *skl* and *ein2* genes. Extensive research has shown the involvement of *EIN2* in plant defense responses. For example, overexpression of *EIN2* in *A. thaliana* *ein2* plants has been shown to restore the induction of plant defense responsive genes like *PDF1* (8). *PDF1* is a marker for the induction of jasmonate-dependent defense responses (149). *A. thaliana* plants carrying a mutant *ein2* gene were shown to be more susceptible to *Botrytis cinerea* (179), *Pseudomonas syringae*, *Xanthomonas campestris* (181) and also to *Erwinia carotovora* (128).

Whereas most of these data are similar, conflicting results have been reported that suggest a minimal role for *ein2* mutation in the defense responses to *X. campestris* and *P. syringe* (20). Recently, Mauch-Mani (158) developed a pathosystem for infection of *A. thaliana* with *P. porri* noting that *ein2*, *etr1* and *jar1* mutants were not compromised in their resistance against this pathogen. *ETR1* codes for an ethylene receptor and its involvement in defense responses has been previously shown (21, 33, 49, 91, 171); *jar1* is a mutant impaired in JA production and its role in plant defense responses has been shown by different groups (17, 119, 189). Interestingly, according to Mauch-Mani (158), neither the destruction of salicylic acid (SA) in salicylate degrading mutants (*nahG*) nor the application of its functional analog, benzothiadiazol, in SA accumulating mutants was effective in preventing disease symptoms in susceptible *A. thaliana* plants infected with *P. porri*. The Mauch-Mani analysis raises questions about the role of ethylene, JA and SA in the resistance of this plant species to this pathogen and suggests a completely different control mechanism mediated by *pad4*, a phytoalexin deficient mutant previously characterized in *A. thaliana* (35, 49). The exploration of these findings in *M. truncatula* is a logical step to further understand *skl* mutation. An analysis of *pad4* homologues, based on the analysis of the *M. truncatula* EST database is was performed but it is not presented here.

Exposing *skl* mutants to the pathogens *C. trifolii*, *M. incognita* and *R. solani* revealed in no apparent increase in susceptibility. The experiment involving *C. trifolii* infection of *M. truncatula* plants showed a hypersensitive response in infected leaves that included localized cell death events. This result is consistent with proposed defense

mechanisms previously observed for resistant alfalfa (135). By contrast, results of infection of *M. truncatula* with *P. ultimum* or *P. irregularum* resulted in slight increase susceptibility of *skl* seedlings when compared to its parental genotype, the A17 plant.

The procedure for *P. ultimum* and *P. irregularum* infection of *M. truncatula* seeds exposes the experimental subjects directly to the pathogen in a non-natural way forcing the expression of resistance in the host if such is present. The North America Alfalfa Improvement Conference (NAAIC) has provided guides to clearly distinguish between *Pythium* sp. resistant and susceptible individuals in such a harsh environment. The guides are tailored to analyze alfalfa cultivars and therefore are adapted for the purpose of this study. The results of the analysis are based on statistical parameters that can be misleading if insufficient population size is used. This was the case with the initial DSI results of A17 and *skl* infection by *Pythium* sp. Collected data suggested that both genotypes respond in similar ways when infected by the pathogens. This assumption was later proved wrong when the same experiment was repeated with a greater sample size. Nonetheless, both of the trials resulted in higher susceptibility of *skl* genotype to infection by these pathogens.

CHAPTER IV
TRANSCRIPTION PROFILING OF GENE HOMOLOGUES IN
MEDICAGO TRUNCATULA

SUMMARY

Bona fide sequence information for proteins involved in phenyl propanoid metabolism, Salicylic Acid (SA) dependent resistance, Jasmonic Acid (JA)/ethylene dependent resistance and stress related metabolism were used in tblastn searches to screen the *Medicago truncatula* EST database for gene homologues. The search resulted in series of contigs sharing a high degree of homology with the query sequences. The EST makeup of each contig was analyzed and normalized to provide an *in silico* based representation of gene expression and to phylogenetically analyze the different gene families investigated. Lastly, the expression profiles of selected gene homologues were used to characterize the transcriptional responses of mutant and A17 *M. truncatula* plants upon infection with *P. medicaginis*. The results of the analysis showed that the *skl* mutant was affected in the generation of signals leading to ethylene production whereas A17 gene expression corroborated a bimodal pattern of ethylene production previously observed. Mutant plants also exhibited upregulation of genes involved in phytoalexin production, as well as stress-related Glutathione S Transferase (GST) proteins. These results suggest that *skl* impairment blocks the ethylene/jasmonate dependent defense response pathway, in agreement with its proposed homology to *Arabidopsis thaliana* ein2 protein.

INTRODUCTION

Medicago truncatula (barrel medic) is a model plant for genetic and physiological analyses in legumes. Research efforts involving *M. truncatula* have been facilitated by an increasing number of tools for genetic, genomic, metabolic, and proteomic analyses (38-39, 82, 141, 188). Among these, the development of Bacterial Artificial Chromosome libraries (BAC libraries) (28, D.R. Cook data not published) has allowed the cloning of important genes involved in symbiotic interactions with nitrogen fixing and mycorrhizal organisms. Random sequencing and fingerprinting of these BAC libraries, in addition to the use of fluorescent in-situ hybridization technologies, has led to the detection of euchromatic and heterochromatic regions of the genome (101, 188). These advances underlie the current effort to determine the sequence of the gene-rich chromosome arms of *M. truncatula* using a BAC-by-BAC strategy (188). Finally, dense genetic maps are providing anchoring points to markers developed in other, more complex legume species like alfalfa, pea, mung bean (*Vigna radiata*), and soybean (34).

Gene analysis in this species is also progressing rapidly, mainly because of the development of EST libraries. Currently, release 7.0 of the *Medicago* Gene Index (MTGI) database (<http://www.tigr.org/tdb/tgi/mtgi/>) contains 189,919 sequences, derived from 38 different cDNA libraries, each one representing a particular environmental or physiological condition (Table 10). The EST in the database have been clustered by sequence identity to create Tentative Contigs (TC), representing an estimated 36,976 unique genes. Of this number, 19,341 sequences are singletons, while 17,635 sequences form contigs of two or more EST.

TABLE 10. Index of DNA libraries used in the *Medicago truncatula* sequencing projects.

LIBRARY Name	TIGR cat#	DESCRIPTION
BNIR	T11031	EST from roots of <i>Medicago truncatula</i> after infection with the nematode <i>Meloidogyne incognita</i>
DSIL	T1748	EST from leaves of <i>Medicago truncatula</i> after inoculation with <i>Colletotrichum trifolii</i>
DSIR	T1581	EST from roots of <i>Medicago truncatula</i> after inoculation with <i>Phytophthora medicaginis</i>
DSLK	T10110	EST from <i>Medicago truncatula</i> leaves and cotyledons
GESD	T10494	EST from developing reproductive tissues (seeds) of <i>Medicago truncatula</i>
GLSD	T11127	EST from late seeds of <i>Medicago truncatula</i>
GPOD	T10493	EST from developing reproductive tissues (pod walls) of <i>Medicago truncatula</i>
GVN	T1617	EST from one month old nitrogen-fixing root nodules of <i>Medicago truncatula</i>
GVSN	T10109	EST from senescent nodules <i>Medicago truncatula</i>
HOGA	T10173	EST from roots of <i>Medicago truncatula</i> treated with oligogalacturonides of DP 6-20
Kiloclone	T10174	EST sequenced and arrayed in microarrays
KV0	T1815	EST from uninoculated seedling roots of <i>Medicago truncatula</i>
KV1	T1841	EST from roots of <i>Medicago truncatula</i> 24 hours after inoculation with <i>Sinorhizobium meliloti</i>
KV2	T1510	EST from roots of <i>Medicago truncatula</i> 48 hours after <i>Rhizobium</i> inoculation
KV3	T1707	EST from roots of <i>Medicago truncatula</i> 72 hours after <i>Rhizobium</i> inoculation
KVVC		EST of cDNA clones selected and re-arrayed from various libraries a.k.a. 1K set
MGHG	T10014	EST from seedling roots of <i>Medicago truncatula</i> after treatment with beta-glucan elicitor preparation from <i>Phytophthora sojae</i>
MHAM	T1682	EST from roots of <i>Medicago truncatula</i> after colonization with <i>Glomus versiforme</i>
MHRP-	T1840	EST from phosphate-starved roots of <i>Medicago truncatula</i>
MTUS		EST of cDNA clones selected and re-arrayed from various libraries. a.k.a. 6K set
MtBA	5518	EST from nitrogen-starved <i>Medicago truncatula</i> root tips
MtBB	5519	EST from <i>Medicago truncatula</i> root nodules
MtBC	5520	EST from roots of <i>Medicago truncatula</i> three weeks after colonization by the arbuscular mycorrhizal fungus <i>Glomus intraradices</i>
MtRHE	1032	EST from <i>Medicago truncatula</i> root hairs and tips
MTAMP		EST from <i>Medicago truncatula</i> mycorrhizal roots inoculated with <i>Glomus intraradices</i>
MTFLOW		EST from <i>Medicago truncatula</i> flowers
MTGIM		EST from <i>Medicago truncatula</i> mycorrhizal roots inoculated with <i>Glomus intraradices</i> subtracted library
MTPOSE		EST from <i>Medicago truncatula</i> pods with seeds
Drought	5413	EST from entire plantlets harvested in a series of days-post-watering time points
Elicited cell cult e	7263	EST from root tissue derived cell cultures
Develop flower	#9D5	EST from pooled <i>Medicago truncatula</i> flowers
Germinating seed	#9D6	EST from <i>Medicago truncatula</i> germinating seeds
Insect herbivory	5414	EST from mature, local and systemic leaves
Irradiated	#9D7	EST from UV and gamma irradiated <i>Medicago truncatula</i> 21-day old seedlings
Developing leaf	4046	EST from a mixture of very young, developing, mature and senescing leaves
Nodulated root	4047	EST from four-week old <i>Rhizobium meliloti</i> inoculated <i>Medicago truncatula</i> roots
Phoma-infected	#A8V	EST from <i>Phoma medicaginis</i> -inoculated leaves of <i>Medicago truncatula</i>
P starved leaf	5415	EST from leaf of phosphate starved <i>Medicago truncatula</i>
Developing root	4048	EST from non-nodulated roots of <i>Medicago truncatula</i> plants grown in nitrate m medium
Developing stem	4049	EST from a mixture of internodal stem segments
R108Mt	2764	EST from <i>Medicago truncatula</i> symbiotic root nodule

The unigene set underlies the recent development of oligonucleotide and cDNA microarrays for gene expression analyses. Ethyl MethaneSulfonate (EMS) mutagenesis and fast neutron mutagenesis are being used to generate plants altered in developmental or physiological responses (147, 188). The analysis of these mutant populations is allowing the characterization of different signal transduction and developmental pathways in this species. Because of the importance of symbiotic nitrogen fixation in agriculture, much of the effort has focused on responses to *Sinorhizobium meliloti* and *Glomus* sp., the natural nitrogen fixing and mycorrhizal symbionts of this plant species. Nonetheless, research on defense responses, host plant and human nutrition, and plant development is progressing steadily as well.

Nodulation screens on *M. truncatula* plants have allowed the isolation of individuals affected in the control and position of nitrogen fixing nodules (148). One of these mutants was found to be insensitive to the plant hormone ethylene. This mutation, called *sickle* (*skl*), was linked to control of the persistence of *Rhizobium* infections in roots, and, therefore, regulation of the number of symbiotic nodules allowed to develop and mature (140, 146, 148). Further analysis of *skl* led to the discovery that defense responses were also hampered in this mutant. Mutant plants were shown to be hypersusceptible to oomycete pathogens, but not to true fungi like *Colletotrichum trifolii* or *Rhizoctonia solani* (see Chapters II and III). In order to further study the role of *skl* mutation, EST information contained in MTGI was used to search for homologues of genes involved in plant defense responses. The extensive search included gene members of pathways that lead to the production of pathogenesis-related proteins (PR proteins),

phytoalexins, ethylene, reactive oxygen species and other stress related proteins. Landmark genes involved in systemic acquired resistance and jasmonate dependent resistance were also sought. A full index of the different genes sought inside the database is presented in Table 11.

TABLE 11. List of gene homologues searched within MTGI.

PATHWAY	GENES	PARALOGUES in MTGI	TARGET for Gene Expression
Ethylene Biosynthesis	<i>Acc Oxidase</i>	5	2
	<i>Acc Synthase</i>	5	0
Ethylene Signal Transduction	<i>ETR1</i>	3	0
	<i>CTR1</i>	2	0
	<i>EIN3</i>	2	0
Pathogen Defense Pathways	<i>EIN2/ Sickle</i>	3	0
	<i>PAD4/EDS1</i>	4	0
	<i>NPR1</i>	3	0
	<i>PR1</i>	7	0
	<i>PR2</i>	6	0
Phenyl Propanoid Metabolism	<i>PR10</i>	3	1
	<i>NDR1/HIN1</i>	3	0
	<i>Lipoxygenase</i>	8	0
	<i>PAL</i>	5	1
	<i>IFR</i>	7	1
Housekeeping Genes and Others	<i>CHS</i>	10	2
	<i>GST</i>	28	2
	<i>Actin</i>	5	1
	<i>Histone H3</i>	12	1

In most of the cases, unique patterns of gene expression were identified, leading to a situation where certain transcripts can serve as "signatures" of pathway activation. The results of this analysis constitute the first half of the current chapter. In the second half, the close homologues of these "signature" genes in *Medicago* serve as the basis of gene transcription studies of the responses of A17 and mutant *M. truncatula* to infection by *P. medicaginis*.

For the EST analysis of *M. truncatula* homologues, bona fide sequence information available in this or other legume species was used as basis for comparison in tblastn searches. When this information was not available for *M. truncatula* or other closely related legume species, gene models developed in distant species like *Arabidopsis thaliana* and *Lycopersicon esculentum* were used. TC with high homology to the query sequence (Table 11) were tabulated into gene families, adjusted for inconsistencies (i.e. sequencing errors, frame shifts, etc), aligned and phylogenetically analyzed. Lastly, TC were further studied based on their EST makeup to obtain a tentative representation of the degree and conditions of expression of each sequence.

With the purpose of finding the onset and duration of expression of genes related with plant defense responses, transcription analysis of gene homologues found through the EST analysis was performed on mRNA isolated from healthy and *P. medicaginis* infected *skl* plants and compared against healthy and *P. medicaginis* infected A17 plants. Transcription profiles of candidate genes were created by time course experiments using real time RTPCR. The gene homologues analyzed in this way were: Gluthatione S Transferases (*GST*) as a stress induced gene; *ACC oxidase*, an enzyme in the ethylene biosynthesis pathway; CHalcone Synthase (*CHS*), IsoFlavone Reductase (*IFR*) and Phenylalanine Ammonia Lyase (*PAL*), important enzymes in the phenyl-propanoid metabolism; and *PR10*, a gene induced by JA and ethylene. The constitutive expressed genes *Histone H3* and *actin* were used as internal controls for the analysis.

Pathways for Defense Responses in Plants

The majority of characterized plant disease resistance phenotypes can be accounted for based on three different signaling pathways: (1) Systemic Acquired Resistance (SAR), (2) Jasmonate/ethylene dependent resistance, and (3) SA/JA/Ethylene independent resistance (50, 102, 104, 160, 167).

In SAR, for example, genes that belong to the phenylpropanoid pathway are often induced. Flavonoid compounds are implicated in stress responses towards a variety of stimuli including high light/uv, wounding, low temperatures, low nitrogen, low phosphorus, low iron, and pathogen attack (46-48, 81). PAL, the first enzyme in the pathway, catalyzes the production of cinnamic acid from the phenylalanine. Cinnamic acid serves as the basic skeleton for several phenylpropanoid derivatives including lignin, coumarin and SA via a series of methylation, hydroxylation and dehydration reactions. These reactions include the condensation reaction of p-coumaroyl-Coenzyme A (CoA) with three molecules of malonyl-CoA, which yields in most species tetrahydroxychalcone. This C₁₅ flavonoid compound can be converted into flavones, flavanones, flavanols and anthocyanins (46). The key enzyme is CHS, which, in conjunction with Chalcone Reductase (CHR) produces trihydroxychalcone. This compound is rearranged by isoflavone synthase to allow the accumulation of several kinds of isoflavonoids. Among them, the main alfalfa phytoalexin medicarpin, is produced after a committed step mediated by IFR. PAL, IFR and CHS were targeted for gene expression analysis in this research. Other stress responses, and in particular detoxification processes, are mediated by enzymes such as Glutathione S transferases.

GST comprises a very large family of proteins with members in all higher organisms. Two GST homologues were studied in transcriptional profiling experiments. SAR induces the expression of some PR protein genes by means of W-boxes located in the promoter regions of the genes. W-boxes are activation targets for a plant-specific class of transcription factors called the WRKY transcription factors (49, 58, 159). Pathogenesis related proteins comprise at least nine families. Among them, PR1 encodes an antifungal protein and perhaps is the most studied protein of this group. Pathogenesis related protein 2 (PR2) and PR3 encode β -1,3-glucanase and chitinase, respectively, and are implicated in the degradation of pathogen cell walls and the production of oligosaccharide elicitors of defense responses. Pathogenesis related protein 4 (PR4) and PR5 code for havein-like and thaumatin-like proteins, antifungal and protein inhibitor compounds, respectively. Finally, PR10 homologues encode small peptides that have been involved with allergic reactions. Pathogenesis related protein 10 (PR10_ is constitutively expressed in *Medicago* nodules, but its role in defense responses has not been clarified yet. For SAR mediated resistance, PR1 and PR2 are considered markers for induction of the pathway (160). For further analysis, PR10 was chosen.

A completely separate plant defense response is mediated by JA and ethylene. The wound response to insects is an example of this response. Upon insect injury, JA accumulation causes the induction of genes for proteinase inhibitors, systemin, THionin (*Thi2.1*) and defensin (*PDF1.2*), which act together to deter insect feeding. Jasmonates are produced through the octadecanoic pathway from cyclopentanone derivatives.

Several enzymes mediate JA biosynthesis, and among these, the LipOXigenases (LOX) comprise an important gene family in which most homologues are correspondingly activated upon insect injury. Jasmonates regulate, among others, plant growth, plant defense responses, and development (52-53, 161, 184).

Jasmonic acid is believed to act through a mechanism involving a MAPK named WIPK (wound induced protein kinase) (49, 167). Interestingly, transgenic tobacco plants that lack WIPK function accumulated SA and PR1, compounds associated with SAR, suggesting a regulatory switch where wound-induced JA suppresses SA-dependent signaling (184). One of the marker genes for JA induction of defense responses is COroinine Insensitive *COII*, which regulates stamen and pollen development in *A. thaliana* (63, 193) and when expressed together with *JARI*, a JA-inducible gene (172), also regulates defense responses (75-76).

Ethylene insensitivity also affects defense responses. This hormone is synthesized in two rapid steps mediated by ACC Synthase (ACS) and ACC Oxidase (ACO) upon pathogen challenge, wounding, and other stress responses. Examples of ethylene involvement in disease resistance include transgenic tobacco expressing a nonfunctional *etr1* (98) and the requirement for ethylene during disease resistance that was observed in *Arabidopsis* plants carrying a defective *ein2* gene. In the latter case, these plants showed increased susceptibility to *Botrytis cinerea* (98,178). Transcription factors known to respond to JA have similarity to ethylene responsive factors (ERF), suggesting commonalities for the regulation of these two hormones, perhaps via *EIN2* dependent or independent pathways (174, 184). Further confirmation of the interactions

of the two pathways comes from the analysis of mutant plants constitutively responding to ethylene (*ctr1*) after treatment with JA (103, 184).

Real Time PCR Analysis of Gene Expression

Polymerase Chain Reaction (PCR) is a technology that allows the perpetual amplification of nucleic acid sequences under controlled circumstances and has revolutionized the scientific field for the past 20 years. Multiple variations have been designed since the early 1980's, when it was introduced, and among them, real time reverse transcription PCR achieves the visualization and analysis of gene products in real time during the progression of the PCR amplification reaction (85).

Real time PCR detection of amplification products is based on compounds that attach or intercalate with the target molecule and in the process generate a signal that reports the progression of the reaction. Different chemistries are available for the detection of PCR products, including intercalating compounds such as Sybr green or ethidium bromide, hybridization probes, molecular beacons, and hydrolysis probes (26-27). In the studies described here Taqman™ probes were used to quantify the expression of transcripts involved in plant defense resistance.

The Taqman™ system is based on the hydrolysis of a fluorescent probe during the DNA replication. Probe hydrolysis, which is accomplished by the 5' exonuclease activity of Taq DNA polymerase, results in an increase in fluorescent signal that is directly proportional to the quantity of the complementary amplicon (79). The fact that the probe is complementary to the amplified product simultaneously improves the specificity of the reaction and facilitates the quantification of the PCR product (26, 85).

The 5' ends of Taqman™ probes have a fluorescent moiety, while the 3' end has a corresponding quenching moiety. Quenching is highly efficient as long as the proximity of the fluorescent molecule and the quenching molecule are maintained. Upon annealing to a complementary amplicon, however, the exonuclease activity of Taq polymerase destroys the probe and releases the fluorescent molecule into solution. The reporter system, typically a camera or a plate reader attached to the PCR machine, detects and quantifies the fluorescent signal, which increases as the amount of replicated nucleic acid increases (26, 72, 74, 85).

During the exponential phase of the PCR reaction, the mathematical expression for a straight line provides an estimate of the amount of template inside the experimental sample (72, 85). This expression correlates the amount of template with the amplification cycle of the PCR. A user-defined threshold is used to distinguish background from true fluorescence and standard curves can be used to calculate initial template concentrations (72, 85).

MATERIALS AND METHODS

P. medicaginis* Infection of *M. truncatula

The protocols for growing *M. truncatula* A17 and *skl* seedlings used in the experiments were described in the previous chapters and were based on the procedures of Cook et al. (37) (Chapter II and III). The experimental plants were grown inside aeroponic tanks Cook et al. (37). The nutrient medium used to grow the plants was that

of Lullien et al. (113). Stock solutions were prepared separately and autoclaved for 20 min, 115°C, and 20 in Hg.

P. medicaginis isolate M2019 provided by D. Samac (USDA ARS- Plant Science Research Unit, St. Paul, MN) was used for the experiments. Zoospore production in this pathogen was induced following the protocol by Maxwell et al. (120) Zoospore suspensions were poured out of the Petri dishes, quantified using hemacytometers and adjusted to 1.5×10^5 zoospores/ml. Infection of *M. truncatula* 2-week-old seedlings was achieved by submerging the roots of the experimental samples into the quantified zoospore suspension, according to the protocols used in Chapter III. Non-inoculated seedlings were mock treated in the same way as presented in Chapter III. Ten plants (one bunch) per genotype (A17 or *skl*) and treatment (*P. medicaginis* infected or mock infected) were sequentially removed from the tank at 0, 2, 6, 12, 24, 32, 48, 72 and 96 h after inoculation. An absolute mock-infected experimental point was taken before exposing the plants to *P. medicaginis*. The time point 0h corresponded to the time when the plants were returned to the tanks after 2 hours of exposure to the pathogen. Experimental samples were frozen in liquid nitrogen and stored at -80°C for later processing and examination. The experiment was repeated two times.

In silico Analysis of Candidate Gene Families

Blast search of candidate genes

M. truncatula EST and TC sequences (154) were accessed through The Institute of Genomic Research (TIGR). *A. thaliana* gene homologue sequences for the

phylogenetic analysis of the different proteins were obtained from the *A. thaliana* sequencing project, which was accessed through The Institute of Genome Research (TIGR). *M. sativa*, *Pisum sativum* and *Glycine max* sequences were retrieved from TIGR and also from the databases that belong to the National Center for Bioinformatics Information (NCBI).

Using bona fide gene information publicly available at NCBI, Basic Local Alignment Search Tools (BLAST) searches were used to query the *M. truncatula* EST database located at TIGR (<http://www.tigr.org/tdb/tgi/mtgi>) (Table 11). To do so, protein information for each of the proposed genes was used as query template against the TIGR non-redundant *M. truncatula* nucleotide database dynamically translated in all six possible reading frames (tblastn). The search results consisted of a series of tentative contigs with variable degrees of relatedness (% of similarity and identity) to the query sequence. Each hit in the database has an associated "expect" value (e-value) representing the likelihood of chance occurrence in a data set of a given size. Therefore, the smaller the e-value the more similar the sequences are. In order to confirm the putative identity of each blast search hit, the nucleotide sequence corresponding to the protein-coding region of each blast search contig hit was used as query template against the non-redundant protein database at NCBI using the tblastx tool at NCBI. Those sequences found to represent anything different than what was expected were removed from analysis.

In silico inference of gene expression

The EST makeup of each tentative contig found by the tblastn search was tabulated according to the library from which its members were sequenced. Data was organized in spreadsheets using Microsoft Excel and used to create plots to show for each TC the corresponding distribution of EST, based on the library of origin. The data was normalized by dividing the corresponding number of sequenced EST coding for a particular contig within each library by the total number of EST present in the corresponding libraries.

Homologue sequence, alignment and analysis

Sequences were trimmed and corrected for mistakes using DNA strider. Multiple sequence alignments for the different protein homologues investigated were performed using ClustalX software (180). Protein trees were created using ClustalX and PAUP software. Distance methods (neighbor joining [162]) for phylogenetic analysis were used at all times and bootstrap analyses based on 1000 iterations of the data, with correction for multiple substitutions were done to evaluate the consistency of the results.

RNA Isolation and Reverse Transcription

RNA from infected and non-infected tissues was isolated using the Qiagen RNeasy mini isolation kit, following manufacturer's instructions. The RNA for analysis was DNase digested and quantified by spectrometer. Total RNA was converted into cDNA by reverse transcription using oligo dT primers. Two μg of total RNA/experimental sample were reverse transcribed using the reagents and protocols

provided by the Taqman™ RTPCR kit (Applied Biosystems, Foster City CA) and shown in the following table:

TABLE 12. Reverse transcription conditions.

Reagent	Working Concentration
Template	2 µg
RT Buffer 10X	1X
25mM MgCl ₂	5.5 mM
dNTPmix (2.5mM each)	500 µM each
50 µM Oligo d(T) ₁₆	2.5 µM
RNase inhibitor (20Unit/µl)	0.4 Units/µl
Multiscribe Reverse transcriptase (50 unit/µl)	1.25 Units/µl
RNase free H ₂ O	Adjust volume

Reaction conditions used were: 10 min at 25°C, 30 min at 48°C and 5 min at 95°C. Reaction tubes without template and without reverse transcriptase were included for control purposes. After the reverse transcription reaction, aliquots (10µl each) of the different RTPCR products were prepared and stored at -20°C freezer for later use and analysis.

Real Time Reverse Transcription PCR

Taqman™ chemistry was employed to perform the amplification of the different transcripts under analysis. The real time PCR machine used for the analysis was the I-cycler from Bio-Rad laboratories, Hercules, CA. This thermal cycler contains a 96 well block to which a high-resolution camera is attached. The system, which uses a tungsten halogen lamp with light filters and mirrors, provides and collects the narrow wavelength

range desired for the optimum excitation and emission fluorescence of the reporter molecules during the reaction. Computer software synchronizes the detection system with the PCR machine during the PCR reaction and, at desired intervals (once every cycle in this case), collects as many pictures as it can of the PCR samples during an allocated user defined time frame. In this case, the time frame for data collection was set to correspond to the first 10 s of the amplification stage of the PCR protocol. During data collection, a graph that relates the average intensity of each sample point with the amplification cycle of the PCR protocol is created by the software and automatically updated until the protocol ends. Once the data is complete, subtraction of the background fluorescence of the system from the raw data is performed to achieve the true amplification plot of the material under quantification.

Primer and probe design

The primers and probes used in this analysis were created using the Primer Express software (Applied Biosystems Foster City, CA). Primers had an annealing temperature of 60°C and were typically 20-24 bp long. According to Taqman™ guidelines, the reporter probes were designed to anneal between the amplification primers and to hybridize to the template at 70°C. The probes had modifications in each of their ends. In the case of target genes, the 5' end was modified with the fluorescent 6-FAM, while the 3' end of target probes had any of the following quenchers attached: DABCYL, BHQ1 or TAMRA. For the internal control genes, the 5' end of the probe was modified with HEX or Texas Red and as quenchers on the 3' end of the oligonucleotides, DABCYL, BHQ1 or TAMRA were used. Tables 13-15 show the

details of the primer and probe sequences used, their positions in the template for amplification and the modifications used. When possible, the primers were designed to span intron sequences of the genes.

Reaction conditions

All the amplification primers and probes were designed to anneal almost at the same temperature with the purpose of having a uniform set of conditions for PCR amplification. PCR conditions for the experimental runs consisted of equal annealing and extension temperatures, plus the required denaturing temperature.

To set up the reactions, Universal Master Mix Real Time PCR reagent kits (Applied Biosystems, Foster City, CA) containing the amplification buffer, MgCl₂, dNTPs, UNG glycosylase (amp erase) and TAQ gold polymerase were used to minimize pipetting errors. Reaction mixes were created by adding to aliquots of the master mix, the necessary internal and target control primers and probe. Experimental and control cDNAs were aliquoted in triplicate and measured aliquots of reaction mixes were added to each of them. After careful mixing, the reagents were distributed in 96 well dishes and the reaction volume in each well was set to 20µl.

Each PCR reaction contained five cDNA standards corresponding to 50, 10, 2, 0.4, and 0.08 ng/µl of total RNA in triplicate samples, plus 10 experimental templates (-2, 0, 2, 6, 12, 24, 32, 48, 72 and 96 h post inoculation) also in triplicate. Reaction tubes without template and without reverse transcriptase were included for control purposes (one each/time point).

TABLE 13. Forward primers used for transcription profiling analysis.

TARGET GENE	MTGI # and Primer name	Start	FORWARD PRIMER			AMPLICON		
			Sequence 5'-3'	Length (bp)	Tm Primer (°C)	cDNA (bp)	Tm (°C)	Genomic (bp)
Histone H3 ^a	TC85197	180	GCT CTT GAT CAG GAA GCT CCC	21	59	107	80	241
	TC6823	373	GGA ATC TCA GAT CCG TCT TGA AA	23	58	73	78	191
Actin	TC85697	184	GGA GAC AGC CAG GAC CAG C	19	59	121	81	121
Acc Oxidase	TC85664	211	CCA AAG GGC TAG AGG CTG TTC	21	59	76	80	76
	TC85507	475	GTT AGT AAC TAC CCT CCT TGT CCT AAG C	28	59	81	79	81
PAL	TC35727	620	CAT TGC CGG TTT ATT AAC GGG	21	60	101	n/a	101
CHS	TC76765	566	TTT GTT CTG AAG TCA CCG CTG TC	23	60	114	79	114
	TC85138	480	CAA CAA GGT TGC TTT GCA GGA	21	60	118	n/a	118
IFR	TC85477	546	TCC TCG GGA TAA AGT TGT CAT TC	23	58	107	77	200
GST	TC78052	287	CCT TGG CTC GTT TTT GGT CTA A	22	59	101	n/a	489
	TC85451	541	AAG TTC ATT GCT TGG GCC AA	20	59	82	n/a	82
PR10	TC76513	320	GGC CAG ATG GAG GAT CCA TT	20	60	117	n/a	117

Primers were designed using Primer Express software (Applied Biosystems). Sequence information for the different genes was retrieved from MTGI and corrected for mistakes. The open reading frame containing the protein sequence of interest was used as template for finding the primers.

^a HisH3 primer TC6823, was initially designed using MTGI release 2. This sequence was later found to be chimeric in release four of MTGI. Therefore primer TC85197 was created.

TABLE 14. Probes used in the analysis.

TARGET GENE	MTGI # and primer name	Start	PROBE ^b		Length (bp)	T _m (°C)
			Sequence 5'-3'			
Histone H3 ^a	TC85197	236	(TxRED) TCA AGA CTG ACC TTC GTT TCC AGA GCC AT (DABCYL)		29	69
	TC 6823	398	(TxRED) TTG AGC AAT TTC ACG GAC AAG ACG CTG (DABCYL)		27	69
Actin	TC85697	252	(TxRED) TCG GAG ACG AGC GTT TCA GAT GTC CA (DABCYL)		26	69
			(HEX) TCG GAG ACG AGC GTT TCA GAT GTC CA (BHQ2)			
Acc Oxidase	TC85664	233	(6-FAM) AAC TGA GGT CAA AGA CAT GGA CTG GGA GAG T (DABCYL)		31	68
	TC85507	504	(6-FAM) TGA TCT CAT CAA GGG ACT TAG AGC ACA CAC A (DABCYL)		31	68
PAL	TC85501	652	(6-FAM) CTA AAG CCG TTG GAC CGT CTG GAG AAA TTC T (BHQ-1)		31	70
			(6-FAM) CTA AAG CCG TTG GAC CGT CTG GAG AAA TTC T (DABCYL)			
CHS	TC76765	612	(6-FAM) TCA CTT GGA CAG TCT TGT TGG ACA AGC ACT ATT T (TAMRA)		34	69
	TC85138	521	(6-FAM) TCA CTT GGA CAG TCT TGT TGG ACA AGC ACT ATT T (BHQ-1)			
IFR	TC85477	596	(6-FAM) TAA AGA TTT AGC TGA AAA CAA CAA AGG TGC TCG TG (TAMRA)		32	70
	TC85477	596	(6-FAM) ATG TCA CTG AGG CTG ATG TTG GGA CTT TTA CC (DABCYL)			
GST	TC78052	327	(6-FAM) TTT GCC TGC AAT ATG GAA TGC TTG TTG GAG T (BHQ-1)		31	71
	TC85451	565	(6-FAM) TTT GCC TGC AAT ATG GAA TGC TTG TTG GAG T (DABCYL)			
PR10	TC85451	565	(6-FAM) TGC ATG CAG GTT GAG AGT ATT TCC AAG TCA C (DABCYL)		31	69
	TC76513	377	(6-FAM) CTG CAC CTA GTG AG AGG AAA TCA AGG GTG G (DABCYL)			

Primers were designed using Primer Express software (Applied Biosystems). Sequence information for the different genes was retrieved from MTGI and corrected for mistakes. The open reading frame containing the protein sequence of interest was used as template for finding the primers.

^a HisH3 primer TC6823, was initially designed using MTGI release 2. This sequence was later found to be chimeric in release four of MTGI. Therefore primer TC85197 was created.

^b The probes were designed using the Primer Express software. In some cases a different combination of reporter and quencher were used for standardization purposes and preliminary experimentation.

TABLE 15. Reverse primers used in the analysis.

TARGET GENE	MTGI # and primer name	Start	REVERSE PRIMER		Length (bp)	Tm (°C)
			Sequence 5'-3'			
Histone H3 ^a	TC85197	286	CCT CTT GCA ATG CAA GCA CA		20	60
	TC6823	445	TTG ATC CGC AAG CTT CCA TT		20	59
Actin	TC85697	304	TAT CAT AGA TGG TTG GAA CAG GAC C		25	59
	TC85664	286	GGT AGG TGA CGC AAA TGG AAA		21	59
Acc Oxidase	TC85507	555	AAG GAT GAT GCC ACC AGC AT		20	59
	TC85501	720	AAC CAA TGC CAG CAA GTT GAA		21	59
PAL	TC76765	685	CAG AGC CAA CAA TAA GAG CAG CA		23	60
	TC85138	598	CCG CGA AAT GTG ACT GCA G		19	58
IFR	TC85477	652	TGT TGG GAT CAT TTG CTG CTT		21	59
	TC78052	387	CTC CAC AGC TTT CTC ACG TCC		21	59
GST	TC85451	622	AGC CAT ACA CCT TAT CTT GAT CAG G		25	59
	TC76513	436	CCT TGA AAA GAC CAT CAC CCC		21	59

Primers were designed using Primer Express software (Applied Biosystems). Sequence information for the different genes was retrieved from MTGI and corrected for mistakes. The open reading frame containing the protein sequence of interest was used as template for finding the primers.

^a HisH3 primer TC6823, was initially designed using MTGI release 2. This sequence was later found to be chimeric in release four of MTGI. Therefore primer TC85197 was created.

Reactions for each of the genotypes under experimentation (A17 and *skl*, infected and mock-infected) were set up and at least 2 independent runs for each target gene were run. The experimental setup was repeated for each set of infected tissue available (see methods above) and for each gene under quantification. The PCR settings used were: Initial UNG glycosilase incubation 2 min at 50°C; initial denaturation, activation of TAQ gold Polymerase: 8 min at 95°C; 40 cycles of 95°C for 20 s, and 60°C for 1 min; final hold at 4°C. The concentrations of reagents used for analysis are presented in Table 16:

TABLE 16. Concentrations of reagents used for analysis.

Reagent	Working Concentration
Template	1 μ l
Taqman™ Buffer A	1X
25mM MgCl ₂	5.5mM
dNTP (A,10mM,C, 10mM ,G, 10mM, U,20mM)	500 μ M each
Amp Erase (1 unit/ μ l)	0.1 units / reaction
TAQ Gold Polymerase (1u/ μ l)	0.05 Units/ reaction
Target and control primers and probes ^a	Varied
RNAse free H ₂ O	Adjust volume to 20 μ l

^a Stock primers and probes were adjusted to 100 pM with Tris-EDTA pH 8.0 made with DEPC treated H₂O. Working solutions were prepared from the stocks at a concentration of 10pM in RNAse Free H₂O and used in a range that varied from 200nM to 600nM based on the results of preliminary assays that yielded the optimum concentration of primers and probes for multiplex amplification of target and control genes.

Methods for data analysis

The method used for quantification of real time PCR data was the comparative cycle threshold (Ct) method ($2^{-\Delta\Delta Ct}$ method) (112). The method provides the relative quantification of a target molecule to the amount of a user defined calibrator (Time 0,

noninoculated A17 samples in this case) and normalized to the amount of a reference molecule (histone H3 or actin). A user defined threshold cycle (Ct) is set to record the cycle number during the PCR amplification protocol at which the signal representing amplified target and reference molecules surpasses an arbitrary value or threshold that differentiates between background and true fluorescence. This threshold is usually set as 10x the standard deviation of the background fluorescence of the system, but can be as low as 3x the standard deviation of the background fluorescence (72, 85). The calibrator is a user-defined sample which Ct value is used as norm to compare the rest of the samples (72, 85, 112).

For each experimental sample, the Ct for target and reference molecules were calculated. To normalize the data, the difference in the Ct of the target and the Ct of the reference, called ΔCt was calculated. The next step was to subtract the ΔCt of each sample from the ΔCt of the calibrator to find the $\Delta\Delta\text{Ct}$ value. Finally, the amount of target normalized to an internal reference and relative to a calibrator sample was calculated by $2^{-\Delta\Delta\text{Ct}}$. Experimental data was expressed as fold change relative to the calibrator. The derivation of the formula is presented in the Appendix.

In order for the method to be valid, the efficiency of target amplification and reference amplification must be similar. This hypothesis was proven by looking at how ΔCt of target and reference molecules changed with template dilution. If the amplification efficiency of both molecules was similar, the absolute value of the slope of log input amount of template vs. ΔCt was expected to be less than 0.1. Therefore, for each of the experiments involving quantification by real time PCR, this validation

experiment was performed (Applied Biosystems User Bulletin #2 or Livak et al. [112]). In the cases that the validation experiment resulted in values above 0.1, absolute quantification of target concentration based on the extrapolation of experimental data from the standards run was used. In those cases, the extrapolated concentration was used to calculate the fold change relative to the initial concentration of the calibrator.

RESULTS

In silico Analysis of Candidate Gene Families

Ethylene biosynthesis pathway homologues

The search for *ACC oxidase* homologues yielded five hits with e^{-} values ranging from 2.1×10^{-71} to 8.8×10^{-133} . The search was done using *ACC oxidase* from *Arabidopsis* (gi: 20141261) as the query. The top 3 hits, TC85507, TC85665, and TC85664, all have high conservation, being 86, 89, and 87 percent similar and 74 percent identical to the query sequence. The three sequences were colinear with the full sequence of the query protein. TC85507 has 154 EST; TC85665 has 27 EST and TC85664 has 44 EST. cDNA library expression analyses showed that *ACC oxidase* was expressed under most conditions and tissues (Fig. 19). The comparison of patterns for TC85507 and TC85664 revealed that TC85507 was heavily induced in the yeast elicited cell culture library (70 EST), while TC85664 only had 1 EST sequenced from this library. A similar pattern was observed upon comparison of the number of EST found for both contigs in roots treated with either beta-glucan or oligogalacturonide elicitors. Symbiotic interaction libraries showed further interesting contrasts. For example,

TC85664 was found at all times during the early developmental stages of the nitrogen fixation interaction, consistent with a role for ethylene during the establishment of this symbiotic interaction (140, 146). This pattern was not observed in TC85507, but surprisingly, TC85507 had strong induction in established nitrogen fixation nodules. Expression of both TC was also observed in mycorrhizal associations with TC85507 showing slightly higher expression than TC85664 (5 and 2 EST respectively). On the other hand, TC85664 had more EST sequenced from *Phoma*-infected and *Colletotrichum*-infected libraries than TC85507. EST from *Phytophthora*-infected roots and insect herbivore libraries were also found in these two contigs (Fig. 19). The differences found in the expression of TC85507 and TC85664 make them ideal candidates for transcription profiling analysis.

Plant defense signal transduction homologues

The search for homologues of genes involved in defense responses such as *PDF1.2*, *PR1*, *PR2*, *PR10*, *NPRI*, *NDRI*, *EDRI*, *LOX* and *PAD4* yielded mixed results. For some of the proteins, few TC were found and when this occurred, the similarity and identity levels were extremely low (less than 15% with e-values higher than 10^{-5}) casting doubts about the annotation of the contigs. In other cases such as the case of LOX homologues, 8 contigs were expressed at high levels (more than 45 EST per contig), and almost under similar conditions, resulting in data that did not show differential responses (Data not shown). LOX derived signals, including jasmonates, are expected to interact in defense responses with signals mediated by ethylene, possibly through a gene called *CEVI* (45).

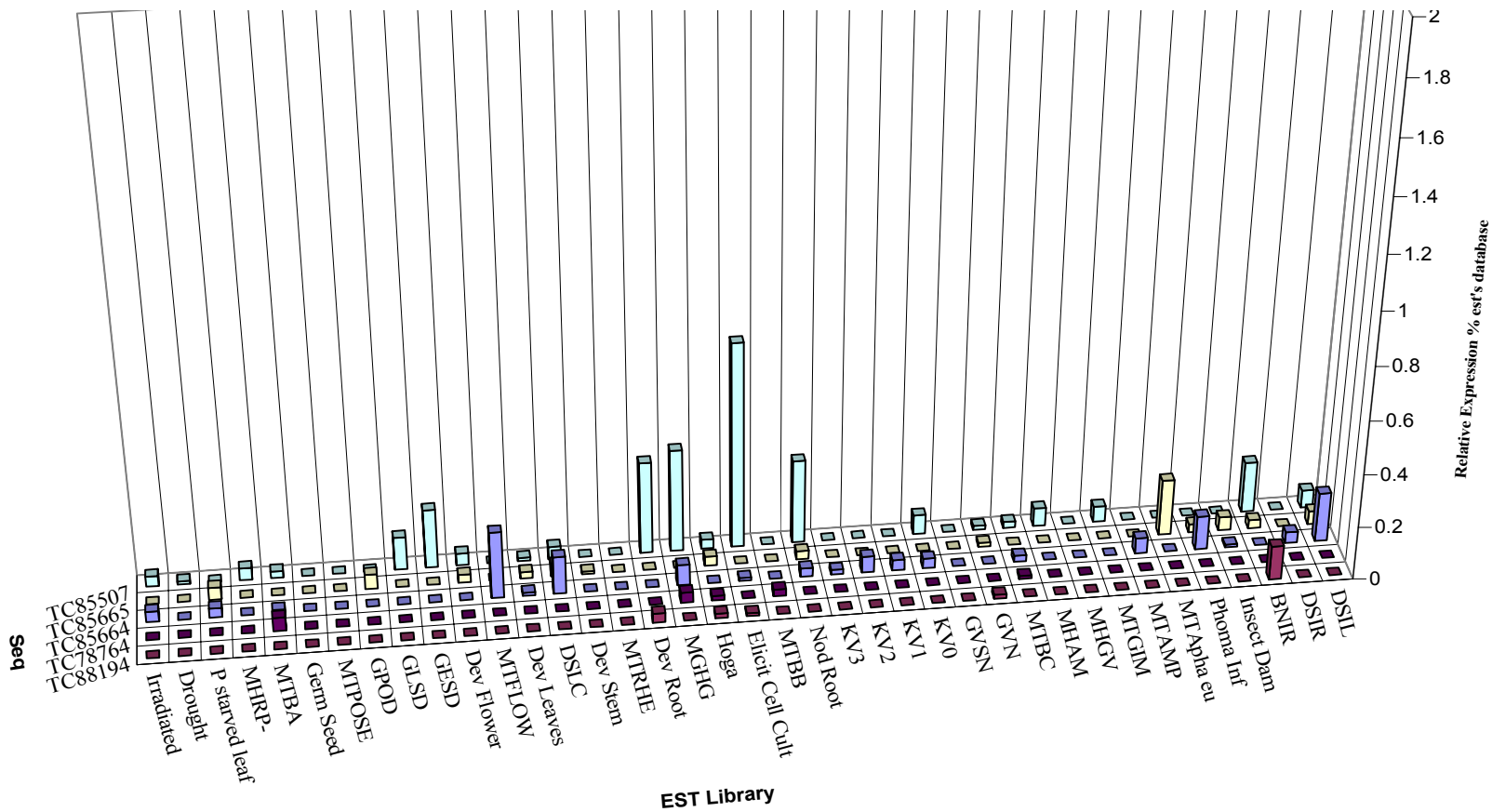


Fig. 19. In silico analysis of ACC oxidase gene expression. The *Medicago truncatula* EST database (MTGI) stored at the Institute of Genomic Research (TIGR) (154) was queried in tblastn searches for transcripts with homology to *A. thaliana* ACC oxidase protein (gi: 20141261). Rows show the results of the search. Each column shows the relative abundance of *M. truncatula* EST in each of the search hits, tabulated according to their library of origin. EST within the database were adjusted for errors and clustered into contigs based on sequence similarity. Each contig (TC) represents the alignment of sequences showing a minimum of 95% identity over a 40 or longer nucleotide region with less than 20 bases mismatched at either end, thus representing partial or full representations of homologous transcripts.

PR10 tblastn searches were based on the constitutively expressed protein PR10 of *M. truncatula* (gi: 1616609). The search yielded several sequences with complete homology at the protein level. Differences at the nucleotide level were found mainly in the untranslated regions of the gene. The homology with this transcript was shared by several more EST, making their placement into particular TC difficult.

MTGI appears to have three *PR10* homologues, TC76513, TC76519 and TC76510. TC76513 corresponded to the actual PR10 protein from *M. truncatula*. It was a strongly expressed transcript, having 379 EST in the contig. EST makeup of TC76513 showed that it was predominantly constituted by sequences derived from roots infected with mycorrhizal organisms (MTAMP). TC76513 was also abundant in hepta β -glucan-treated (MGHG) cDNA libraries. Interestingly, irradiated tissues and nematode-infected roots also expressed this transcript abundantly. The expression profile for TC76519 almost mirrors that of TC76513 but at a smaller scale (Fig. 20). Because of the high induction of PR10 and its expected responsiveness to ethylene/jasmonate signals, TC76513 was chosen for transcription profiling analysis.

Stress and detoxifying pathways

A large number of stress and detoxification responses are handled by proteins such as GST. Homologues of this protein were identified in MTGI using an auxin-inducible *GST* from soybean (gi: 2920666) as the query. Soybean GST protein family and, in general, plant GSTs are members of large gene families; therefore, it was no surprise to find several tentative contigs sharing high homology to the soybean sequence.

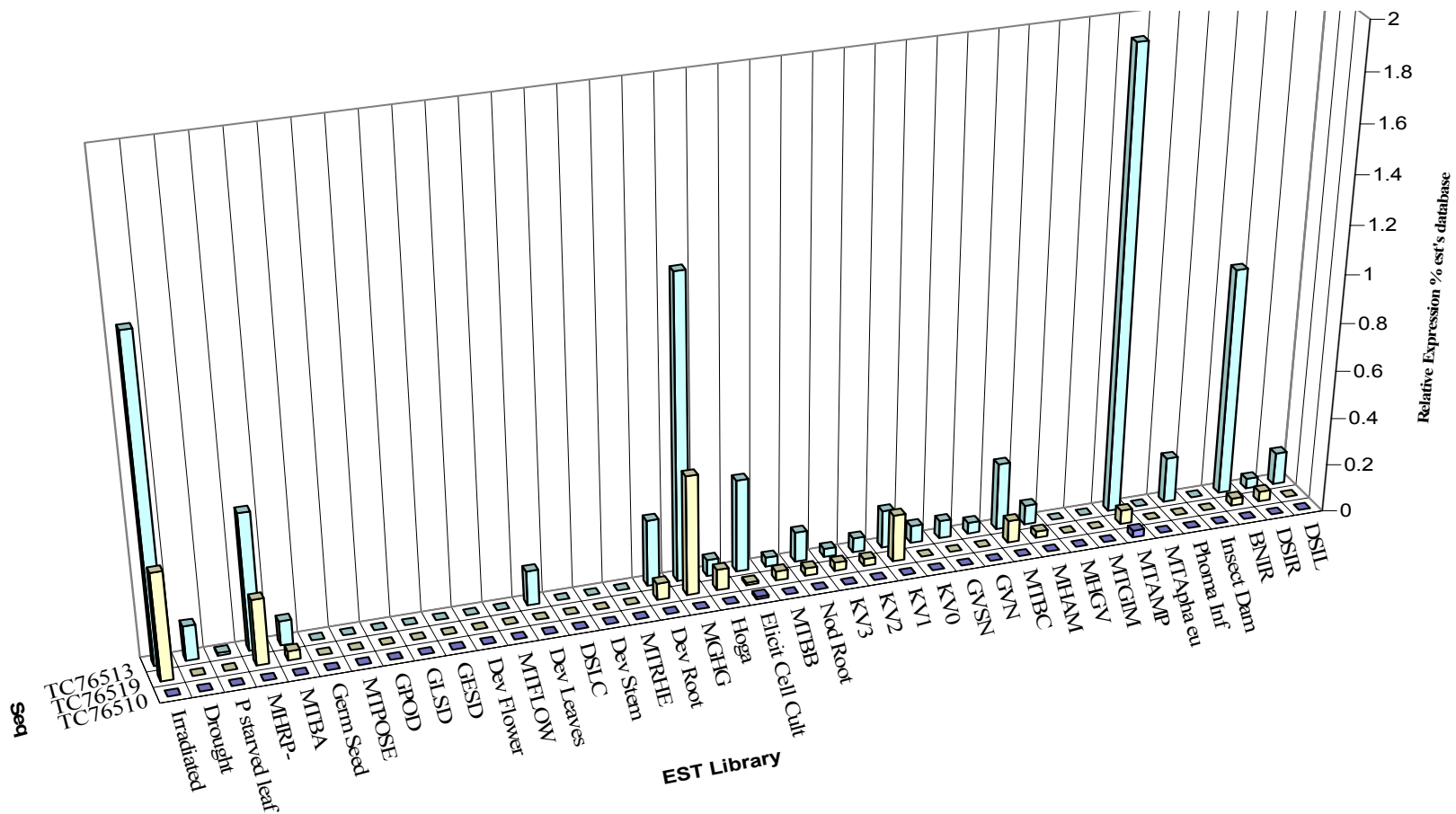


Fig. 20. In silico analysis of PR10 gene expression. The *Medicago truncatula* EST database (MTGI) stored at the Institute of Genomic Research (TIGR) (154) was queried in tblastn searches for transcripts with homology to PR10 protein of *M. truncatula* (gi: 1616609). Rows show the results of the search. Each column shows the relative abundance of *M. truncatula* EST in each of the search hits, tabulated according to their library of origin. EST within the database were adjusted for errors and clustered into contigs based on sequence similarity. Each contig (TC) represents the alignment of sequences showing a minimum of 95% identity over a 40 or longer nucleotide region with less than 20 bases mismatched at either end, thus representing partial or full representations of homologous transcripts.

In total, 28 contigs were identified, the great majority of which appear to contain full-length protein coding regions. The e-values for the different hits ranged from 1.3×10^{-102} for the closest homologue, to 5.0×10^{-30} for the most diverged sequence analyzed. At the amino acid level, identity and similarity values ranged from 81% identity and 94% similarity for the closest hit to 40% identity and 55% similarity for the most distant homologue.

In silica expression analysis revealed that most contigs were expressed in many different cDNA libraries. TC85451, the closest homologue to the query sequence, was the most highly expressed, with 188 EST making up the contig. The EST forming this contig were sequenced from a variety of tissues and conditions including leaves infected with *C. trifolii* and roots treated with hepta β -glucan elicitors. TC85451 also had several EST sequenced from plant tissues taken at different stages of plant development, including healthy leaves and stems, developing flowers, developing leaves, seeds and pods. TC85451 was also well represented in abiotic stress libraries, including drought and N or P starvation. EST for TC85451 were also encountered in roots infected with *P. medicaginis* or *M. incognita*, as well as in leaves infected by *Phoma medicaginis* or fed on by insects. Although the remaining GST contigs were expressed at low levels and in different libraries, common patterns in regulation seemed to be biotic and abiotic stress. Whereas scattered, the induction of GST homologues in response to fungal, oomycete, nematode, insect feeding, and mycorrhizal fungi can be seen in Fig. 21.

Abiotic factors, including UV irradiation, yeast elicitor, and fungal and plant cell wall oligosaccharides also were correlated with gene expression. The highest induction

of any *GST* homologue was found to be that of TC85868 after *Glomus intraradices* (MGIM) expression. TC85868 seemed to be expressed at the very high value of 2.2% of the EST in MGIM, well above the scale of the graph (0.5%).

By contrast to TC85451, TC78052 was not expressed in hepta β glucan treated tissue. A very low level of expression was seen for TC78052 in *Phytophthora* infected roots (DSIR) and *Colletotrichum* infected leaves (DSIL) (only 1 EST was sequenced in each case). Interestingly, elicited cell cultures KV1, MHAM, MTBC, and MTBA contained both TC85451 and TC78052. TC78052 and TC85451 were chosen for transcription profiling analysis.

Phenylpropanoid metabolism homologues

Three proteins from the phenylpropanoid pathway were mined from the EST data set: PAL, the first enzyme in the process, CHS, an intermediate enzyme, and IFR, one of the last enzymes involved in the production of the phytoalexin medicarpin.

PAL homologues. The search for PAL homologues was based on *M. sativa* PAL (gi: 129590). The results showed extremely high conservation between the query sequence and three MTGI tentative contigs (Table 17). Two additional sequences, TC85503 and TC85504, were also detected but were only partial hits, with 27% and 22% coverage, respectively. Nonetheless, in all the cases, the close phylogenetic relationship among the two organisms was reflected in the degree of homology among the sequences (Table 17).

The expression analysis of the contigs showed that TC85501, the second closest hit, was composed of 90 EST. TC85502, the closest homologue, had 37 EST in its contig. *PAL* homologues were expressed in libraries derived from pathogen-infected tissues such as *C. trifolii*, *P. medicaginis*, *Phoma medicaginis* and *Aphanomyces euteiches*. Libraries derived from cultures treated with different elicitors confirmed this observation. Developing tissues, with the exception of pods and stems, had limited expression of *PAL*-like sequences. TC85502, the closest hit to the query, had its highest representation in *A. euteiches* and *Phoma medicaginis*-infected libraries. EST comprising TC85502 were also sequenced from mycorrhiza-infected and *Rhizobium*-infected plants. Interestingly, the induction by nitrogen fixing bacteria seemed to be higher than the responses elicited by *G. versiforme* or *G. intraradices*.

TC85501 was observed to follow similar patterns, and, in general, similar levels of induction as TC85502. Nonetheless, this transcript was expressed in more libraries than TC85502. For this reason, TC85501 was chosen for subsequent transcription profiling analysis, Fig. 22.

TABLE 18. *Medicago truncatula* CHS homologues.

Target	% Coverage	% Identity	% Similarity	Tentative Annotation
TC85169	100	96	97	<i>CHS9 Medicago sativa</i>
TC85150	100	95	97	<i>CHS9</i> homologue <i>M. sativa</i>
TC85146	100	93	96	<i>CHS2</i> homologue <i>M. sativa</i>
TC85138	100	93	96	<i>CHS8</i> homologue <i>M. sativa</i>
TC76767	100	93	95	<i>CHS2</i> homologue <i>M. sativa</i>
TC76765	100	93	95	Putative <i>CHS M.truncatula</i>
TC79835	100	88	94	<i>CHS B</i> Pea homologue
TC85145	98	78	89	<i>CHS Vitis vinifera</i>
TC85174	82	90	93	<i>CHS 4 Medicago sativa</i>
TC79323	100	66	83	<i>CHS Vitis vinifera</i>

Data was generated by tblastn search of *M. sativa* CHS (gi: 166362) against MTGI. A cutoff value of 1×10^{-120} was used to separate other possible homologues from the rest of the retrieved hits.

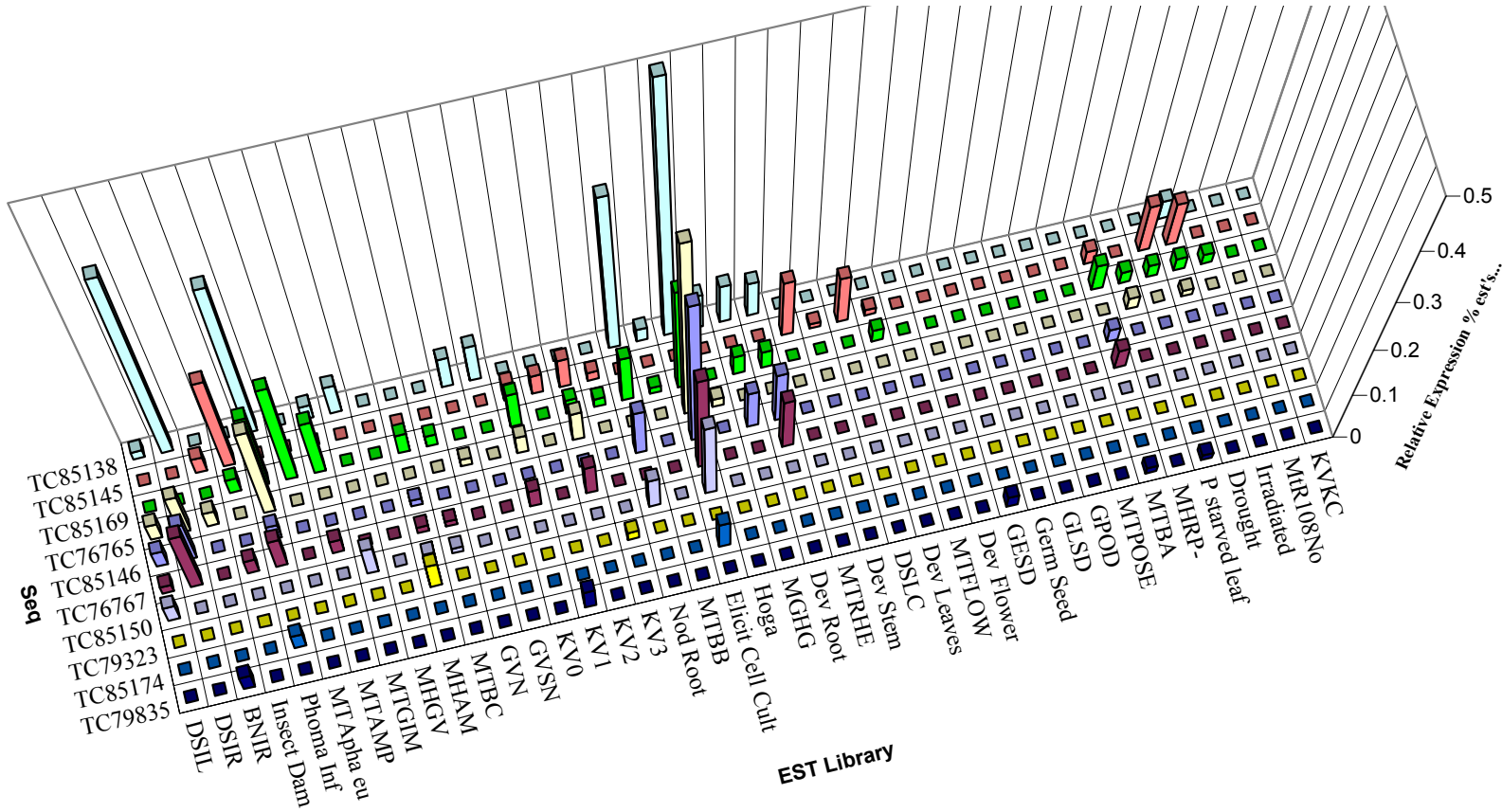


Fig. 22. In silico analysis of PAL gene expression. The *Medicago truncatula* EST database (MTGI) stored at the Institute of Genomic Research (TIGR) (154) was queried in tblastn searches for transcripts with homology to *M. sativa* PAL (gi: 129590). Rows show the results of the search. Each column shows the relative abundance of *M. truncatula* EST in each of the search hits, tabulated according to their library of origin. EST within the database were adjusted for errors and clustered into contigs based on sequence similarity. Each contig (TC) represents the alignment of sequences showing a minimum of 95% identity over a 40 or longer nucleotide region with less than 20 bases mismatched at either end, thus representing partial or full representations of homologous transcripts.

Chalcone Synthase homologues. This search was based on *M. sativa* CHS1 (gi: 166362), and 10 hits were found to contain high homology to CHS1. Most of the hits covered the entire length of the query protein (Table 18). Expression analyses of the contigs showed that most of them were expressed under pathogen attack or following elicitor treatment. Interestingly, the abundance of EST induced by symbiotic organisms (*Rhizobium* and *Glomus*) was lower than that observed after pathogen challenge. Minimal induction of *CHS* transcripts (less than 4 EST) was seen in most of the flower- and seed-derived libraries, libraries from developing leaves and stems, or tissue under abiotic stress including nitrogen or phosphate starvation or drought.

The strongest induction observed was for TC85138 upon exposure to yeast elicitors. Roots and leaves inoculated with *P. medicaginis* and *Phoma medicaginis* also strongly induced this same transcript. TC85138 was not found in most of the libraries derived from *Rhizobium* infection, but its transcripts were found highly expressed in established symbiotic interactions with *Rhizobium* (Nod roots, 10 EST). Conversely, other transcripts were expressed in the different *Rhizobium*-infected libraries (KV0, KV1, KV2, KV3, GVN, GVSN, etc). The high levels of expression seen under these three conditions suggest that TC85138 is a good candidate for transcription profiling analysis. A different homologue, TC76765, was also expressed at high levels and in libraries such as DSIL (*C. trifolii* infected), DSIR (*P. medicaginis* infected), NBIR (*M. incognita* infected) and *Phoma medicaginis* infected. Expression of TC76765 in elicited cell cultures was high, but curiously its expression was almost nonexistent in HOGA or

MGHG. These last two libraries represent treatments where elicitors of defense responses were also used. TC85138, for example, was present in all these three libraries. TC76765 was also almost silent in symbiotic responses to *S. meliloti* (low expression in KV0, KV2 and GVN), and in this sense, TC76765 shows different regulation and induction conditions than TC85138 and somewhat similar conditions to TC85145 and other homologues. Expression of TC76765 in roots infected with *P. medicaginis* (2 EST) was also lower than TC85138 (8 EST), but both transcripts were similarly induced by *Phoma medicaginis* infection. The observed different regulation and expression conditions of TC76765 make it another good candidate for transcription profiling analysis, Fig. 23.

Isoflavone Reductase homologues. The query sequence used for the tblastn search was *M. sativa* IFR (gi: 19620). This protein is 318 aa long and its comparison against MTGI yielded seven sequences sharing homology. Of the seven hits, only one had an almost perfect match with the query sequence. TC85477 had 98% identity and 99% similarity, for an e-value of 6.6×10^{-167} (Table 19). Besides these seven sequences, an additional hit was found to partially cover the C-terminal end of the query protein. The homology of this contig was high, being 98% identical and 99% similar to the query sequence. Two singletons were also found to have homology to the query. Table 19 shows the different findings.

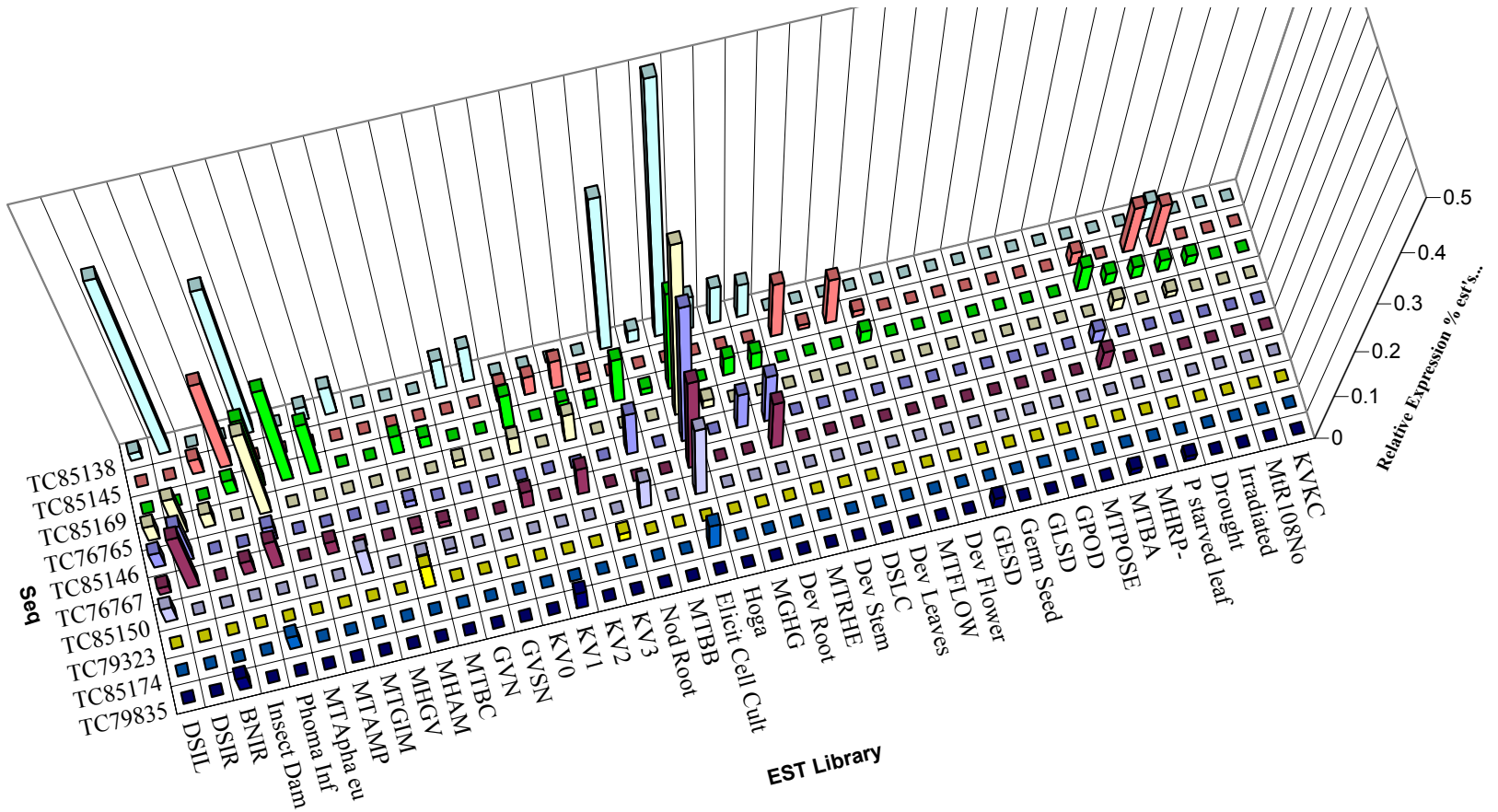


Fig. 23. In silico analysis of CHS gene expression. The *Medicago truncatula* EST database (MTGI) stored at the Institute of Genomic Research (TIGR) (154) was queried in tblastn searches for transcripts with homology to *M. sativa* CHS1 (gi: 166362). Rows show the results of the search. Each column shows the relative abundance of *M. truncatula* EST in each of the search hits, tabulated according to their library of origin. EST within the database were adjusted for errors and clustered into contigs based on sequence similarity. Each contig (TC) represents the alignment of sequences showing a minimum of 95% identity over a 40 or longer nucleotide region with less than 20 bases mismatched at either end, thus representing partial or full representations of homologous transcripts.

TABLE 19. *Medicago truncatula* IFR homologues.

Target	% Coverage	% Identity	% Similarity	Tentative Annotation
TC85477	100	98	99	IFR <i>M.truncatula</i>
TC77184	100	59	75	IFR homologue <i>G. max</i>
TC86142	100	57	73	IFR-like NADPH dep. <i>M. sativa</i>
TC88037	93	49	65	IFR related prot. <i>Pyrus communis</i>
TC87311	81	54	72	IFR homologue 2, <i>G. max</i>
TC79537	100	42	62	IFR homologue <i>Lupinus albus</i>
TC86455	100	40	61	IFR1 homologue <i>Lupinus albus</i>

Data was generated by tblastn search of *M. sativa* IFR (gi: 19620) against MTGI. A cutoff value of 1×10^{-55} was used to separate other possible homologues from the rest of the retrieved hits.

At the expression level, EST abundance analysis indicated that half of the contigs had more than 20 EST. These EST were sequenced from a wide variety of libraries, but most were isolated from pathogen- and symbiont-infected libraries. Elicitor-derived libraries (HOGA, Elicited cell cultures and MGHG) also induced the expression of these transcripts.

IFR homologue's expression was not abundant in plant development-derived libraries and the two closest homologues (TC85477 and TC77184) to the query sequence were almost solely induced upon biotic and abiotic stress conditions. Yeast elicited cell cultures and MGHG treated tissues accounted for most of the IFR EST. With a few notable exceptions (Fig. 24), the top two hits (TC85477 and TC77184) possessed very similar patterns of expression. The main difference between the two transcripts was the relative abundance of EST coding for them. The abundant expression of TC85477 in symbiotic and pathogen-induced libraries makes it a prime candidate for transcription profiling analysis, Fig. 24.

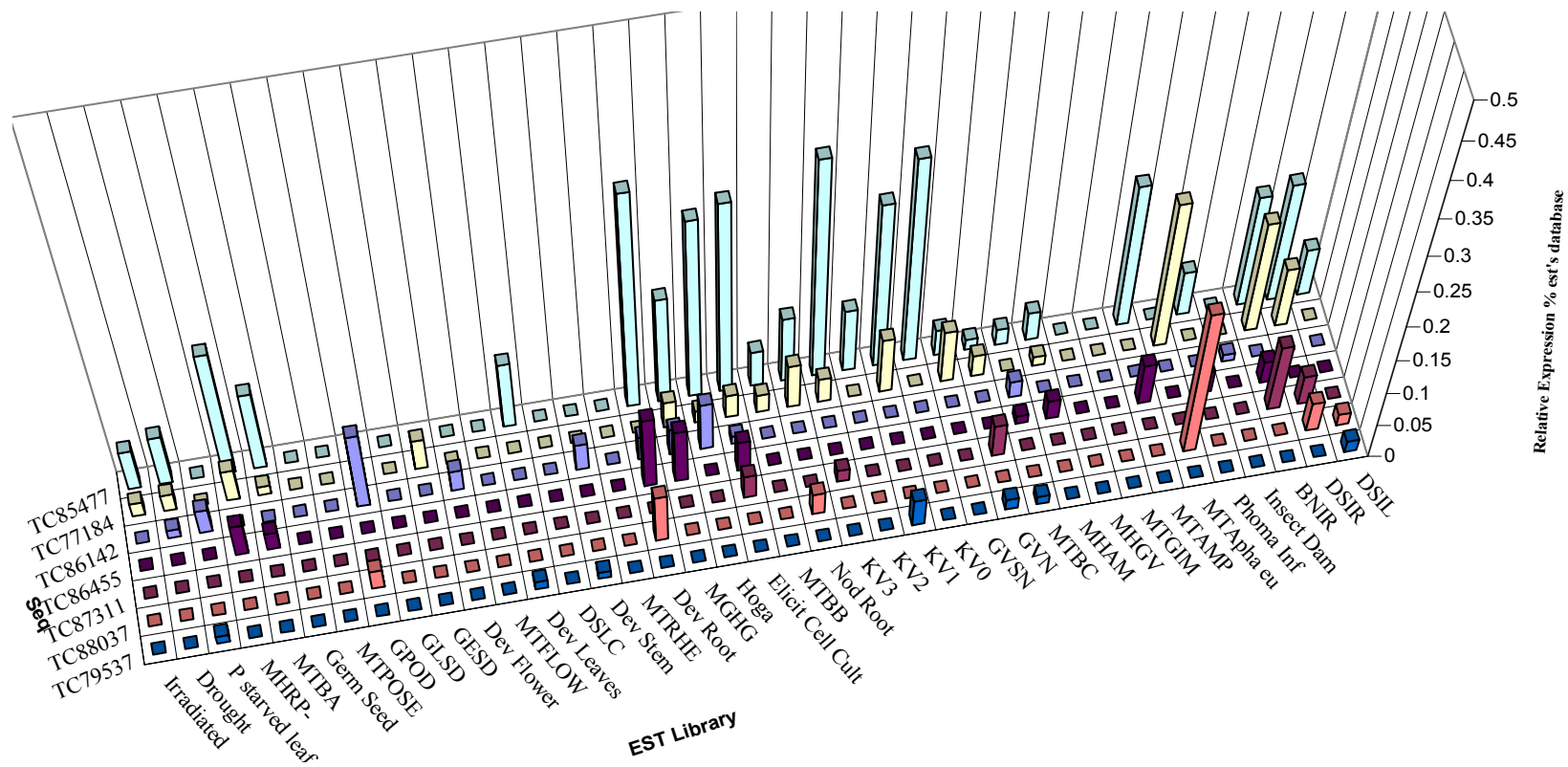


Fig. 24. In silica analysis of IFR gene expression. The *Medicago truncatula* EST database (MTGI) stored at the Institute of Genomic Research (TIGR) (154) was queried in tblastn searches for transcripts with homology to *M. sativa* IFR (gi: 19620). Rows show the results of the search. Each column shows the relative abundance of *M. truncatula* EST in each of the search hits, tabulated according to their library of origin. EST within the database were adjusted for errors and clustered into contigs based on sequence similarity. Each contig (TC) represents the alignment of sequences showing a minimum of 95% identity over a 40 or longer nucleotide region with less than 20 bases mismatched at either end, thus representing partial or full representations of homologous transcripts.

The comparison of expression profiles between *CHS* homologues and *IFR* homologues showed interesting parallels. For example, both proteins were highly expressed in elicited cell cultures, nodulated roots, and *Phytophthora*-infected roots. On the other hand, these proteins were not to be highly expressed in leaves, pods or flowers.

A low level of induction was similarly observed after infection with mycorrhizal fungi. Intriguingly, the abundance of EST coding for *IFR* homologues was higher than the number of EST coding for *CHS* homologues in *S. meliloti*-induced libraries. In this same sense, nematode infection of roots (BNIR) induced the expression of *CHS* and *IFR* homologues, but again the induction levels for *CHS* was lower than the observed *IFR* levels. This might indicate that the activity of IFR enzyme is required at higher levels in those particular interactions suggesting medicarpin production.

CHS levels were higher than *IFR* levels when the plants were exposed to *Phoma medicaginis*, an observation that suggests a different response program in the plant towards this pathogen. *PAL* expression seems to be lower than *CHS*, but it is seen to occur in the same tissues and conditions as *IFR* and *CHS*. *CHS*, which in itself seems to be the highest expressed of all three enzymes, was also the one with the most number of homologues found, suggesting a very complex and tightly regulated exchange of signals within the phenylpropanoid pathway.

Real Time PCR Analysis of *M. truncatula* Homologues

Choice of internal controls for analysis

The control transcripts chosen to normalize the expression profiling experiments were two constitutively expressed genes, *Actin* and *Histone H3*. Analysis of expression based on the abundance of EST coding for these two sequences is shown in Figures 25 and 26.

To demonstrate the utility of these genes for real time PCR experimentation, they were initially amplified using *M. truncatula* genomic DNA. The results of four reactions per gene with 50 cycles of PCR demonstrated that each target yielded a single product with the expected size (data not shown). Standard curves for these transcripts using serial dilutions of template indicated that it was possible to detect a template concentration ranging from 0.04 ng – 400 ng of DNA (Fig. 27).

To test the amplification of actin and histone controls in a two-target multiplex, where template concentration of one gene varied relative to the second, a known amount (1 ng) of *Homo sapiens* DNA was added to the samples of *M. truncatula* genomic DNA. Control reactions amplified extremely well when the amount of *M. truncatula* template was below 40ng/ μ l. The flat line response observed (Fig. 28) means that the amplification of GAPDH during the PCR reaction was not affected by any template concentration below that point and that it was possible to generate standard curves for amplification using both Actin and His H3. These results also demonstrated a high degree of technical precision, as noted by the similarity in the amplification curves for GAPDH in experiments using actin as compared to histone.

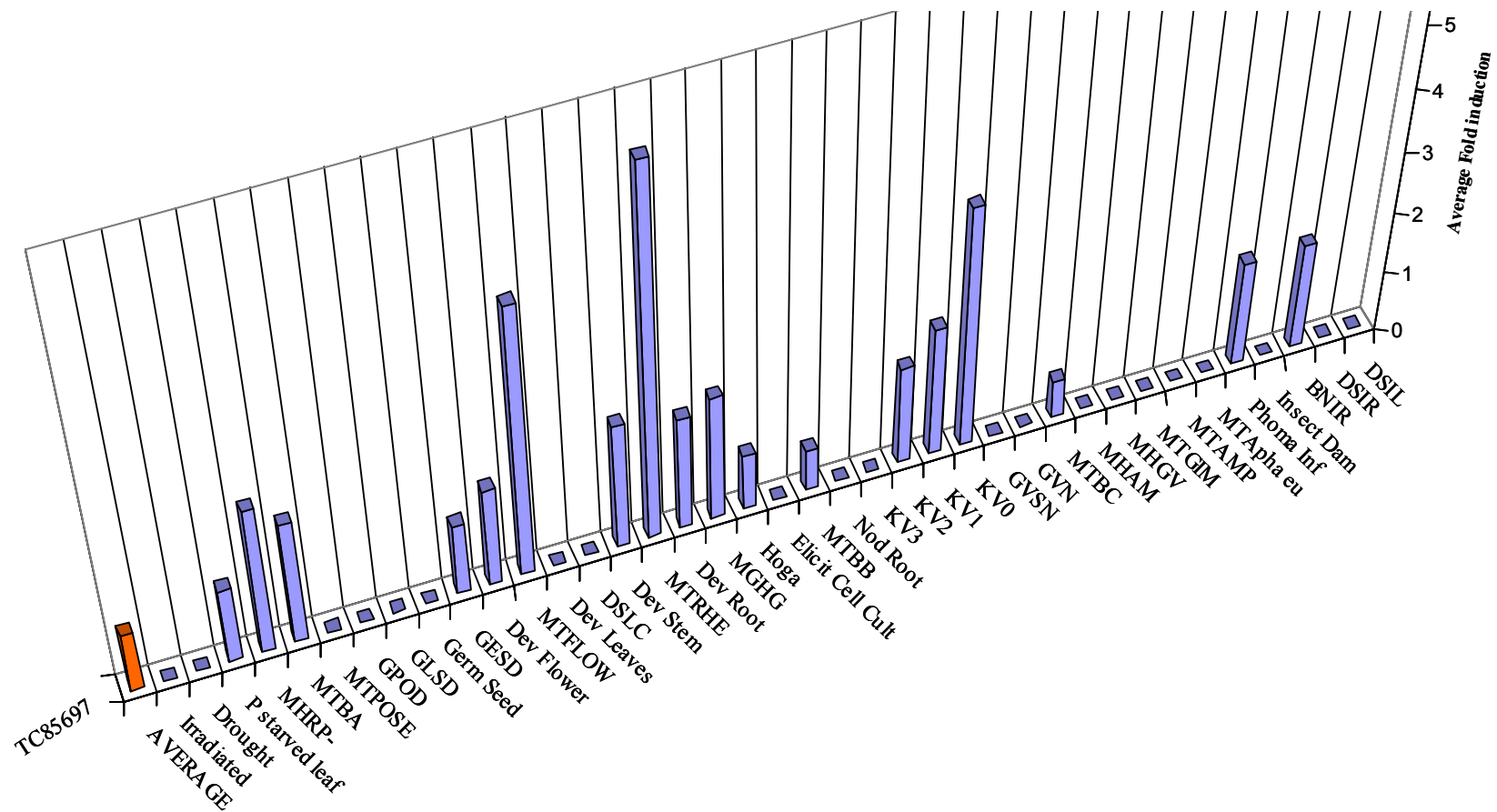


Fig. 25. In silica analysis of *Actin* homologue TC85697.

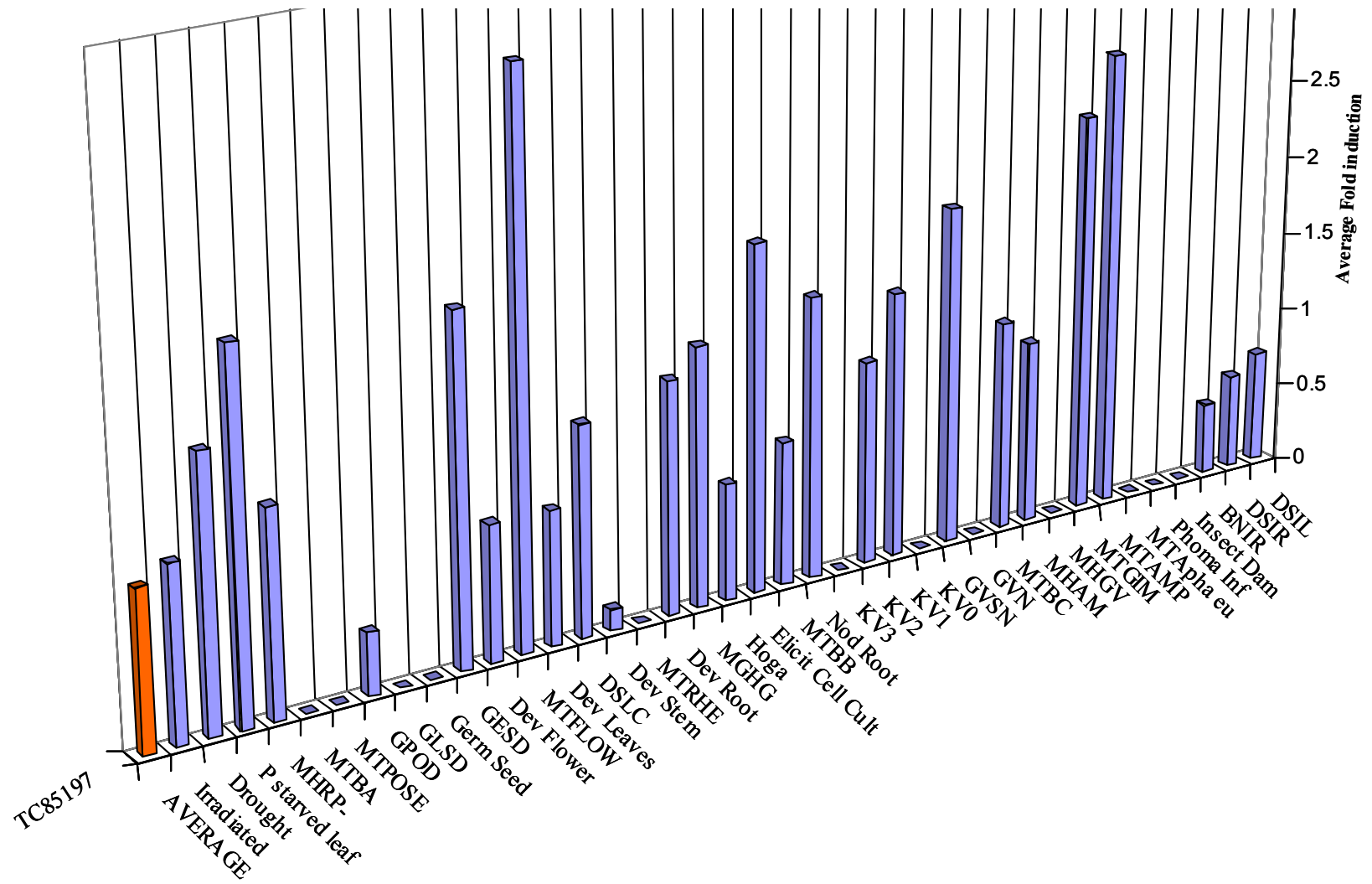
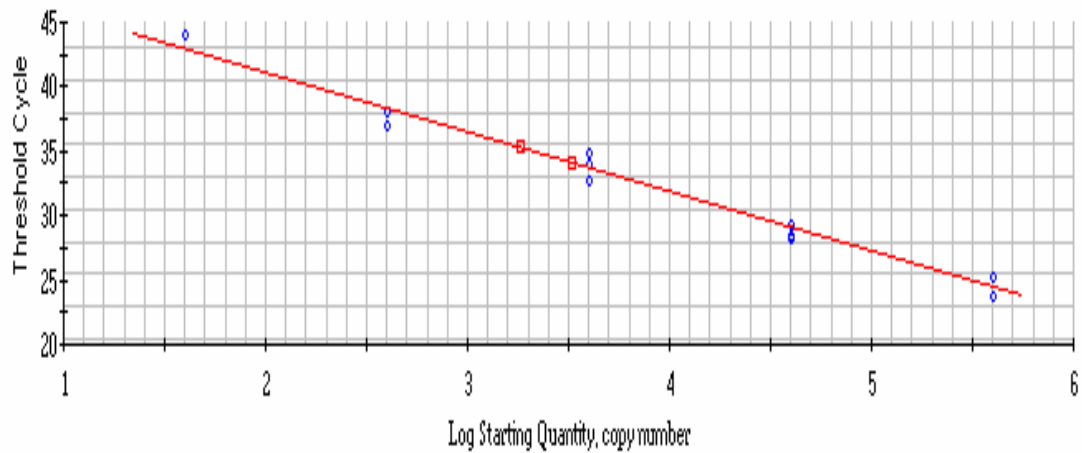


Fig. 26. In silico analysis of *His H3*, TC85197.

Standard Curve Chart for *Actin*

Correlation Coefficient: 0.991 Slope: -4.630 Intercept: 50.422 $Y = -4.630X + 50.422$

□ Unknowns
○ Standards



Standard Curve Chart for *Acc Oxidase (TC85664)*

Correlation Coefficient: 0.999 Slope: -3.200 Intercept: 40.048 $Y = -3.200X + 40.048$

□ Unknowns
○ Standards

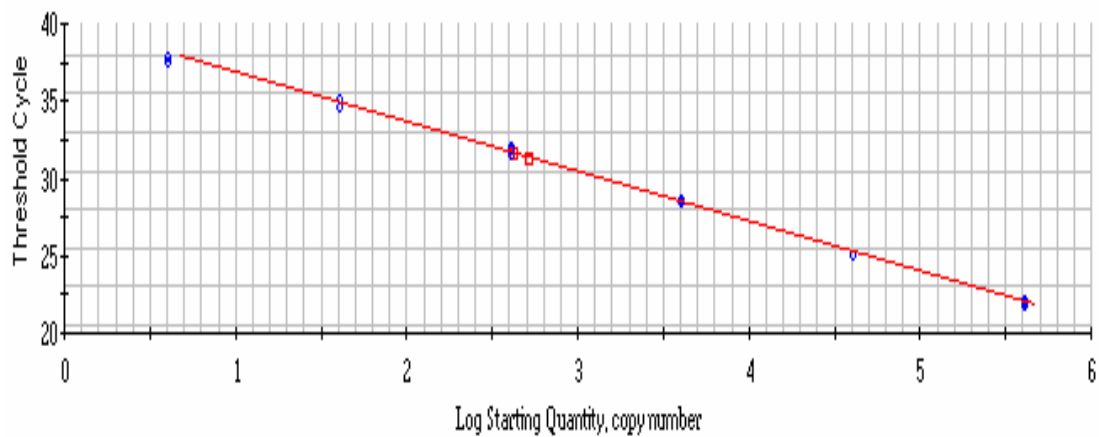


Fig. 27. Multiplex of target and reference genes. Subset of results.

Based on the multiplex analysis with GAPDH and either actin or histone, it was concluded that the fluorophore combinations of 6-FAM and Texas Red or 6-FAM and Hex work well for simultaneous quantification of gene products (123). However, standard curves generated using genomic DNA (Fig. 28), and in particular the comparison of slopes for the regression curves of internal control and target genes, (Fig. 27) demonstrated that adjustment of primer/probe concentration would later be required to achieve similar amplification efficiencies in both, control and target genes.

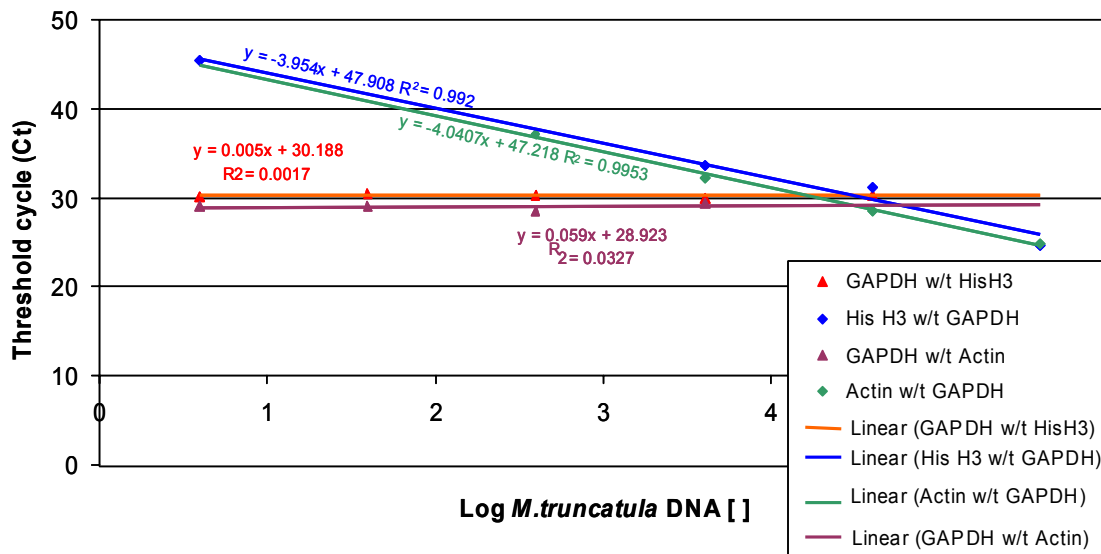


Fig. 28. Standard curves for amplification of *Actin* and *His H3* in multiplex with *GAPDH*.

Expression profiling of skl an ethylene insensitive mutant of M. truncatula

Expression profiling of ACO homologues. Penmetsa and Cook reported that *M. truncatula skl* mutation was insensitive to the hormone ethylene (146). In Chapters II and III of this dissertation, experiments to characterize *skl* mutation upon infection with

different pathogens demonstrated that *skl* plants were hyper-susceptible to infection by oomycete pathogens. Results of gas chromatography of *P. medicaginis*-infected roots showed that *skl* roots produced ethylene upon infection, but the intensity of the detected ethylene burst was smaller than the levels observed for infected A17 plants (Chapter III).

To characterize the expression profile of ethylene forming enzymes during infection by *P. medicaginis*, amplification of homologues of the ethylene-forming enzyme ACC oxidase using real time polymerase chain reaction was performed. Based on in silico analysis of the *M. truncatula* database (this chapter, previous results), two contigs with homology to *ACC oxidases* were chosen for analysis. According to the in silico analyses, both contigs were highly expressed but showed different expression profiles according to the treatments and conditions from which each of the EST comprising the contigs were sequenced. Therefore, these contigs represented good candidates to analyze differential responses to pathogen infection.

Real time PCR of TC85507 and TC85664 in A17 and *skl* infected roots revealed different profiles. Upon *P. medicaginis* infection, A17 plants expressed both homologues. In the case of the TC85664 transcript, A17 plants showed a strong initial induction that was followed by a decrease to almost basal levels during the first 12 hours after inoculation. At 24 hours, it was possible to see again an increase in transcript accumulation that peaked at 32 hours, Fig. 29. Later experiments showed that another increase in expression was observed beginning at 72 hours and continuing through 96 hours (data not shown). TC85507 exhibited a different pattern of expression, with a low

level of expression observed at early time points, and a large increase (between 70 and 150 fold increase) in expression at 24 and 32 h (Fig. 30).

skl plants also responded to pathogen inoculation. TC85664 expression was not that different from A17 plants. By contrast, TC85507 was unaffected by *P. medicaginis* infection in *skl*. The combined results suggest that TC85507 is regulated in an ethylene (*skl*) dependent manner, while TC85664 is regulated independent of ethylene perception.

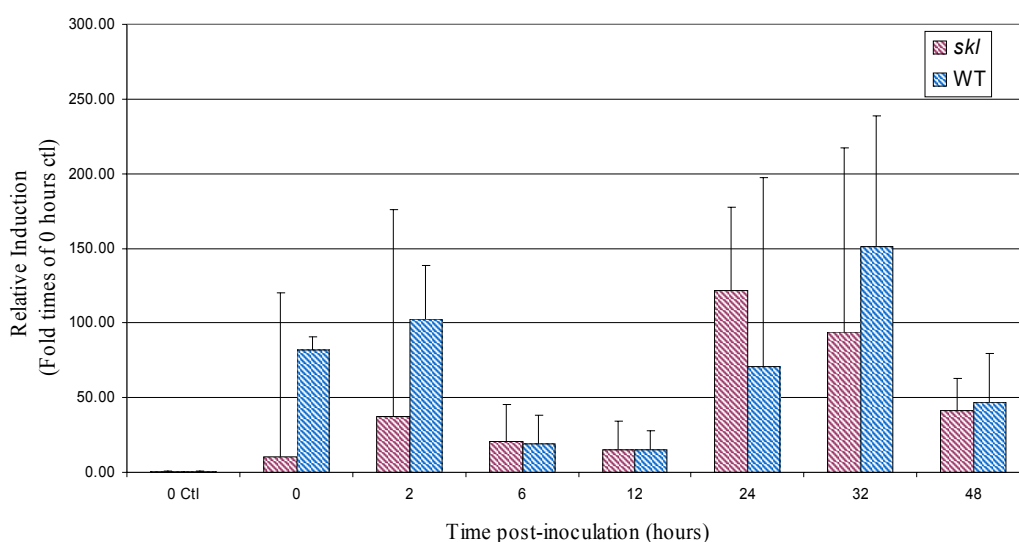


Fig. 29. Transcription profiling of *ACO* TC85664. Data is the average of two independent experiments. Each experiment was replicated at least two times. Plants growing inside aeroponic tanks were retrieved and inoculated with zoospores of *P. medicaginis*. Control plants were mock inoculated with the exudates of not inoculated V8-agar dishes that were flooded with sterile water. The inoculation time was 2 hours. Time 0 ctl corresponds to roots that never were exposed to zoospores or mock-inoculum. Time 0 represents the point at which treated plants were returned to the aeroponic tanks and it is the actual start of the time course experiment. Primers and probes with homology to the target and control genes were used to amplify by real time PCR, cDNA templates prepared from the roots of *M. truncatula* infected and not infected *skl* and A17 genotypes. Relative induction of target genes was calculated with the formula of Livak K. et al. (112). As sample for calibration of experimental results the non-inoculated 0 hours control (0 ctl) was used. Amplification data was normalized to *Actin* or *His H3* levels.

Expression profiling of *PR10* homologues. *PR10* gene is considered to be constitutively expressed in nodulated roots and this was confirmed by the real time PCR

results. Nonetheless, the experiments showed that its expression followed the pattern observed for ACC oxidase, i.e. there was strong induction after initial exposure to the pathogen was first seen, followed by a reduction in expression of the gene between 6 and 24 hours and then a second peak that was observed at 32 and 48 hours after inoculation.

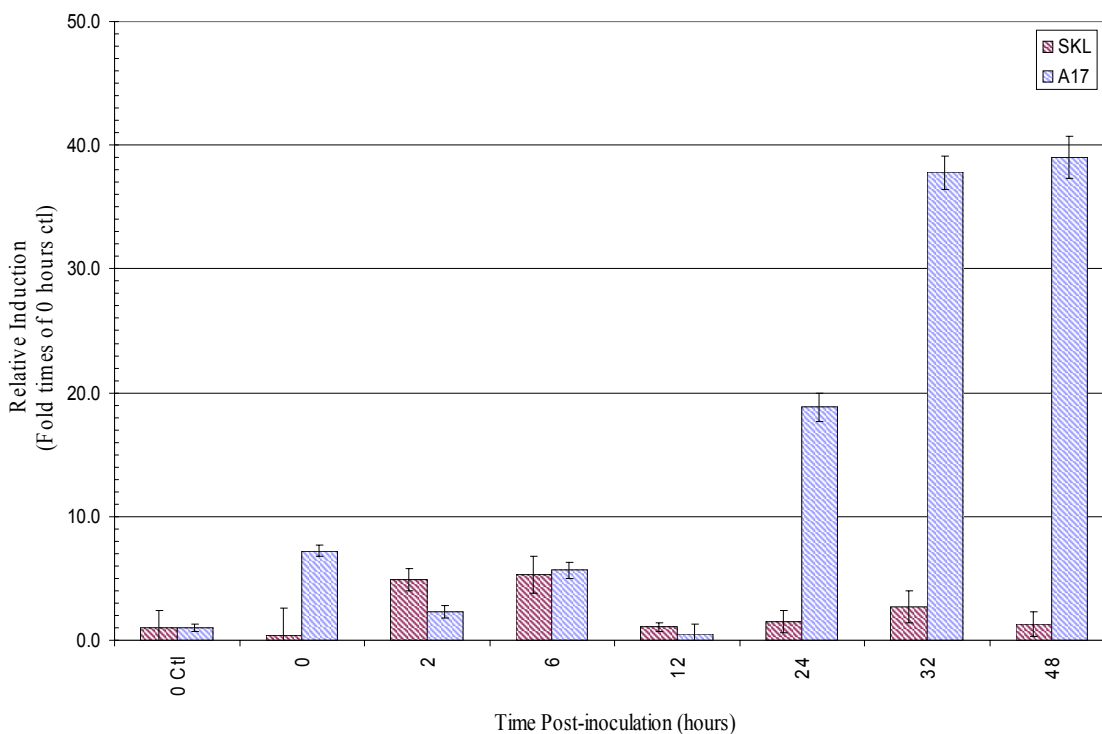


Fig. 30. Transcription profiling of *ACO* TC85507. Data is the average of two independent experiments. Each experiment was replicated at least two times. Plants growing inside aeroponic tanks were retrieved and inoculated with zoospores of *P. medicaginis*. Control plants were mock inoculated with the exudates of not inoculated V8-agar dishes that were flooded with sterile water. The inoculation time was 2 hours. Time 0 ctl corresponds to roots that never were exposed to zoospores or mock-inoculum. Time 0 represents the point at which treated plants were returned to the aeroponic tanks and it is the actual start of the time course experiment. Primers and probes with homology to the target and control genes were used to amplify by real time PCR, cDNA templates prepared from the roots of *M. truncatula* infected and not infected *skl* and A17 genotypes. Relative induction of target genes was calculated with the formula of Livak K. et al. (112). As sample for calibration of experimental results the non-inoculated 0 hours control (0 ctl) was used. Amplification data was normalized to *Actin* or *His H3* levels.

Interestingly, the expression pattern of *skl* and A17 were similar enough to rule out possible direct effects of *skl* mutation in the induction of this gene. The only

noticeable difference occurred at time 0 after inoculation, where A17 plants showed a stronger induction than *skl* infected plants (Fig. 31). Although little is known about the role of PR10 in plant defense responses, the results suggested that this gene is induced upon pathogen challenge, independent of a requirement for ethylene signaling.

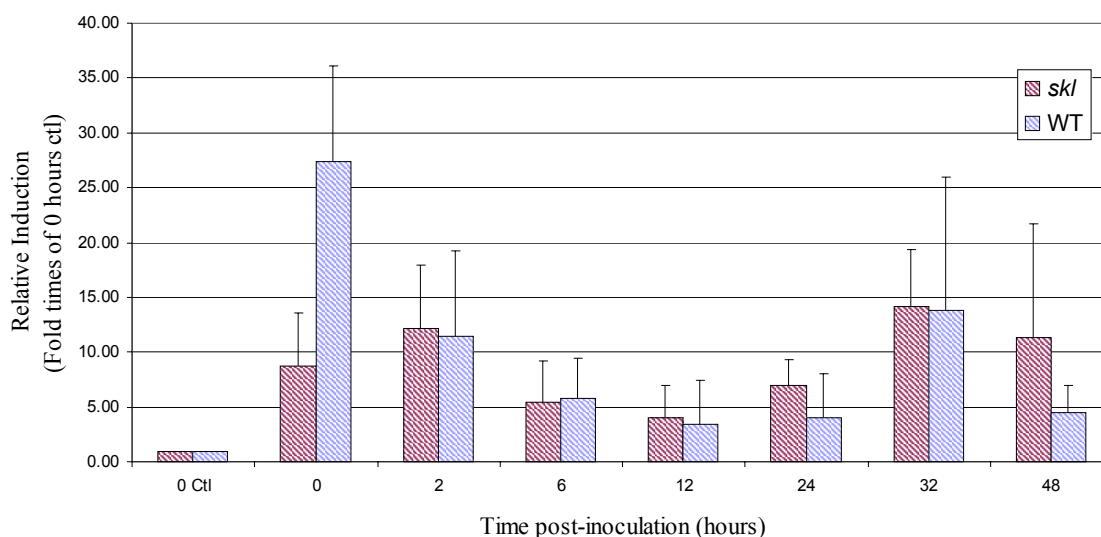


Fig. 31. Transcription profiling of *PR10* (TC76513). Data is the average of two independent experiments. Each experiment was replicated at least two times. Plants growing inside aeroponic tanks were retrieved and inoculated with zoospores of *P. medicaginis*. Control plants were mock inoculated with the exudates of not inoculated V8-agar dishes that were flooded with sterile water. The inoculation time was 2 hours. Time 0 ctl corresponds to roots that never were exposed to zoospores or mock-inoculum. Time 0 represents the point at which treated plants were returned to the aeroponic tanks and it is the actual start of the time course experiment. Primers and probes with homology to the target and control genes were used to amplify by real time PCR, cDNA templates prepared from the roots of *M. truncatula* infected and not infected *skl* and A17 genotypes. Relative induction of target genes was calculated with the formula of Livak K. et al. (112). As sample for calibration of experimental results the non-inoculated 0 hours control (0 ctl) was used. Amplification data was normalized to *Actin* or *His H3* levels.

Transcriptional analysis of gene members in the phenylpropanoid metabolism.

Transcriptional regulation of the phenylpropanoid pathway was assayed by monitoring the expression of four genes, representing PAL, CHS (2 paralogues), and IFR. As

shown in Fig. 32, the PAL homologue TC35727 was generally expressed at higher levels in *skl* than in A17 following inoculation with *P. medicaginis*.

Despite the high variation between experiments, the same trend was observed in each case. Both *skl* and A17 demonstrated a rapid response to inoculation (the 0 hr control represents 2 hrs incubation in the presence of zoospores). However, expression in A17 rapidly returned to basal levels, while it generally remained high in *skl* plants. The negative relationship between PAL induction and ethylene perception might be explained by the fact that *skl* plants experience a greater amount of pathogen infection (as measured by an increase in pathogen reproduction). Thus, *PAL* expression might be regulated by infection per se, in an ethylene independent manner.

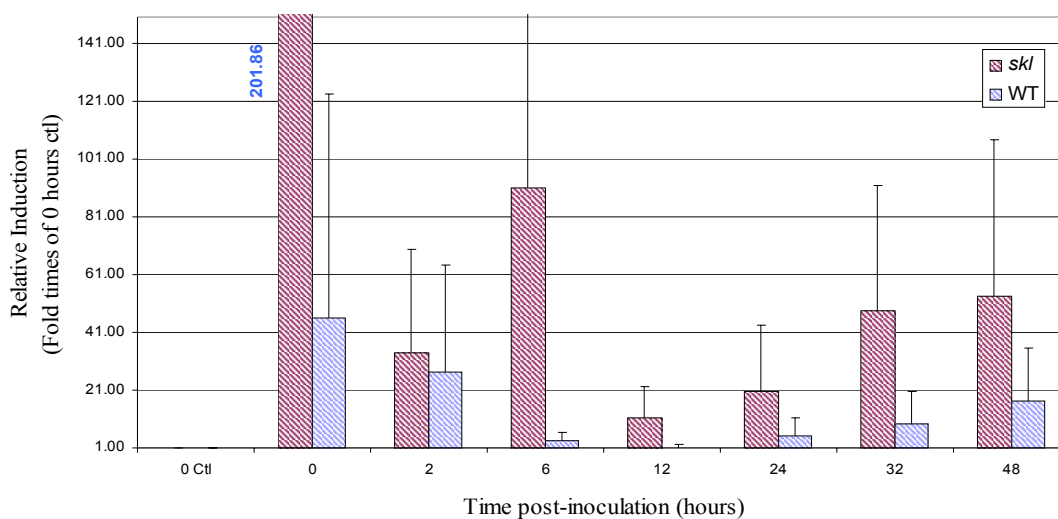


Fig. 32. Transcription profiling of *PAL* TC85501. Data is the average of two independent experiments. Each experiment was replicated at least two times. Plants growing inside aeroponic tanks were retrieved and inoculated with zoospores of *P. medicaginis*. Control plants were mock inoculated with the exudates of not inoculated V8-agar dishes that were flooded with sterile water. The inoculation time was 2 hours. Time 0 ctl corresponds to roots that never were exposed to zoospores or mock-inoculum. Time 0 represents the point at which treated plants were returned to the aeroponic tanks and it is the actual start of the time course experiment. Primers and probes with homology to the target and control genes were used to amplify by real time PCR, cDNA templates prepared from the roots of *M. truncatula* infected and not infected *skl* and A17 genotypes. Relative induction of target genes was calculated with the formula of Livak K. et al. (112). As sample for calibration of experimental results the non-inoculated 0 hours control (0 ctl) was used. Amplification data was normalized to Actin or His H3 levels.

Two different transcripts were chosen for the analysis of chalcone synthase expression: *CHS* TC76765 and *CHS* TC85138. As in the case of *PAL* homologues, replicate experiments revealed substantial variation between data sets (Fig. 33 and 34). Despite this experimental variation, the data are consistent with two general conclusions. First, both *CHS* paralogues are induced following inoculation with *P. medicaginis* (compare 0 hr non-inoculated control with 0 hr inoculated control). Second, expression was similar between *skl* and A17, suggesting that *CHS* transcription is regulated independent of ethylene perception.

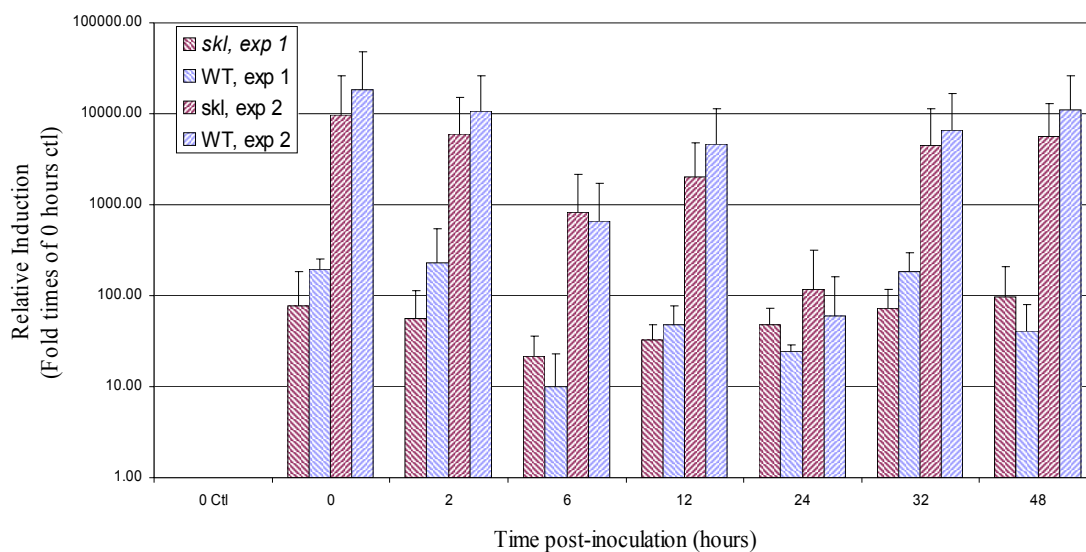


Fig. 33. Transcription profiling of *CHS* TC76765. Data is the average of two independent experiments. Each experiment was replicated at least two times. Plants growing inside aeroponic tanks were retrieved and inoculated with zoospores of *P. medicaginis*. Control plants were mock inoculated with the exudates of not inoculated V8-agar dishes that were flooded with sterile water. The inoculation time was 2 hours. Time 0 ctl corresponds to roots that never were exposed to zoospores or mock-inoculum. Time 0 represents the point at which treated plants were returned to the aeroponic tanks and it is the actual start of the time course experiment. Primers and probes with homology to the target and control genes were used to amplify by real time PCR, cDNA templates prepared from the roots of *M. truncatula* infected and not infected *skl* and A17 genotypes. Relative induction of target genes was calculated with the formula of Livak K. et al. (112). As sample for calibration of experimental results the non-inoculated 0 hours control (0 ctl) was used. Amplification data was normalized to *Actin* or *His H3* levels.

Transcription analysis of *IFR* (TC85477) showed that, in A17 infected roots, expression of this transcript seemed to be high at 0 and 2 hours after inoculation, which is consistent with the results previously observed for *PAL* and *CHS* transcripts. At 6 and 12 hours after inoculation, *IFR* levels were reduced to almost the basal levels, but a slight increase was again observed at 24 and 32 hours after inoculation.

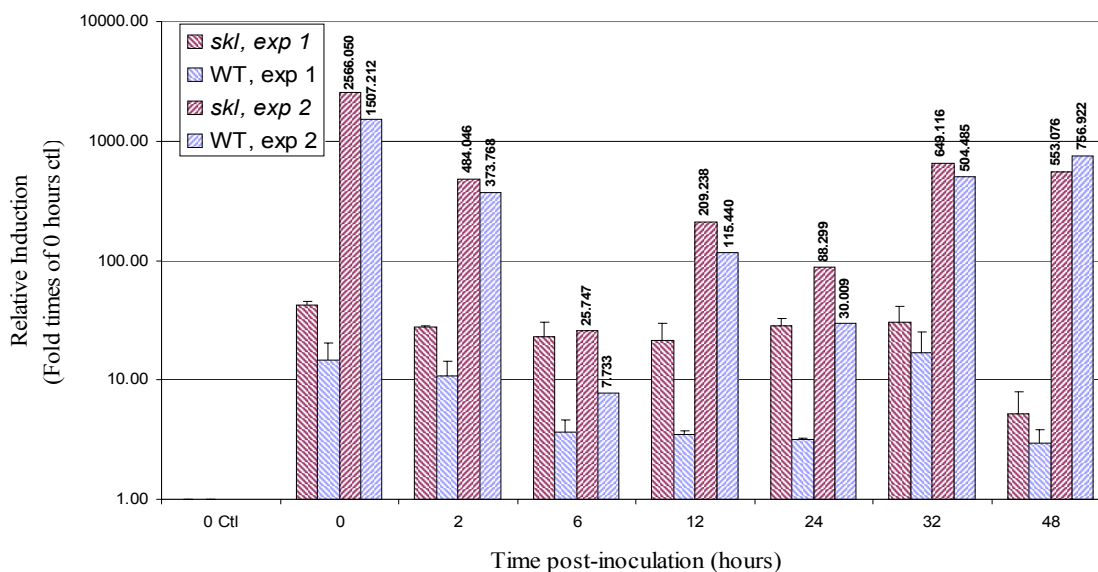


Fig. 34. Transcription profiling of *CHS* TC85138. Data is the average of two independent experiments. Each experiment was replicated at least two times. Plants growing inside aeroponic tanks were retrieved and inoculated with zoospores of *P. medicaginis*. Control plants were mock inoculated with the exudates of not inoculated V8-agar dishes that were flooded with sterile water. The inoculation time was 2 hours. Time 0 ctl corresponds to roots that never were exposed to zoospores or mock-inoculum. Time 0 represents the point at which treated plants were returned to the aeroponic tanks and it is the actual start of the time course experiment. Primers and probes with homology to the target and control genes were used to amplify by real time PCR, cDNA templates prepared from the roots of *M. truncatula* infected and not infected *skl* and A17 genotypes. Relative induction of target genes was calculated with the formula of Livak K. et al. (112). As sample for calibration of experimental results the non-inoculated 0 hours control (0 ctl) was used. Amplification data was normalized to *Actin* or *His H3* levels.

Transcription profiling of GST homologues. In the case of *GST* paralogues TC85451 and TC78052, real time PCR analysis suggested differences in the level of induction between the two paralogues, as well as differences in their dependence on ethylene. In

A17 plants, only TC78052 was induced upon *P. medicaginis* infection. Similar to the results obtained with *PAL* and *IFR*, TC78052 exhibited a bi-phasic pattern of expression, with a peak upon inoculation and then at 32 h post-inoculation.

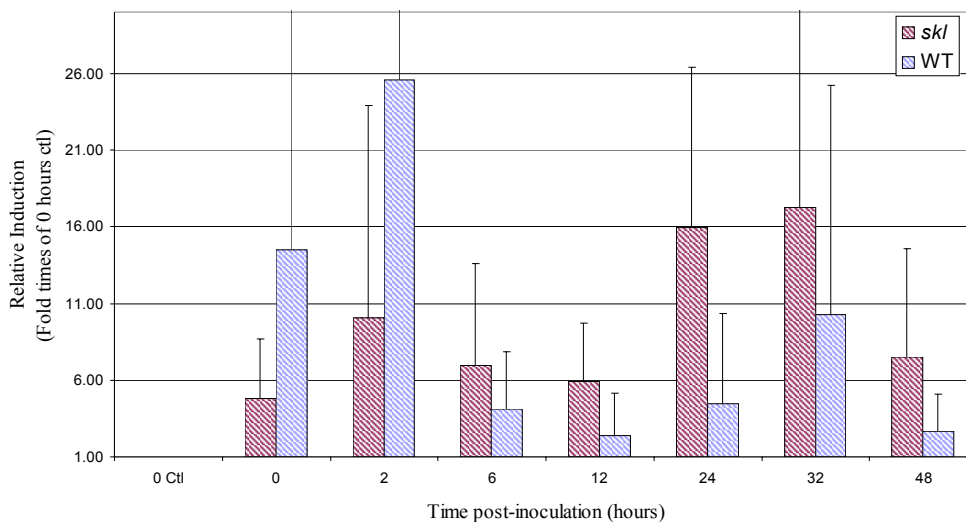


Fig. 35. Transcription profiling of *IFR* TC85477. Data is the average of two independent experiments. Each experiment was replicated at least two times. Plants growing inside aeroponic tanks were retrieved and inoculated with zoospores of *P. medicaginis*. Control plants were mock inoculated with the exudates of not inoculated V8-agar dishes that were flooded with sterile water. The inoculation time was 2 hours. Time 0 ctl corresponds to roots that never were exposed to zoospores or mock-inoculum. Time 0 represents the point at which treated plants were returned to the aeroponic tanks and it is the actual start of the time course experiment. Primers and probes with homology to the target and control genes were used to amplify by real time PCR, cDNA templates prepared from the roots of *M. truncatula* infected and not infected *skl* and A17 genotypes. Relative induction of target genes was calculated with the formula of Livak K. et al. (112). As sample for calibration of experimental results the non-inoculated 0 hours control (0 ctl) was used. Amplification data was normalized to *Actin* or *His H3* levels.

TC78052 appeared to be induced in a similar manner in the *skl* genotype, although with higher than average transcript levels at most time points. Interestingly, TC85451, which failed to respond to *P. medicaginis* in A17, was rapidly induced upon inoculation of *skl*. Transcript levels were maximal immediately following inoculation, declining to lower but still detectable levels at most subsequent time points Figures 36 (TC85451) and 37 (TC78052).

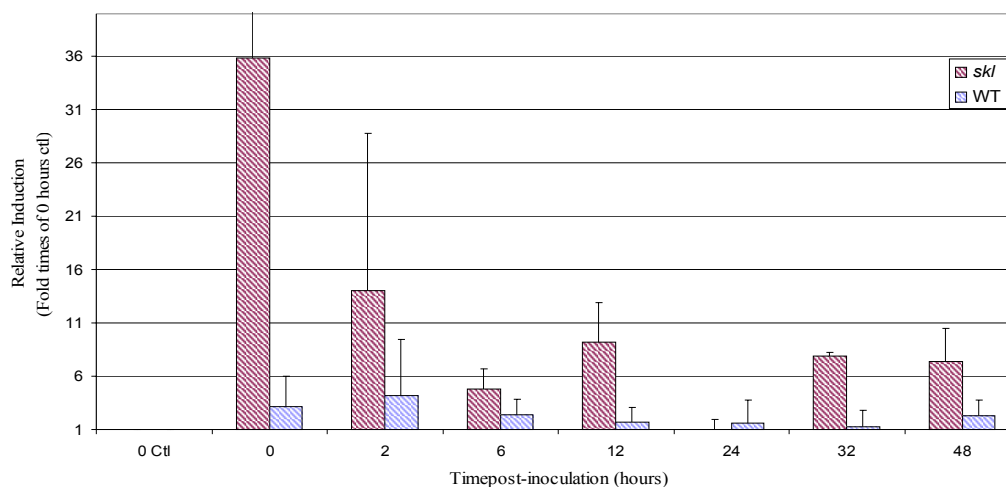


Fig. 36. Transcription profiling of *GST* TC85451. Data is the average of two independent experiments. Each experiment was replicated at least two times. Plants growing inside aeroponic tanks were retrieved and inoculated with zoospores of *P. medicaginis*. Control plants were mock inoculated with the exudates of not inoculated V8-agar dishes that were flooded with sterile water. The inoculation time was 2 hours. Time 0 ctl corresponds to roots that never were exposed to zoospores or mock-inoculum. Time 0 represents the point at which treated plants were returned to the aeroponic tanks and it is the actual start of the time course experiment. Primers and probes with homology to the target and control genes were used to amplify by real time PCR, cDNA templates prepared from the roots of *M. truncatula* infected and not infected *skl* and A17 genotypes. Relative induction of target genes was calculated with the formula of Livak K. et al. (112). As sample for calibration of experimental results the non-inoculated 0 hours control (0 ctl) was used. Amplification data was normalized to Actin or His H3 levels.

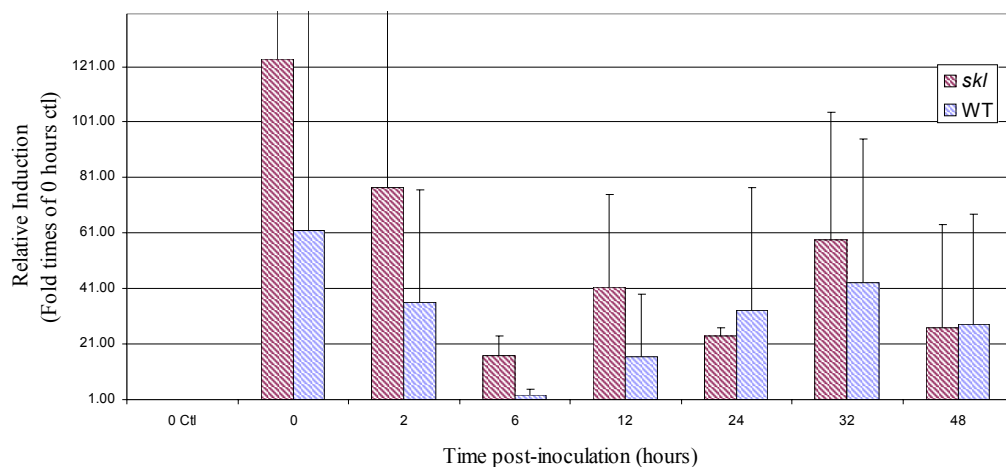


Fig. 37. Transcription profiling of *GST* TC78052. Data is the average of two independent experiments. Each experiment was replicated at least two times. Plants growing inside aeroponic tanks were retrieved and inoculated with zoospores of *P. medicaginis*. Control plants were mock inoculated with the exudates of not inoculated V8-agar dishes that were flooded with sterile water. The inoculation time was 2 hours. Time 0 ctl corresponds to roots that never were exposed to zoospores or mock-inoculum. Time 0 represents the point at which treated plants were returned to the aeroponic tanks and it is the actual start of the time course experiment. Primers and probes with homology to the target and control genes were used to amplify by real time PCR, cDNA templates prepared from the roots of *M. truncatula* infected and not infected *skl* and A17 genotypes. Relative induction of target genes was calculated with the formula of Livak K. et al. (112). As sample for calibration of experimental results the non-inoculated 0 hours control (0 ctl) was used. Amplification data was normalized to Actin or His H3 levels.

DISCUSSION

In silico Analysis of Gene Homologues

The *M. truncatula* EST database was analyzed to identify candidate genes involved in plant defense responses. Literature searches and computational resources (blast searches and phylogenetic analysis programs) were used to find homologous sequences for a large set of proteins and pathways involved in plant defense responses. The various sequences were analyzed for their homology and phylogenetic relationship with other closely related sequences. The analyses also provided an estimate of gene expression based on the EST frequency of *Medicago truncatula* Gene Index (MTGI), stored at TIGR. Although extensive, the performed analysis needs to be corroborated through extensive experimentation.

The characterization and use of *M. truncatula* EST libraries has been previously demonstrated (41, 61, 80, 93). These studies emphasized nodule-derived transcripts to complement studies describing the symbiotic relationships between *M. truncatula* and its nitrogen-fixing symbiont, the bacteria *S. meliloti*. The analysis presented here represents the first step towards the characterization and potential cloning of defense-related genes and compares defense responses in *M. truncatula* with other plant models such as *A. thaliana* and *Nicotiana tabacum*. This data will also enhance and complement the information available from the shotgun sequencing and fingerprinting of BAC libraries of *M. truncatula* (188).

Data mining of EST information has allowed the establishment of the first comparisons of gene expression profiles (2, 68, 106, 138,139) that ultimately were used

to provide experimental model analyses for medical and biochemical purposes. Currently, the availability of several plant EST databases has permitted this type of analysis to be done with agronomically important species (1, 22, 40, 59, 61,62, 100, 115, 165).

Most “in silico” analyses rely on the accumulation of a large number of EST to deduce the expression patterns from the EST frequency within the library. Other approaches such as Fedorova et al. (61) used logical queries to characterize MTGI and find sequences that fulfilled certain requirements including expression in symbiont-derived libraries, but not in developmental- or stress-conditioned libraries. Venn diagrams, each one representing each of the different EST libraries and secondary diagrams, (the product of the queries) were used to find a subset of 340 out of over 140.000 transcripts within 30 libraries, which were induced only as a response to nitrogen fixation symbiotic development. These results were validated by microarray and northern analyses of this subset of transcripts. To validate in silico analyses, statistical methods have also been employed (59, 173). As a partial validation of the in silico approach used in this study, real time PCR amplification of a subset of the gene homologues found in this analysis was accomplished.

Because EST libraries are sequenced from different tissues and conditions, the relative abundance of a particular transcript in a specific library is an index of its expression (106). This quality was exploited in this work to find the candidate transcripts for PCR analyses. The approach used gave emphasis to those contigs seemingly

expressed in mainly pathogen-infected derived libraries, due to the interest in the responses elicited by *M. truncatula* upon pathogen infection.

Correct analysis of transcript abundance requires that the contribution of each transcript in the overall database be the same. In MTGI, each EST library has a different number of sequences, that if not normalized will skew the results of the analysis. Therefore, all the data were normalized to a basal level that was independent of the depth at which each EST library was sequenced. The normalization procedure allowed the visualization of the treatment or tissue that generated the highest proportion of EST in a given contig; providing a relative representation of gene expression. Phylogenetic analysis and multiple sequence alignment of the different gene families were used to establish the closeness of the homologues identified. This approach provided information regarding the evolutionary history of the transcripts, which was useful in the selection process of the contigs used in real time PCR amplification. Multiple sequence alignment data were used to design amplification primers and probes around regions with low homology to assure amplification of the desired contigs and to distinguish among very closely related paralogues.

The usefulness of in silico analyses has been limited by factors such as the extension, coverage and quality of the available EST databases (138,139). The extension and coverage of the database is directly related to the manner in which the EST information is processed prior to study. For example, with larger EST datasets, more contigs can be made, and the completeness of the representation of the expressed mRNA is enhanced (109, 154). In addition, the likelihood of finding a particular mRNA

species depends on the copy number of the gene in question, its expression level and turnover rate. Thus, the mRNA population inside a cell can be classified as highly abundant, moderately abundant or rare. According to Lee et al. (106), if the EST database contains more than 3,000 sequences, the probability of finding a highly abundant mRNA species is higher than 99%. For moderately abundant transcripts, the probability is higher than 85%, and for rare transcripts it is less than 5%. As most of the libraries comprising MTGI were sequenced in sufficient depth, there is a high degree of confidence that most of the transcripts will be found in the database.

During the construction of EST, mistakes can be introduced. A study to analyze EST sequencing errors was previously performed by Liang and Quakenbusch (109) with the purpose of optimizing the process of EST clustering and creation of TC. Nonetheless, TC can still harbor chimerical sequences that have high homology among them. This type of error was observed for some of the *PAL* and *GST* homologues (data not shown), and it is particularly evident when new releases of the EST database, containing greater datasets showed that a sequence could be split into two or three different contigs, based on the new clustering of the EST.

Although the dataset was extensive, candidate genes for most of the pathways analyzed were not found. For example, the EST search of gene homologues for PR1, PR2, PAD4, NPR1, NDR1 and CPR1 yielded mixed results or lowly expressed transcripts or transcripts that were similarly regulated. Under these conditions, it was not expected that these transcripts would be affected in *skl* mutation. These gene homologues were not further studied. Something similar was observed for gene

homologues such as *PDF1.2* and thionin. However, the search for *LOX* homologues produced eight different contig sequences, all sharing high homology with the query sequence and coordinately induced in the different libraries. Furthermore, the number of EST in each of the contigs was high, suggestive of high expression levels. The lack of a differential response in pathogen-derived or elicitor-derived libraries for these contigs suggested that the usefulness of Lox homologues in subsequent analysis of *skl* mutation was not clear (data not shown).

EST analysis for genes involved in the transduction of ethylene signals, such as *ETR1*, *CTR1*, *EIN2* and *EIN3*, yielded a low number of contigs with homology to the query sequences. In some of the cases, the homology was restricted to known protein motifs that are present in other proteins, severely limiting the confidence in these results. However, the EST search of *ACC oxidase* and *ACC synthase* homologues yielded sequences that were highly expressed according to the number of EST comprising each of the contigs. These results were particularly clear in the case of *ACC oxidase* and therefore subsequent analysis focused on this protein.

Transcription Profiling of Gene Homologues

Real time PCR

The success of real time PCR, irrespective of the chemistry or quantification method used, depends upon the normalization process. A reliable quantification of RT-PCR requires correction for experimental variation at both the reverse transcription and the PCR efficiencies (74). Constitutive expressed genes have been used as controls to

normalize data in a wide array of experimental assays because they are expressed at a constant level among the different tissues of an organism, and their expression is neither affected by the treatment nor the stage of development of the organism (26, 74). Of the different housekeeping genes available, the most commonly used are *Actin*, *ribosomal RNA* and *Histone H3*, but other genes, such as *Hypoxanthine-guanine phosphoribosyltransferase*, *ciclophilin*, *mitochondrial ATP synthase*, have been used as well as controls in gene quantification experiments (74). *Histone H3* (*HisH3*) encodes a protein involved in chromatin organization. The *HisH3* transcript amplified in this work was TC85197, the homologue of *HisH3* gene from *Lycopersicon sculentum*. TC85197 is a contig assembled with 126 EST and is expressed across 26 different libraries. In silica analysis of expression levels in TC85197 showed that the levels were quite similar among the different libraries (Fig. 26). The same analysis also showed that *HisH3* was mildly induced by pathogens, although artificial elicitation with yeast cells or Heptaglucons seemed to induce this gene in higher proportions. Nonetheless, this *HisH3* apparent induction was lower than the level seen for this same transcript in the developing leaves EST library, which presented the highest induction of all ($\approx 3.5X$ the average induction level or 0.25% of the number of EST in the database). Interestingly, this transcript was present at above average levels in mycorrhizal and *S. meliloti* induced libraries, suggesting that it might not be a good control for analysis in experiments involving such treatments.

Actin encodes a cytoskeleton protein and was expressed in almost all cell types examined. The *actin* transcript analyzed was TC85697, the homologue of *Actin 11* of *A.*

thaliana. TC85697 is formed by 27 EST sequenced from 18 different libraries (Fig. 25). This transcript is also present in the Kiloclone set, an EST library prepared with the clones present in the microarray slides that the *M. truncatula* consortium is printing. As in the case of *His H3*, this transcript was mildly induced in tissues infected by pathogens. TC85697 was shown to be strongly induced in libraries derived from elicited tissues exposed to yeast cells or Hepta-glucans. The in silico study also showed that nitrogen fixing bacteria seemed to induce this transcript. TC85697 had its highest expression in root hairs and developing leaves, which is consistent with developing tissues and cells engaged in active reproduction. Thus, it was not surprising to find induction of this transcript in root cells infected with *S. meliloti* from libraries such as KV0, KV1 and KV2 that represent the initial stages of plant-microbe interactions leading to nitrogen fixation. In this context the expression of TC85697 corresponds to the expected modification of sub-cellular structures in cells undergoing changes that will lead to the development of nitrogen fixing nodules. The expression of this transcript in roots and its very low or almost non existent induction by pathogens makes this transcript a very good control for the purposes of these transcription profiling experiments.

The goal of the initial control experiments was to identify the possibility of amplifying target and control molecules in single reactions. The main advantage of multiplexing target and control genes is that the number of samples that can be processed in a determined time frame is greatly increased (72). Multiplexing also reduces the amount of PCR template needed to achieve the experiments, a very important factor if the amount of the experimental sample is limited. On the other hand,

multiplexing requires a comparatively longer preparation time than the time required to prepare the amplification of a single PCR product. Similarly, multiplexing requires experiments geared to adjust the conditions for the PCR amplification, which can increase the final cost of the experiment in terms of reagents (PCR Polymerase, dNTPs, MgCl₂, PCR buffer) (107). Nonetheless, simultaneous amplification of target and control genes in different tubes may be the preference if a suitable primer and probe combinations for target and control genes cannot be determined (190). This choice is also useful if the number of target genes for analysis and the number of reactions to be performed is small. But more importantly, data analysis of real time PCR reactions can be accurate under multiplex or separate tube amplification (112). Because the goal of the experiment was to amplify nine different genes plus an internal control in time course experiments involving as many as eight different time points in replicated experiments, the most reasonable approach seemed to adjust amplification conditions for multiplexing of target and internal control genes. The major concern with the multiplexing strategy was to not restrict the amplification of any of the gene species and to ensure that the reporter system would be adequate to clearly distinguish the signals from target and control molecules.

Independent amplification of PCR targets is important because in real time PCR, data are analyzed when the fluorescence of the target gene is above an arbitrary point called the Threshold Cycle (Ct) (72, 85). The threshold cycle is defined as the PCR cycle at which the fluorescence of a sample is above the background fluorescence of the experimental system. It is usually calibrated at 10x the standard deviation of the average

background fluorescence of the system (85). Thus, when adjusting the primer and probe concentrations for both internal and target genes, the primer and probe concentration subsequently used in the real time experiments was the one that minimized the time required for the PCR to reach the threshold cycle for both genes.

Color multiplexing is one of the ways by which different PCR products can be identified in a reaction mixture. Other ways to achieve this is by using physical properties that will discriminate among the simultaneously amplified templates such as denaturing temperature or size of the PCR amplicon (190). Color multiplexing relies on the use of external artificial tags present at the extremes of a third oligonucleotide called a probe. Upon probe and template hybridization, the tags are detected during the PCR reaction by typical fluorescence resonance energy transfer mechanisms (26, 190). Efficient energy transfer between the 5' and 3' modifications largely depends on how far apart the locations of both modifications are within the probe. The distance these molecules can be placed apart depends on the Förster radius of the fluorogenic molecules employed (177). The farther apart the two molecules are, the less likely will be the transferring of electrons or photons among them. A higher likelihood of achieving an efficient electromagnetic interaction between the molecules occurs when the two fluorogenic molecules are close to each other (177).

As shown in the experimental results section, real time amplification data was inconsistent. Factors that could have influenced this outcome would include photobleaching of reporter probes, activity of DNA polymerase, stability of RNA and cDNA molecules, and choice of reporters. The mechanism by which Taqman™ probes

work can also be improved. A new generation of these probes is currently available and is designed to bind to the minor groove of the cDNA template. This type of binding is expected to be more robust and reliable, allowing a better disintegration of the probe during the amplification. Also, new probes are shorter than the ones used in this study. Shorter probes should be more effective in quenching fluorescence when not hybridized and hydrolyzed. In addition, new methods for synthesis of reporter compounds are yielding probes that are more stable and less prone to degradation (123).

Gene expression profiling

Few expression profiling studies in *M. truncatula* that aim to characterize the defense responses upon pathogen infection have been published. The expression profiles of chitinase homologues in *M. truncatula* under conditions of mycorrhiza and pathogen infection have been demonstrated (163). However, the expression patterns of only eight different chitinase homologues were examined. The objective of the current study was to provide a possible framework to study defense-responses against pathogens on a much broader scale.

Equally scarce are data that correlate gene expression information with microarray data in *M. truncatula*. Recently, Mitra et al. (121) used microarray technology to screen for changes in the expression profile of mutated genes in *M. truncatula*. With this novel approach Mitra et al. were able to clone *M. truncatula dmi3*, a gene involved in the signal transduction program of symbiotic interactions between *M. truncatula* and organisms such as *S. meliloti* and *G. versiforme*. A publication has been

provided by Harrison et al. (110) that has insights about transcription profiling in mycorrhizally infected roots. Also, real time PCR has been used to create expression profiles of genes involved in root development upon auxin exposure in this plant species (127). Currently experiments are being performed to analyze transcription profiling of *Medicago truncatula* pathogenic interactions using microarray technology (188).

To adapt to changing environments, higher organisms differentially regulate gene families (65). Lipoxygenases, for example, comprise a fairly large gene family with at least 8 members in *M. truncatula*. This enzyme is involved in the production of multiple compounds implicated with plant growth and development, resistance to insects and pathogens, senescence, cold tolerance, and drought. The specific regulation of some of these homologues has been correlated with their specific function and tissue location (99). The evolution of triterpene synthases in *M. truncatula* is another example of differential regulation of gene families. Some of the triterpene synthase homologues are involved in gravitropism, whereas others are needed for cellulose synthesis or to produce saponins involved in antimicrobial activity (90). Therefore, it is expected that gene homologues involved with defense responses have also adapted to respond to different biotical stresses, thus being differentially regulated. Under this framework, it is expected that genes that are differentially regulated in *skl* mutation be found, therefore facilitating the characterization and study of this plant mutation.

In Chapter III of this dissertation, it was shown that *P. medicaginis* infection of *M. truncatula* seedlings induced ethylene production. Gas chromatographic assays of *skl* and A17 infected seedlings showed that the pattern of ethylene evolution had bimodal

characteristics. Using real time PCR those results were able to be corroborated with gene expression data from genes coding for ACC oxidase. Using the same conditions of pathogen infection, it was possible to trace the gene expression pattern of two *ACO* homologues. One was not responsive in *skl* infected plants, possibly contributing to the lack of ethylene production in these mutant plants.

Expression profiling of the ACO homologue TC85507 matched the results of the gas chromatography assay. The expression levels were clearly induced in A17 plants but almost absent in *skl*. On the other hand, the second ACO homologue, TC85664, was similarly induced in both genotypes. The fact that TC85507 exhibited a different expression pattern in A17 and *skl* plants suggests independent pathways for the control of the expression of these genes. Perhaps TC85507 represents an *ACO* homologue induced upon pathogen challenge, while TC85664 may be an *ACC oxidase* homologue induced by autocatalytic ethylene. In agreement with this hypothesis, an ortholog of TC85664 from lima bean was induced by herbivore-induced volatiles and ethylene in a timeframe similar to the one observed here (12). Visual and microscopical observations of *P. medicaginis*-infected plants, in *skl* and A17 plants at 96 hours post inoculation (data not shown) demonstrated that *skl* infected plants had considerably more necrosis at the root level than the necrosis observed in infected A17 plants. The aerial parts were almost completely wilted in *skl* plants. These factors together could trigger the production of autocatalytic ethylene and explain the similar induction seen for TC85664 both *skl* and A17 infected plants.

PR10 expression after infection with *P. medicaginis* in both A17 and *skl* infected tissues followed the patterns obtained for *ACC oxidase*. *PR10* is a gene constitutively expressed in nodules of *M. truncatula*, but its function is not clear. PR10 family of pathogenesis related proteins are seen as providers of small peptides with antifungal properties. Because PR10 proteins are expressed in reaction to ethylene and jasmonic acid defense responses, the intent of this experiment was to follow the expression pattern of this gene and determine the extent of impairment of *skl* defense responses. Unfortunately, the constitutively expression of this transcript precluded it being a useful gene to characterize *skl* mutation.

The comparison of gene expression data for *PAL*, *IFR* and *CHS* homologues suggested that their expression was coordinated after pathogen infection. In this study, the specific amplification of particular transcripts was attempted to find those cases of coordinated gene induction.

However, the expression profiling analysis of *PAL*, *CHS* and *IFR* homologues was difficult to assess. In the case of *CHS* homologues, the experimental results from two experiments were different, but the patterns obtained remained constant. In one of the experiments, at time 0 before inoculation, the basal levels for the transcripts were found to be low. The use of the time 0 not inoculated samples as the calibrator to deduce the induction or repression pattern of the time course experiment generated high values of relative induction in all the infected time points. The values found were in some cases a hundred-to a thousand-fold higher than in the replicated experiment, which used a different set of equally treated plants. Furthermore, in both sets of plants, the TC values

for the internal control gene were always in the same range as in infected tissues, suggesting different initial calibrator concentration in the template instead of different concentration of cDNA template for that particular control sample during real time PCR. To resolve the inconsistency between experiments, each experiment was analyzed independently rather than as a single dataset. The fact that this problem was only observed for *CHS* transcripts suggested a localized induction of this transcript created by a unique, undetected stress response generated during the development of the experiment, instead of a general contamination of the experiment.

Phytoalexin production in *M. truncatula* begins with the production of flavonoid compounds in a series of reactions involving the enzymes PAL and CHS. IFR and O-methyltransferase (IOMT) are required in the later stages of the process to transform the deoxyflavonoid daidzein into medicarpin, the major phytoalexin of alfalfa and *M. truncatula*. The pathway leading to medicarpin production is highly regulated and involves many more than these four enzymes (46-48). Several analyses have characterized the different steps involved in medicarpin production and its importance in disease resistance (46-48, 84, 199). Medicarpin and other phytoalexin detoxifying metabolic pathways have been described in plant pathogenic fungi, suggesting the importance of this plant antibiotic in disease resistance (170). Recently, the studies of Mundodi et al. (124,125) suggested that upon pathogen infection, the biosynthesis of antifungal phytoalexins in alfalfa and other legumes was correlated with higher resistance to fungal pathogens. Other research suggests that medicarpin accumulation occurred faster and its effect lasted longer in incompatible interactions involving fungal

pathogens (46-48). Studies such as Stevenson et al. (175), and Samac et al. (14), previously suggested the importance of the phytoalexins medicarpin and maackiain in the control of *F. oxisporum* f.sp. *ciceri* in chickpea and *Pratylenchus penetrans* in alfalfa.

In this study, it was shown that the pathways leading to medicarpin accumulation was activated in both *skl* and A17 infected plants. The results of the transcription profiling experiments suggested that *skl* plants should produce medicarpin, but the time and intensity of the response might be different than in A17. Testing of this hypothesis requires the characterization of root exudates by liquid chromatography in a similarly designed time course experiment. *skl* plants infected with *P. medicaginis* were severely affected by the pathogen, suggesting that additional defense mechanisms other than medicarpin production are present in A17 plants but impaired in *skl* mutants. Quantification of reactive oxygen species and real time PCR of genes induced by salicylic acid production or jasmonic acid production may provide further insights into the *skl* mutation. Another experiment that may assist in clarifying *skl*'s role in defense responses is the transcription profiling of *skl* and A17 plants upon infection with natural symbionts such as *S. meliloti* and *Glomus sp.*

Data analysis of the *GST* homologues showed that both transcripts were expressed in A17 and *skl* infected tissues. The gene expression analysis of the *GST* homologues demonstrated that these transcripts were expressed at higher levels in *skl* mutants than in A17, suggesting a similar regulation pattern as *PAL*, *CHS* and *IFR* genes. Because *GST* had an extremely high number of homologues, the biological

significance of the real time PCR results is difficult to understand. Nonetheless, a possible mechanistic process can be proposed. GSTs are thought to be involved in the protection of cells against oxidative damage. GSTs work by reducing the energy of reactive molecules with the addition of tripeptide glutathione (GSH), but the mechanisms involved in such protection are not clear (117). Ethylene production in *P. medicaginis* infected plants trigger secondary defense responses such as localized cell death mechanisms, as well as the induction of genes involved in defense responses, therefore the activation of protection mechanisms mediated by GST molecules is expected. The role of GSTs in the degradation of xenobiotic compounds as well as GST induction after exposure to plant hormones such as abscisic acid, gibberelic acid, ethylene and auxin has been reported (117). Plant exposure to pathogens, bright light, dehydration, and wounding also induced transcripts of this gene family (117). Experiments to measure the production of reactive species as a result of pathogen exposure could clarify the role of this gene family not only in *skl* background, but also in the general defense responses of this model species.

Recently, *skl* was shown to be the *EIN2* homologue of *A. thaliana*. The in silico analysis performed in this study was unable to establish the number of *EIN2* homologues in this model legume. Efforts to find them using EST databases were hampered by the extensive homology of this gene to protein kinases. The results observed for the genes involved in the phenylpropanoid metabolism, ethylene production, as well as the expression profile of *GST* homologues, can be explained on the basis of decreased signal transduction of ethylene derived responses. The salicylic acid derived defense responses

that are normally counteracted by the ethylene-JA signal transduction become partially unblocked. It is accepted that ethylene-jasmonic acid defense responses cross talk to repress the salicylic acid derived defense responses (49), and *skl* impairment in the ethylene signaling pathway could remove the repression of the responses induced by salicylic acid accumulation. Under the regulation of SA, the increase in *PAL* (TC85501), *CHS* (TC85138) and *IFR* (TC 85477) would be explained, while the expression of *CHS* (TC76765) could be dependent on ethylene accumulation after pathogen infection. The almost totally opposite expression pattern found for both *CHS* homologues suggested different regulation of these proteins at the transcriptional level. An examination of the in silica expression pattern found for both *CHS* homologues corroborates this assessment. TC85138 was highly expressed in *Phytophthora* infected roots, while TC76765 was also expressed under this condition, but at a considerably lower level. It is possible that TC85138 is globally regulated, while TC76765 is pathogen dependent. Experiments designed to test *skl* deficiencies under an *npr1* or *nahG* background could further clarify the role of *skl* in defense responses.

CHAPTER V

SUMMARY

In this dissertation, the analysis of *M. truncatula* lines with a mutation in *skl*, a gene homologous to *A. thaliana ein2* was accomplished. The analysis of *skl* was performed at two levels. Initially, the response of individuals with the *skl* mutation to pathogens such as *P. medicaginis*, *C. trifolii*, *R. solani*, *P. ultimum* and *P. irregulare* was assessed. Plants with the *skl* mutation were hyperinfected by the oomycete pathogens, but not by the true fungi *C. trifolii* or *R. solani*. A time course experiment to characterize the response of *skl* to *P. medicaginis* indicated that the mutant plants were almost invariably killed by the pathogen whereas the control genotype (A17) had only 30% mortality. Quantification of oomycete reproductive structures showed the extraordinary ease with which the pathogen colonized the mutant plants. Quantification of ethylene production following infection by *P. medicaginis* of A17 and *skl* genotypes showed a bi-modal pattern of ethylene evolution. The ethylene burst in A17 was determined to be higher than in *skl*, but the ethylene production in the mutant was higher than in the non-inoculated controls.

To determine the relative response of *M. truncatula* plants to infection by *P. medicaginis*, 96 ecotypes and commercial cultivars representing populations from Algeria, France, Spain, Portugal and Greece were inoculated with oospores of the pathogen. The results indicated that the genotype A17 is a resistant ecotype. Four other populations, including GRE065 and FRA20031 from Greece and France respectively,

demonstrated higher resistance than A17. On the other hand, *skl* mutation, as well as DZA220 and DZA222 from Algeria, plus 19 other ecotypes and cultivars mainly from Spain and Algeria were within a group of populations susceptible to *P. medicaginis* infection.

Characterization of the *skl* mutation at the transcriptional level was attempted by real time RTPCR. Literature searches for genes and pathways involved in plant defense responses towards pathogens and pests provided a list of candidate genes for analysis, that were suspected of being regulated by the *skl* mutation. Sequence information for such genes were mined from the *M. truncatula* EST database (MTGI), using Basic Local Alignment Search Tools (Blast). Data were corrected for inconsistencies and analyzed in silico. Putative gene homologues that seemed to satisfy expression conditions, such as a high expression in EST libraries derived from plant tissues exposed to pathogens or expression in EST libraries derived from elicitors of pathogen interactions and that had the greatest potential to detreat *skl*'s impairments were chosen for further study.

Real time RTPCR of replicated time course experiments, involving *skl* and A17 plants infected with *P. medicaginis*, indicated that *skl* was hampered in its ability to induce transcription of downstream genes involved in *Phytophthora* resistance, such as *ACC oxidase* homologues. *skl*'s inability to correctly induce transcriptional responses seemed to cause an increase in the transcriptional response of genes, such as *GST*, *IFR*, *CHS* and *PAL* that act through the SAR pathway. These results are in agreement with a mechanism where the block of SAR signals that is expected to occur upon activation of defense responses mediated by JA/ethylene is not present, and likely due to the lack of

ethylene derived defense signals mediated by *skl*. The observed results also provided evidence of functional homology between *skl* and its orthologous sequence, the *Arabidopsis thaliana* *EIN2* gene.

LITERATURE CITED

1. Ablett, E., Seaton, G., Scott, K., Shelton, D., Graham, M. W., Baverstock, P., Slade, L., and Henry, R. 2000. Analysis of grape EST: global gene expression patterns in leaf and berry. *Plant Science* 159: 87–95.
2. Adams, M. D., Kerlavage, A. R., Fleischmann, R. D., Fuldner, R. A., Bult C. J., Lee, N. H., Kirkness, E. F., Weinstock, K. G., Gocayne, J. D., and White, O. 1995. Initial assessment of human gene diversity and expression patterns based upon 83 million nucleotides of cDNA sequence. *Nature* 377 (6547 suppl.): 3-174.
3. Agrios, G. N. 1997. Control of plant diseases. Pages 173-221 in: *Plant pathology*. G. N., Agrios, ed. Academic Press. San Diego. CA.
4. Agrios, G. N. 1997. Genetics of plant disease. Pages 115-142 in: *Plant pathology*. G. N., Agrios, ed. Academic Press. San Diego. CA.
5. Alexopoulos, C. J., Mims, C. W., and Blackwell, M. 1996. Phylum Oomycota. Pages 683-737 in: *Introductory mycology*. C. J. Alexopoulos, C. W. Mims, and M. Blackwell, eds. John Wiley & Sons, Inc, New York, NY.
6. Allen, D. J. 1983. Introduction. Pages 1-17 in: *The pathology of tropical food legumes : disease resistance in crop improvement*, D. J. Allen, ed. John Wiley & sons. New York, NY.
7. Allen, D. J., and Lenné, J. M. 1998. Disease as a constraint to production of legumes in agriculture. Pages 1-61 in: *The pathology of food and pasture legumes*, D. J. Allen, and J. M. Lenné, eds. ICRISAT & CAB International, New York, NY.
8. Alonso, J. M., Hirayama, T., Roman, G., Nourizadeh, S., and Ecker, J. R. 1999. EIN2, a bifunctional transducer of ethylene and stress responses in *Arabidopsis*, *Science* 284: 2148-2152.
9. Altier, N. A., Barnes, D. K., Thies, J. A., and Samac, D. A. 1995. *Pythium* seed rot and damping-off resistance in: Standard tests to characterize alfalfa cultivars. North America Alfalfa Improvement Conference (NAAIC). Oklahoma State University, Stillwater, OK. <http://www.naaic.org/stdtests/pythium.htm>.
10. Altier, N. A., and Thies J. A. 1995. Identification of resistance to *Pythium* seedling diseases in alfalfa using a culture plate method. *Plant Dis.* 79: 341-346.

11. Ané, J. M., Kiss, G. B., Riely, B. K., Penmetsa, R. V., Oldroyd G. E. D., Ayax, C., Lévy, J., Debellé, F., Baek, J. M., Kalo, P., Rosenberg, C., Roe, B. A., Long, S. R., Dénarié, J., and Cook D. R. 2004. *Medicago truncatula DM11* required for bacterial and fungal symbioses in legumes. *Science* 303: 1364-1367.
12. Arimura, G., Ozawa, R., Nishioka, T., Boland, W., Koch, T., Kühnemann, F., and Takabayashi, J. 2002. Herbivore-induced volatiles induce the emission of ethylene in neighboring lima bean plants. *Plant Journal* 29: 87-98.
13. Bajaj, Y. P. S. 1990. Wide hybridization, transformation, cryopreservation. Pages 1-20 in: *Biotechnology in agriculture and forestry: legumes and oilseed crops*. Y. P. S. Bajaj, ed. Springer-Verlag. Berlin, Germany.
14. Baldridge, G. D., and O'Neill, N. R., Samac, D. A. 1998. Alfalfa (*Medicago sativa* L.) resistance to the root-lesion nematode, *Pratylenchus penetrans*: defense-response gene mRNA and isoflavonoid phytoalexin levels in roots. *Plant Mol. Biol.* 38: 999-1010.
15. Barbetti, M. J. 1989. Response of *Medicago* cultivars to fungal root pathogens associated with *Trifolium subterraneum*. *Plant Protection Quarterly* 4: 75-77.
16. Bartnicki-Garcia, S., and Wong, M. C. 1983. Biochemical aspects of morphogenesis in *Phytophthora*. Pages 121-137 in: *Phytophthora: its biology, taxonomy, ecology and pathology*. D. C. Erwin, S. Bartnicki-Garcia, and P. M. Tsao, eds. The American Phytopathological Society Press, St. Paul, MN.
17. Bell, E., and Mullet, J. 1993. Characterization of an *Arabidopsis* lipoxigenases gene responsive to methyl jasmonate and wounding. *Plant Physiol.* 103: 1133-1137.
18. Ben Amor, B., Shaw, S. L., Oldroyd, G. E. D., Maillet, F., Penmetsa, R. V., Cook, D. R., Long, S. R., Dénarié, J., and Gough, C. 2003. The NFP locus of *Medicago truncatula* controls an early step of Nod factor signal transduction upstream of a rapid calcium flux and root hair formation. *Plant Journal* 34: 495-506.
19. Bent, A. 2001. Plant mitogen-activated protein kinase cascades: negative regulatory roles turn out positive. *Proc. Natl. Acad. Sci. USA* 98: 784-786.
20. Bent, A. F., Innes, R. W., Ecker, J. R., and Staskawicz, B. J. 1992. Disease development in ethylene-insensitive *Arabidopsis thaliana* infected with virulent and avirulent *Pseudomonas* and *Xanthomonas* pathogens. *Mol. Plant-Microbe Interact.* 5: 372-378.

21. Bleecker, A. B. 1999. Ethylene perception and signaling: an evolutionary perspective. *Trends in Plant Science* 4: 269-274.
22. Bohnert, H. J., Ayoubi, P., Borchert, C., Bressan, R. A., Burnap, R. L., Cushman, J. C., Cushman, M. A., Deyholos, M., Fischer, R., and Galbraith, D. W. 2001. A genomics approach towards salt stress tolerance. *Plant Physiol. Biochem.* 39: 295–311.
23. Boisson-Dernier, A., Chabaud, M., Garcia, F., Bécard, G., Rosenberg, C., and Barker, D. G. 2001. *Agrobacterium rhizogenes*-transformed roots of *Medicago truncatula* for the study of nitrogen-fixing and endomycorrhizal symbiotic associations. *Mol. Plant-Microbe Interact.* 14: 693-700.
24. Borlaug, N. E. 2000. Ending world hunger. The promise of biotechnology and the threat of antisience zealotry. *Plant Physiol.* 124: 487–490.
25. Brady, N. C. 1998. Food legume research sponsored by the United States Agency for International Development (AID). Pages 3-6 in: *World crops: cool season food legumes*. R. J. Summerfield, ed. Kluwer Academic Publishers. Boston, MA.
26. Bustin, S. A. 2000. Absolute quantification of mRNA using real-time reverse transcription polymerase chain reaction assays. *J. Molec. Endocr.* 25: 169-193.
27. Bustin, S. A. 2002. Quantification of mRNA using real-time reverse transcription PCR (RT-PCR): trends and problems. *J. Molec. Endocr.* 29: 23-39.
28. Cao, H., Li, X., and Dong, X. 1998. Generation of broad-spectrum disease resistance by overexpression of an essential regulatory gene in systemic acquired resistance. *Proc. Natl. Acad. Sci. USA* 95: 6531-6536.
29. Carlile, M. 1983. Motility, taxis, and tropism in *Phytophthora*. Pages 95-105 in: *Phytophthora: its biology, taxonomy, ecology and pathology*. D.C. Erwin, S. Bartnicki-Garcia, and P. M. Tsao, eds. The American Phytopathological Society Press, St. Paul, MN.
30. Catoira, R., Galera, C., de Billy, F., Journet, E. P., Maillet, F., Penmetsa, V., Rosenberg, C., Gough, C., Cook, D. and Dénarié, J. 2000. Four genes of *Medicago truncatula* controlling components of a Nod factor transduction pathway. *Plant Cell* 12: 1647–1665.
31. Century, K. S., Holub, E. B., and Staskawicz, B. J. 1995. *NDR1*, a locus of *Arabidopsis thaliana* that is required for disease resistance to both a bacterial and a fungal pathogen. *Proc. Natl. Acad. Sci. USA* 92: 6597-6601.

32. Century, K. S., Shapiro, A. D., Repetti, P. P., Dahlbeck, D., Holub, E., and Staskawicz, B. J. 1997. NDR1, a pathogen-induced component required for *Arabidopsis* disease resistance. *Science* 278: 1963-1965.
33. Chang, C., and Shokey, J. A. 1999. The ethylene-response pathway: signal perception to gene regulation. *Curr. Op. Plant Biol.* 2: 352-358.
34. Choi, H. K., Kim, D., Uhm, T., Limpens, E., Lim, H., Mun, J. H., Kalo, P., Penmetsa, R. V., Seres, A., Kulikova, O., Roe, B. A., Bisseling, T., Kiss, G. B., and Cook, D. R. 2004. A sequence-based genetic map of *Medicago truncatula* and comparison of marker colinearity with *M. sativa*. *Genetics* 166: 1463-1502.
35. Clarke, J. D., Liu, Y., Klessig, D. F., and Dong, X. 1998. Uncoupling PR gene expression from *NPR1* and bacterial resistance: characterization of the dominant *Arabidopsis cpr6-1* mutant. *Plant Cell* 10: 557-569.
36. Clough, S., Fengler, K. A., Yu, I. C., Lippok, B., Smith, R. K., and Bent, A. F. 2000. The *Arabidopsis dnd1* “defense, no death” gene encodes a mutated cyclic nucleotide-gated ion channel. *Proc. Natl. Acad. Sci. USA* 97: 9323-9328.
37. Cook, D., Dreyer, D., Bonnet, D., Howell, M., Nony, E., and VandenBosch, K. 1995. Transient induction of a peroxidase gene in *Medicago truncatula* precedes infection by *Rhizobium meliloti*. *Plant Cell* 7: 43-55.
38. Cook, D. R. 1999. *Medicago truncatula* – a model in the making. *Curr. Op. Plant Biol.* 2: 301-304.
39. Cook, D. R., VandenBosch, K., De Bruijn, F., and Huguet, T. 1997. Model legumes get the nod. *Plant Cell* 9: 275-281.
40. Cooke, R., Raynal, M., Laudié, M., Grellet, F., Delseny, M., Morris, P. C., Guerrier, D., Giraudat, J., Quigley, F., and Clabault, G. 1996. Further progress towards a catalogue of all *Arabidopsis* genes: analysis of a set of 5000 non-redundant ESTs. *Plant Journal* 9: 101–124.
41. Covitz, P. A., Smith, L.S. and Long, S.R. 1998. Expressed sequence tags from a root-hair-enriched *Medicago truncatula* cDNA library. *Plant Physiol.* 117: 1325-1332.
42. De la Fuente, L., Quagliotto, L., Bajsa, N., Fabiano, E., Altier, N., and Arias, A. 2002. Inoculation with *Pseudomonas fluorescens* does not affect the symbiosis between rhizobia and forage legumes. *Soil Biol. Biochem.* 34: 545-548.

43. De Wit, P. J. G. M. 1992. Molecular characterization of gene-for-gene systems in plant-fungus interactions and the application of avirulence genes in control of plant pathogens. *Annu. Rev. Phytopathol.* 30: 391-418.
44. Delaney, T. P., Uknes, S. J., Vernooij, B., Friedrich, L., Weymann, K., Negrotto, D., Gaffney, T., Gut-Rella, M., Kessmann, H., Ward, E., and Ryals, J. 1994. A central role of salicylic acid in plant disease resistance. *Science* 266: 1247-1249.
45. Devoto, A., and Turner, J. G. 2003. Regulation of jasmonate-mediated plant responses in *Arabidopsis*. *Annals of Botany* 92: 329-337.
46. Dixon, R. 2001. Natural products and plant disease resistance. *Nature* 411: 843-847.
47. Dixon, R. A., and Paiva, N. 1995. Stress induced phenylpropanoid metabolism. *Plant Cell* 7: 1085-1097.
48. Dixon, R. A., and Steele, C.L. 1999. Flavonoids and isoflavonoids a gold mine for metabolic engineering. *Trends in Plant Science* 4: 394-400.
49. Dong, X. 1998. SA, JA, ethylene and disease resistance in plants. *Curr. Op. Plant Biol.* 1: 316-323.
50. Dong, X. 2001. Genetic dissection of systemic acquired resistance. *Curr. Op. Plant Biol.* 4: 309-314.
51. Ecker J. R. 1995. The ethylene signal transduction pathway in plants. *Science* 268: 667-675.
52. Ellis, C., Karafyllidis, L., Wasternack, C., and Turner, J. G. 2002. The *Arabidopsis* mutant *cevl* links cell wall signaling to jasmonate and ethylene responses. *Plant Cell* 14: 1557-1566.
53. Ellis, C., and Turner, J. G. 2001. The *Arabidopsis* mutant *cevl* has constitutively active jasmonate and ethylene signal pathways and enhanced resistance to pathogens. *Plant Cell* 13: 1025-1033.
54. Endre, G., Kereszt, A., Kevei, Z., Mihacea, S., Kaló, P., and Kiss, G. B. 2002. A receptor kinase gene regulating symbiotic nodule development. *Nature* 417: 962-966.
55. Epple, P., Apel, K., and Bohlmann, H. 1995. An *Arabidopsis thaliana* thionin gene is inducible via a signal transduction pathway different from that for pathogenesis-related proteins. *Plant Physiol.* 109: 813-820.

56. Erwin, D. C., and Ribeiro, O. K. 1996. Control by host resistance. Pages 186-210 in: *Phytophthora*, diseases worldwide. D. C. Erwin, and O. K. Ribeiro, eds. The American Phytopathological Society Press, St. Paul, MN.
57. Erwin, D. C., and Ribeiro, O. K. 1996. Culture, physiology and genetics. Pages 43-95 in: *Phytophthora*, diseases worldwide. D. C. Erwin, and O. K. Ribeiro, eds. The American Phytopathological Society Press, St. Paul, MN.
58. Eulgem T., Rushton, P. J., Robatzek, S., and Somssichet I. E. 2000. The WRKY superfamily of plant transcription factors. *Trends in Plant Science* 5: 199-206.
59. Ewing, R. M., Kahla, A. B., Poirot, O., Lopez, F., Audic, S., and Claverie, J. M. 1999. Large scale statistical analyses of rice EST reveal correlated patterns of gene expression. *Genome Res.* 9: 950-959.
60. Falk, A., Feys, B. J., Frost, L. N., Jones, J. D. G., Daniels, M. J., and Parker, J. E. 1999. *EDSI*, an essential component of R gene-mediated disease resistance in *Arabidopsis* has homology to eukaryotic lipases. *Proc. Natl. Acad. Sci. USA* 96: 3292-3297.
61. Fedorova, M., Van De Mortel, J., Matsumoto, P. A., Cho, J., Town, C. D., VandenBosch, K. A., Gantt, J. S., and Vance, C. P. 2002. Genome-wide identification of nodule-specific transcripts in the model legume *Medicago truncatula*. *Plant Physiol.* 130: 519-537.
62. Fernandes, J., Brendel, V., Gai, X., Lal, S., Chandler, V. L., Elumalai, R. P., Galbraith, D. W., Pierson, E. A., and Walbot, V. 2002. Comparison of RNA expression profiles based on maize expression sequence tag frequency analysis and micro-array hybridization. *Plant Physiol.* 128: 896-910.
63. Feys, B. J. F., Benedetti, C. E., Penfold, C. N., and Turner, J. G. 1994. *Arabidopsis* mutants selected for resistance to the phytotoxin coronatine are male-sterile, insensitive to methyl jasmonate, and resistant to a bacterial pathogen. *Plant Cell* 6: 751-759.
64. Finlayson, S. A., Lee, I. J., and Morgan, P. W. 1998. Phytochrome B and the regulation of circadian ethylene production in sorghum. *Plant Physiol.* 116: 17-25.
65. Fisher, A. J. Grimes, H. D., and Fall, R. 2003. The biochemical origin of pentenol emissions from wounded leaves. *Phytochemistry.* 62: 159-163.

66. Flemming, M. D., and Andrews, N. C. 1998. Mammalian iron transport: an unexpected link between metal homeostasis and host defense. *J. Lab. Clin. Med.* 132: 464-468.
67. Flor, H. H. 1946. Genetics of pathogenicity of *Melampsora lini*. *J. Agricultural Research* 74: 241-262.
68. Franco, G. R., Rabelo, E. M., Azevedo, V., Pena, H. B., Ortega, J. M., Santos, T. M., Meira, W. S., Rodrigues, N. A., Dias, C. M., Harrop, R., Wilson, A., Saber, M., Abdel-Hamid, H., Faria, M. S., Margutti, M. E., Parra, J. C., and Pena, S. D. 1997. Evaluation of cDNA libraries from different developmental stages of *Schistosoma mansoni* for production of expressed sequence tags (EST). *DNA Research* 4: 231-240.
69. Freeman, W. M., Walker, S. J., and Vrana, K. E. 1999. Quantitative RT-PCR: pitfalls and potential. *Biotechniques* 26: 112-125.
70. Frye, C., Tang, D., and Innes, R. W. 2001. Negative regulation of defense responses in plants by a conserved MAPKK kinase. *Proc. Natl. Acad. Sci. USA* 98: 373-378.
71. Gallusci, P., Dedieu, A., Journet, E. P., Huguet, T., and Barker, D. G. 1991. Synchronous expression of leghaemoglobin genes in *Medicago truncatula* during nitrogen-fixing root nodule development and response to exogenously supplied nitrate. *Plant Mol. Biol.* 17: 335-349.
72. Gibson U. E. M., Heid, C. A., and Williams P. M. 1996. A novel method for real time quantitative RT-PCR. *Genome Res.* 6: 995-1001.
73. Gilchrist, D. G. 1998. Programmed cell death in plant disease: the purpose and promise of cellular suicide. *Annu. Rev. Phytopathol.* 36: 393-414.
74. Giulletti, A., Overbergh, L., Valckx, D., Decallonne, B., Bouillon, R., and Mathieu, C. 2001. An overview of real time PCR. *Methods* 25: 386-401.
75. Glazebrook, J. 1999. Genes controlling expression of defense responses in *Arabidopsis*. *Curr. Op. Plant Biol.* 2: 280-286.
76. Glazebrook, J. 2001. Genes controlling expression of defense responses in *Arabidopsis* - 2001 status. *Curr. Op. Plant Biol.* 4: 301-308.
77. Goodman, R. N., and Novacky, A. J. 1994. The hypersensitive reaction in plants to pathogens: a resistance phenomenon. Pages 45-56. The American Phytopathological Society Press. St. Paul, MN.

78. Guinel, F. C., and Sloetjes, L. L. 2000. Ethylene is involved in the nodulation phenotype of *Pisum sativum* R50 (*sym 16*), a pleiotropic mutant that nodulates poorly and has pale green leaves. *J. Exp. Bot.* 51: 885-894.
79. Gut, M., Leutenegger, C. M., Huder, J. B., Pedersen, N. C., and Lutz, H. 1999. One-tube fluorogenic reverse transcription-polymerase chain reaction for the quantitation of feline coronaviruses. *J. Virol. Methods* 77: 37-46.
80. Györgyey, J., Vaubert, D., Jiménez-Zurdo, J. I., Charon, C., Troussard, L., Kondorosi, A., and Kondorosi, E. 2000. Analysis of *Medicago truncatula* nodule expressed sequence tags. *Mol. Plant-Microbe Interact.* 13: 62-71.
81. Hammerschmidt, R. 1999. Phytoalexins: What have we learned after 60 years? *Annu. Rev. Phytopathology.* 37: 285-306.
82. Harrison, M. J. 2000. Molecular genetics of model legumes. *Trends in Plant Science* 5: 414-415.
83. Havey, M. J., and Maxwell, D. P. 1987. Inheritance of *Phytophthora* root rot resistance in two diploid alfalfa species. *Crop Science* 27: 225-228.
84. He, X. Z., and Dixon, R. A. 2000. Genetic manipulation of isoflavone 7-O-methyltransferase enhances biosynthesis of 4'-O-methylated isoflavonoid phytoalexins and disease resistance in alfalfa. *Plant Cell* 12: 1689-1702.
85. Heid, C., Stevens, J., Livak, K. J., and Williams, P. M. 1996. Real time quantitative PCR. *Genome Res.* 6: 986-994.
86. Heidstra, R., Yang, W. C., Yalcin, Y., Peck, S., Emons, A. M., van Kammen, A., and Bisseling, T. 1997. Ethylene provides positional information on cortical cell division but is not involved in Nod factor-induced root hair tip growth in *Rhizobium*-legume interaction. *Development* 124: 1781-1787.
87. Hirayama, T. and Alonso, J. M. 2000. Ethylene captures a metal! Metal ions are involved in ethylene perception and signal transduction. *Plant Cell Physiol.* 41: 548-555.
88. Hohrein, B. A., and Bean, G. A. 1983. Greenhouse technique to evaluate alfalfa resistance to *Phytophthora megasperma* f. sp. *medicaginis*. *Plant Dis.* 67: 1332-1333.
89. Innes, R. W. 1998. Genetic dissection of R gene signal transduction pathways. *Curr. Op. Plant Biol.* 1: 229-304.

90. Iturbe-Ormaetxe, I., Haralampidis, K., Papadopoulou, K., and Osbourn, A. E. 2003. Molecular cloning and characterization of triterpene synthases from *Medicago truncatula* and *Lotus japonicus*. *Plant Mol. Biol.* 51: 731-743.
91. Jhonson, P. R., and Ecker, J. R. 1998. The ethylene signal transduction pathway: a molecular perspective. *Annu. Rev. Genet.* 32: 227-254.
92. Jones, C. R., and Samac, D. A. 1996. Biological control of fungi causing alfalfa seedling damping-off with a disease-suppressive strain of *Streptomyces*. *Biological Control* 7: 196-204.
93. Journet, E. P., van Tuinen, D., Gouzy, J., Crespeau, H., Carreau, V., Farmer, M. J., Niebel, A., Schiex, T., Jaillon, O., Chatagnier, O., Godiard, L., Micheli, F., Kahn, D., Gianinazzi-Pearson, V., and Gamas, P. 2002. Exploring root symbiotic programs in the model legume *Medicago truncatula* using EST analysis. *Nucleic Acids Res.* 30: 5579-5592.
94. Kamaté, K., Rodriguez-Llorente, I. D., Scholte, M., Durand, P., Ratet, P., Kondorosi, E., Kondorosi, A., and Trinh, T. H. 2000. Transformation of floral organs with GFP in *Medicago truncatula*. *Plant Cell Reports* 19: 647-653.
95. Keen, N. T., and Yoshikawa, M. 1983. Physiology of disease and the nature of resistance to *Phytophthora*. Pages 279-287 in: *Phytophthora: its biology, taxonomy, ecology and pathology*. D. C. Erwin, S. Bartnicki-Garcia, and P. M. Tsao, eds. The American Phytopathological Society Press, St. Paul, MN.
96. Kieber, J. J., Rothenberg, M., Roman, G., Feldmann, K. A., and Ecker, J. R. 1993. *CTR1*, a negative regulator of the ethylene response pathway in *Arabidopsis*, encodes a member of the RAF family of protein kinases. *Cell.* 72: 427-441.
97. Kinkema, M., Fan, W., and Dong, X. 2000. Nuclear localization of NPR1 Is required for activation of PR gene expression. *Plant Cell* 12: 2339-2350.
98. Knoester, M., van Loon, L. C., and van den Heuvel, J. 1998. Ethylene-insensitive tobacco lacks non-host resistance against soil-borne fungi. *Proc. Natl. Acad. Sci. USA* 95: 1933-1937.
99. Kolomiets, M. V., Chen, H., Gladon, R. J., and Hannapel, D. J. 2000. A leaf lipoxygenase of potato induced specifically by pathogen infection. *Plant Physiol.* 124: 1121-1130.

100. Kruger, W. M., Pritsch, C., Chao, S., and Muehlbauer, G. J. 2002. Functional and comparative bioinformatic analysis of expressed genes from wheat spikes infected with *Fusarium graminearum*. *Mol. Plant-Microbe Interact.* 15: 445–455.
101. Kulikova, O., Gualtieri, G., Geurts, R., Kim, D. J., Cook, D., Huguet, T., de Jong, J. H., Fransz, P. F., and Bisseling, T. 2001. Integration of the FISH pachytene and genetic maps of *Medicago truncatula*. *Plant Journal* 27: 49-58.
102. Kumar, D., and Klessig, D. F. 2000. Differential induction of tobacco MAP kinases by the defense signals nitric oxide, salicylic acid, ethylene, and jasmonic acid. *Mol. Plant-Microbe Interact.* 13: 347-351.
103. Kunkel, B. N., and Brooks, D. M. 2002. Cross talk between signaling pathways in pathogen defense. *Curr. Op. Plant Biol.* 5: 325–331.
104. Lamb, C., and Dixon, R. A. 1996. The oxidative burst in plant disease resistance. *Annu. Rev. Plant Physiol. Plant Mol. Biol.* 48: 251-275.
105. Lebel, E., Heifetz, P., Thorne, L., Uknes, S., Ryals, J., and Wardet, E. 1998. Functional analysis of regulatory sequences controlling *PR-1* gene expression in *Arabidopsis*. *Plant Journal* 16: 223-233.
106. Lee, N. H., Weinstock, K. G., Kirkness, E. F., Earle-Hugues, J. A., Fuldner, R. A., Marmaros, S., Glodek, A., Gocayne, J. D., Adams, M. D., and Kerlavage, A. R. 1995. Comparative expressed-tag analysis of differential gene expression profiles in PC-12 cells before and after nerve growth factor treatment. *Proc. Natl. Acad. Sci. USA* 92: 8303-8307.
107. Leutenegger, C. M., Mislin, C. N., Sigrist, B., Ehrenguber, M. U., Hofmann-Lehmann, R., and Lutz, H. 1999. Quantitative real-time PCR for the measurement of feline cytokine mRNA. *Vet. Immunol. Immunopathol.* 71: 291-305.
108. Li, X., Clarke, J. D., Zhang, Y., and Dong, X. 2001. Activation of an EDS1-mediated R-gene pathway in the *sncl* mutant leads to constitutive, NPR1-independent pathogen resistance. *Mol. Plant-Microbe Interact.* 14: 1131-1139.
109. Liang, F., Holt, I., Perteau, G., Karamycheva, S., Salzberg, S. L., and Quackenbush, J. 2000. An optimized protocol for analysis of EST sequences. *Nucleic Acids Res.* 28: 3657-3665.

110. Liu, J., Blaylock, L. A., Endre, G., Cho, J., Town, C. D., VandenBosch, K. A., and Harrison, M. J. 2003. Transcript profiling coupled with spatial expression analyses reveals genes involved in distinct developmental stages of an arbuscular mycorrhizal symbiosis. *Plant Cell* 15: 2106-2123.
111. Liu, Y., Zhang, S., and Klessig, D. F. 2000. Molecular cloning and characterization of a tobacco MAP kinase kinase that interacts with SIPK. *Mol. Plant-Microbe Interact.* 13: 229-124.
112. Livak, K. J., and Schmittgen, T. D. 2001. Analysis of relative gene expression data using real time quantitative PCR and the 2- $\Delta\Delta$ Ct method. *Methods* 25: 402-408.
113. Lullien, V., Barker, D. G., de Lajudie, P., and Huguet, T. 1987. Plant gene expression in effective and ineffective root nodules of alfalfa (*Medicago sativa*). *Plant Mol. Biol.* 9: 469-478.
114. Mackay, I. M., Arden, K. E., and Nitsche, A. 2002. Real-time PCR in virology. *Nucleic Acids Res.* 30: 1292-1305.
115. Maleck, K., Levine, A., Eulgem, T., Morgan, A., Schmid, J., Lawton, K. A., Dangel, J. L., and Dietrich, R. A. 2000. The transcriptome of *Arabidopsis thaliana* during systemic acquired resistance. *Nature Genet.* 26: 403-410.
116. Mangalathu, R., Ranamukhaarachchi, D. G., Vernon, S. D., and Unger, E. R. 2001. Use of Real-Time Quantitative PCR to validate the results of cDNA array and differential display PCR technologies. *Methods* 25: 443-451.
117. McGonigle, B., Keeler, S. J., Lau S. C. L., Koeppe, M. K., and O'Keefe, D. P. 2000. A genomics approach to the comprehensive analysis of the *Glutathione S-Transferase* gene family in soybean and maize. *Plant Physiol.* 124: 1105-1120.
118. McGrath, R., and Ecker, J. R. 1998. Ethylene signaling in *Arabidopsis*: events from the membrane to the nucleus. *Plant Physiol. Biochem.* 36: 103-113.
119. Melan, M., Dong, X., Endara, M. E., Davis, K. R., Ausubel, F. M., and Peterman, T. K. 1993. An *Arabidopsis thaliana* lipoxygenase gene can be induced by pathogens, abscisic acid, and methyl jasmonate. *Plant Physiol.* 101: 441-450.
120. Miller, S., and Maxwell, D. P. 1984. Light microscope observations of susceptible, host resistant, and nonhost resistant interactions of alfalfa with *Phytophthora megasperma*. *Can. J. Bot.* 62: 109-116.

121. Mitra, R. M., Gleason, C. A., Edwards, A., Hadfield, J., Downie, J. A., Oldroyd, G. E. D., and Long S. R. 2004. A Ca²⁺/calmodulin-dependent protein kinase required for symbiotic nodule development: gene identification by transcript-based cloning. *Proc. Nat. Acad. Sci. USA* 101: 4701-4705.
122. Mitra, R. M., and Long, S. R. 2004. Plant and bacterial symbiotic mutants define three transcriptionally distinct stages in the development of the *Medicago truncatula*/*Sinorhizobium meliloti* symbiosis. *Plant Physiol.* 134: 595–604.
123. Molecular Probes, Inc. 2004. Handbook of fluorescent probes and research products. Section 1.1: Introduction to amine modification. <http://www.probes.com/handbook/sections/0101.html>.
124. Mundodi, S. R., and Paiva, N. L. 2000. Expression of a medicarpin detoxification gene in alfalfa. (Abstr.) *Plant Biology Meeting (ASPB)*: 281.
125. Mundodi, S. R., Watson, B. S., Lopez-Meyer, M., and Paiva, N. L. 2001. Functional expression and subcellular localization of the *Nectria haematococca* Mak1 phytoalexin detoxification enzyme in transgenic tobacco. *Plant Mol. Biol.* 46: 421-432.
126. Nam, Y-W., Penmetsa, R. V., Endre, G., Uribe, P., Kim, D., and Cook, D. R. 1999. Construction of a bacterial artificial chromosome library of *Medicago truncatula* and identification of clones containing ethylene-response genes. *Theor. Applied Genetics.* 98: 638-646.
127. Nolan, K. E., Irwanto, R., and Rose, R. J. 2003. Auxin up-regulates *MtSERK1* expression in both *Medicago truncatula* root-forming and embryogenic cultures. *Plant Physiol.* 133: 218-230.
128. Norman-Setterblad, C., Vidal, S., and Palva, E. T. 2000. Interacting signal pathways control defense gene expression in *Arabidopsis* in response to cell wall-degrading enzymes from *Erwinia carotovora*. *Mol. Plant-Microbe Interact.* 13: 430-438.
129. Nürnberger, T., and Scheel, D. 2001. Signal transmission in the plant immune response. *Trends in Plant Science* 6: 372-379.
130. Nygaard, S., Tofte, J., and Barnes, D. K. 1995. *Phytophthora* root rot-seedling in: Standard tests to characterize alfalfa cultivars. North America Alfalfa Improvement Conference (NAAIC). Oklahoma State University, Stillwater, OK. <http://www.naaic.org/stdtests/phytoptseeds.htm>.

131. Nygaard, S. L., and Grau, C. R. 1989. *Phytophthora megasperma* virulence to alfalfa measured using single-isolate zoospore suspensions. *Can. J. Plant Pathol.* 11: 101-108.
132. O'Neill, N. R. 1991. Anthracnose in: Standard tests to characterize alfalfa cultivars. North America Alfalfa Improvement Conference (NAAIC). Third edition (1991). Oklahoma State University, Stillwater, OK. <http://www.naaic.org/stdtests/anthracn.html>.
133. O'Neill, N. R. 1996. Defense expression in protected tissues of *Medicago sativa* is enhanced during compatible interactions with *Colletotrichum trifolii*. *Phytopathology* 86: 1045-1050.
134. O'Neill, N. R. 1996. Pathogenic variability and host resistance in the *Colletotrichum trifolii* / *Medicago sativa* pathosystem. *Plant Dis.* 80: 450-457.
135. O'Neill, N. R., Bauchan, G. R., and Samac, D. A. 2003. Reactions in the annual *Medicago spp.* core germplasm collection to *Phoma medicaginis*. *Plant Dis.* 87: 557-562.
136. O'Neill, N. R., and Saunders, J. A. 1994. Compatible and incompatible responses in alfalfa cotyledons to races 1 and 2 of *Colletotrichum trifolii*. *Phytopathology* 84: 283-287.
137. Oklahoma Cooperative Extension Service. 2003. Root and crown diseases. Pages 30-33 in: E-826, Alfalfa production guide for the southern great plains. Oklahoma State University. Stillwater, OK.
138. Okubo, K., Hori, N., Matoba, R., Niiyama, T., Fukushima, A., Kojima, Y., and Matsubara, K. 1992. Large scale cDNA sequencing for analysis of quantitative and qualitative aspects of gene expression. *Nature Genet.* 2: 173-179.
139. Okubo, K., Itoh, K., Fukushima, A., Yoshii, J., and Matsubara, K. 1995. Monitoring cell physiology by expression profiles and discovering cell type-specific genes by compiled expression profiles. *Genomics* 30: 178-186.
140. Oldroyd, G., Engstrom, E., and Long, S. R. 2001. Ethylene inhibits the Nod factor signal transduction pathway of *Medicago truncatula*. *Plant Cell* 13: 1835-1849.
141. Oldroyd, G., and Geurts, R. 2001. *Medicago truncatula*, going where no plant has gone before. *Trends in Plant Science.* 6: 552-554.

142. Oldroyd, G., Mitra, R. M., Wais, R. J., and Long, S. R. 2001. Evidence for structurally specific negative feedback in the Nod factor signal transduction pathway. *Plant Journal* 28: 191-199.
143. Oldroyd, G.E.D. 2001. Dissecting symbiosis: developments in Nod factor signal transduction. *Annals of Bot.* 87: 709-718.
144. Orozco-Cárdenas, M. L., Narváez-Vásquez, J., and Ryan, C. A. 2001. Hydrogen peroxide acts as a second messenger for the induction of defense genes in tomato plants in response to wounding, systemin, and methyl jasmonate. *Plant Cell* 13: 179-191.
145. Parker, J. E., Knoegge, W., and Scheel, D. 1989. Molecular aspects of host-pathogen interactions in *Phytophthora*. Pages 91-103 in: *Phytophthora*. J.A. Lucas, R. C. Shas, D. C. Shaw, and L. R. Cooke, eds. Cambridge University Press. Cambridge, United Kingdom.
146. Penmetsa, R. V., and Cook, D. R. 1997. A legume ethylene-insensitive mutant hyperinfected by its rhizobial symbiont. *Science* 275: 527-530.
147. Penmetsa, R. V., and Cook, D. R. 2000. Production and characterization of diverse developmental mutants of *Medicago truncatula*. *Plant Physiol.* 123: 1387-1397.
148. Penmetsa, V., Frugoli, J., Smith, L. S., Long, S. R., and Cook, D. R. 2003. Dual genetic pathways controlling nodule number in *Medicago truncatula*. *Plant Physiol.* 131: 998-1008.
149. Penninckx, I., Eggermont, K., Terras, F., and Thomma, B. 1996. Pathogen-induced systemic activation of a plant defensin gene in *Arabidopsis* follows a salicylic acid-independent pathway. *Plant Cell* 8: 2309-2323.
150. Perfect, S. E., Hughes, H. B., O'Connell, R. J., and Green, J. R. 1999. *Colletotrichum*: A model genus for studies on pathology and fungal-plant interactions. *Fungal Genetics & Biology* 27: 186-198.
151. Petersen, M., Brodersen, P., Naested, H., Andreasson, E., Lindhart, U., Johansen, B., Nielsen, H. B., Lacy, M., Austin, M. J., Parker, J. E. Sharma, S. B., Klessig, D. F., Martienssen, R., Mattsson, O., Jensen, A. B., and Mundy, J. 2000. *Arabidopsis* MAP kinase 4 negatively regulates systemic acquired resistance. *Cell* 103: 1111-1120.

152. Pieterse, C., van Wees, S., and van Pelt, J. 1998. A novel signaling pathway controlling induced systemic resistance in *Arabidopsis*. *Plant Cell*. 10: 1571-1580.
153. Powell, N. T., Meléndez, P. L., and Batten, C. K. 1971. Disease complexes in tobacco involving *Meloidogyne incognita* and certain soil-borne fungi. *Phytopathology* 61: 1332-1337.
154. Quackenbush, J., Cho, J., Lee, D., Liang, F., Holt, I., Karamycheva, S., Parvizi, B., Pertea, G., Sultana, R., and White, J. 2001. The TIGR Gene Indices: analysis of gene transcript sequences in highly sampled eukaryotic species. *Nucleic Acids Res.* 29: 159-164.
155. Ramu, S. K., Peng, H. M., and Cook, D. R. 2002. Nod factor induction of reactive oxygen species production is correlated with expression of the early nodulin gene *rip1* in *Medicago truncatula*. *Mol. Plant-Microbe Interact.* 15: 522-528.
156. Reddy, M. V., Raju, T. N., and Lenné, J. M. 1998. Diseases of pigeonpea. Pages 517-558 in: *The pathology of food and pasture legumes*, D. J. Allen, and J. M. Lenné, eds. ICRISAT & CAB International, New York, NY.
157. Reue, K. 1998. mRNA quantitation techniques: considerations for experimental design and application. *Journal of Nutrition* 128: 2038-2044.
158. Roetschi, A., Si-Ammour, A., Belbahri, L., Mauch, F., and Mauch-Mani, B. 2001. Characterization of an *Arabidopsis-Phytophthora* pathosystem: Resistance requires a functional *PAD2* gene and is independent of salicylic acid, ethylene and jasmonic acid signaling. *Plant Journal* 28: 293-305.
159. Rushton, P. J., Torres, J. T., Parniske, M., Wernert, P., Hahlbrock, K., and Somssich, I. E. 1996. Interaction of elicitor-induced DNA-binding proteins with elicitor response elements in the promoters of parsley *PR1* genes. *EMBO J.* 15: 5690-5700.
160. Ryals, J. A., Neuenschwander, U. H., Willits, M. G., Molina, A., Steiner, H. Y., and Hunt, M. D. 1996. Systemic acquired resistance. *Plant Cell* 8: 1809-1819.
161. Ryan, C. A., Pearce, G., Johnson, S., McGurl, B., Orozco-Cardenas, M., and Farmer, E. 1993. Systemin, a polypeptide signal for proteinase inhibitor gene expression in plants. Pages 196-201 in: *Developments in plant pathology; mechanisms of plant defense responses*. B. Fritig, and M. Legrand, eds. Vol. 2. Kluwer Academic Publishers, Boston, MA.

162. Saitou, N., and Nei, M. 1987. The neighbor-joining method: a new method for reconstructing phylogenetic trees. *Mol. Biol. Evol.* 4: 406-425.
163. Salzer, P., Bonanomi, A., Beyer, K., Vögeli-Lange, R., Aeschbacher, R. A., Lange, J., Wiemken, A., Kim, D., Cook, D. R., and Boller, T. 2000. Differential expression of eight chitinase genes in *Medicago truncatula* roots during mycorrhiza formation, nodulation, and pathogen infection. *Mol. Plant-Microbe Interact.* 13: 763–777.
164. Sambrook, J., and Russell, D. W. 2001. *Molecular cloning: A laboratory manual*. Cold Spring Harbor Laboratory Press. Cold Spring Harbor, NY.
165. Sasaki, T., Song, J., Koga-Ban, Y., Matsui, E., Fang, F., Higo, H., Nagasaki, H., Hori, M., Miya, M., and Murayama-Kayano, E. 1994. Toward cataloguing all rice genes: large-scale sequencing of randomly chosen rice cDNAs from a callus cDNA library. *Plant Journal* 6: 615–624.
166. Schenk, P. M., Kazan, K., Wilson, L., Anderson, J. P., Richmond, T., Somerville, S. C., and Manners, J. M. 2000. Coordinated plant defense responses in *Arabidopsis* revealed by microarray analysis. *Proc. Natl. Acad. Sci. USA.* 97: 11655-11660.
167. Seo, S., Sano, H., and Ohashi, Y. 1999. Jasmonate-based wound signal transduction requires activation of WIPK, a tobacco mitogen-activated protein kinase. *Plant Cell* 11: 289-298.
168. Shah, J., Kachroo, P., and Klessig, D. F. 1999. The *Arabidopsis ssi1* mutation restores pathogenesis-related gene expression in *npr1* plants and renders defensin gene expression salicylic acid dependent. *Plant Cell* 11: 191-206.
169. Shah, J., Kachroo, P., Nandi, A., and Klessig, D. F. 2001. A recessive mutation in the *Arabidopsis SSI2* gene confers SA- and NPR1-independent expression of PR genes and resistance against bacterial and oomycete pathogens. *Plant Journal* 25: 563-574.
170. Soby, S., Caldera, S., Bates, R., and Vanetten, H. 1996. Detoxification of the phytoalexins maackiain and medicarpin by fungal pathogens of alfalfa. *Phytochemistry* 41: 759-765.
171. Solano, R., Stepanova, A., Chao, Q., and Ecker, J. R. 1998. Nuclear events in ethylene signaling: A transcriptional cascade mediated by ethylene-insensitive3 and ethylene-response-factor1. *Genes & Development* 12: 3703-3714.

172. Staskawicz, B. J., Asubel, F. M., Baker, B. J., Ellis, J. E., and Jones, J. D. G. 1995. Molecular genetics of plant disease resistance. *Science* 268: 661-667.
173. Stekel, D. J., Git, Y., and Falciani, F. 2000. The comparison of gene expression from multiple cDNA libraries. *Genome Res.* 10: 2055–2061.
174. Stepanova, A. N., and Ecker, J. R. 2000. Ethylene signaling: from mutants to molecules. *Curr. Op. Plant Biol.* 3: 353-360.
175. Stevenson, P. C., Padgham, D. E., and Haware, M. P. 1994. The chemical basis of resistance in chickpeas, *Cicer arietinum L.*, to fusarium wilt, *Fusarium oxisporum* f.sp. *ciceri*. *Acta Hort. (ISHS)* 381: 631-637.
176. Stougaard, J. 2000. Regulators and regulation of legume root nodule development. *Plant Physiol.* 124: 531-540.
177. Stryer, L., and Haugland, R. P. 1967. Energy transfer: a spectroscopic ruler. *Proc. Natl. Acad. Sci. USA* 58: 719-726.
178. Thomma, B., Eggermont, K., and Penninckx, I. 1998. Separate jasmonate-dependent and salicylate-dependent defense-response pathways in *Arabidopsis* are essential for resistance to distinct microbial pathogens. *Proc. Natl. Acad. Sci. USA* 95: 15107-15111.
179. Thomma, B., Eggermont, K., Tierens, K., and Broekaert, W. 1999. Requirement of functional *Ethylene-Insensitive 2* Gene for efficient resistance of *Arabidopsis* to infection by *Botrytis cinerea*. *Plant Physiol.* 121: 1093-1101.
180. Thompson, J. D., Gibson, T. J., Plewniak, F., Jeanmougin, F., and Higgins, D. G. 1997. The ClustalX windows interface: flexible strategies for multiple sequence alignment aided by quality analysis tools. *Nucleic Acids Res.* 24: 4876-4882.
181. Ton, J., van Pelt, J. A., van Loon, L. C., and Pieterse, C. M. J. 2002. Differential effectiveness of salicylate-dependent and jasmonate/ethylene-dependent induced resistance in *Arabidopsis*. *Mol. Plant-Microbe Interact.* 15: 27-34.
182. Trinh, T. H., Ratet, P., Kondorosi, E., Durand, P., Kamaté, K., Bauer, P., and Kondorosi, A. 1998. Rapid and efficient transformation of diploid *Medicago truncatula* and *Medicago sativa* ssp. *falcata* lines improved in somatic embryogenesis. *Plant Cell Reports* 17: 345-355.
183. Truesdell, G. M., and Dickman, M. B. 1997. Isolation of pathogen/stress-inducible cDNAs from alfalfa by mRNA differential display. *Plant Mol. Biology* 33: 737-743.

184. Turner, J. G., Ellis, C., and Devoto, A. 2002. The Jasmonate Signal Pathway. (Abstr.) *Plant Cell* (suppl.): S153–S164.
185. Tuzun, S., and Bent, E. 1999. The role of hydrolytic enzymes in multigenic and microbially-induced resistance in plants. Pages 95-115 in: *Induced plant defenses against pathogens and herbivores*. A. Agrawal, S. Tuzun, and E. Bent, eds. The American Phytopathological Society Press. St. Paul, MN.
186. van Spronsen, P. C., Gronlund, M., Bras, C. P., Spaink, H. P., and Kijne J. W. 2001. Cell biological changes of outer cortical root cells in early determinate nodulation. *Mol. Plant-Microbe Interact.* 14: 839–847.
187. van Wees, S. C. M., De Swart, E. A. M., van Pelt, J. A., van Loon L. C., and Pieterse, C. M. J. 2000. Enhancement of induced disease resistance by simultaneous activation of salicylate and jasmonate-dependent defense pathways in *Arabidopsis thaliana*. *Proc. Natl. Acad. Sci. USA* 97: 8711-8716.
188. VandenBosch, K., and Stacey, G. (Monitoring editors). 2003. Summaries of legume genomics projects from around the globe. Community resources for crops and models. *Plant Physiol.* 131: 840-865.
189. Vijayan, P., Shockey, J., Levesque, C. A., Cook, R. J., and Browse, J. 1998. A role for jasmonate in pathogen defense of *Arabidopsis*. *Proc. Natl. Acad. Sci. USA* 95: 7209-7214.
190. Wittwer, C. T., Herrmann, M. G., Gundry, C. N., and Elenitoba-Johnson, K. S. J. 2001. Real time multiplex PCR assays. *Methods* 25: 430-442.
191. Wright, B., Rowse, H. R., and Whipps, J. M. 2003. Application of beneficial microorganisms to seeds during drum priming. *Biocontrol Science and Technology* 13: 599-614.
192. Wu, S. H., Ramonell, K., Gollub, J., and Somerville, S. 2001. Plant gene expression profiling with DNA microarrays. *Plant Physiol. Biochem.* 39: 917-926.
193. Xie, D. X., Feys, B. F., James, S., Nieto-Rostro, M., and Turner, J. G. 1998. COI1: An *Arabidopsis* gene required for jasmonate-regulated defense and fertility. *Science* 280: 1091–1094.
194. Yang, K., Liu, Y., and Zhang, S. 2001. Activation of mitogen-activated protein kinase is involved in disease resistance in tobacco. *Proc. Natl. Acad. Sci. USA* 98: 741-746.

195. Yu, I., Parker, J., and Bent, A. 1998. Gene-for-gene disease resistance without the hypersensitive response in *Arabidopsis dnd1* mutant. Proc. Natl. Acad. Sci. USA 95: 7819-7824.
196. Zhang, S., and Klessig, D. F. 2001. MAPK cascades in plant defense responses. Trends in Plant Science 11: 520-527.
197. Zhang Y., Fan, W., Kinkema, M., Li, X., and Dong X. 1999. Interaction of NPR1 with basic leucine zipper protein transcription factors that bind sequences required for salicylic acid induction of the *PR-1* gene. Proc. Natl. Acad. Sci. USA 96: 6523-6528.
198. Zhu, H., Cannon, S. B., Young, N. D., and Cook, D. R. 2002. Phylogeny and genomic organization of the TIR and non-TIR NBS-LRR resistance gene family in *Medicago truncatula*. Mol. Plant-Microbe Interact. 15: 529-539.
199. Zubieta, C., Dixon, R. A., and Noel, J. P. 2001. Crystal structures of chalcone O-methyltransferase and isoflavone O-methyltransferase reveal the structural basis for substrate specificity in plant O-methyltransferases. Nature Struct. Biol. 8: 271-279.

APPENDIX

Formula Derivation for the comparative $2^{-\Delta\Delta CT}$ method for real time PCR amplification data analysis (112).

The equation that describes the exponential amplification of PCR is:

$$X_n = X_o \times (1 - E_x)^n \quad \text{Where}$$

X_n = number of target molecules at cycle n
 X_o = number of initial target molecules
 E_x = Efficiency of target amplification

Therefore;

$$X_T = X_o \times (1 + E_x)^{CT,X} = K_X \quad X_T = \text{Threshold number of target molecules}$$

CT,X = Threshold number of target amplification
 K_X = Constant

A similar equation describes the amplification of the endogenous reference:

$$R_T = R_o \times (1 + E_x)^{CT,R} = K_R$$

R_o = number of initial reference molecules
 R_T = Threshold number of reference molecules
 E_R = Efficiency of target amplification
 CT,R = Threshold number of reference amplification
 K_R = Constant

$$\frac{X_T}{R_T} = \frac{X_o \times (1 + E_x)^{CT,X}}{R_o \times (1 + E_x)^{CT,R}} = \frac{K_X}{K_R} = K$$

X_T and R_T depend on several factors like the reporter dye used in the probe, its purity, the sequence context effects on the fluorescence of the probe, the efficiency of probe cleavage and the setting of the threshold cycle of fluorescence. So K does not have to be equal to 1.

If the efficiency of amplification of target and reference molecules is the same, the equation can be simplified to:

$$\frac{X_o}{R_o} \times (1+E)^{CT,X - CT,R} = K$$

Solving for some of the terms results in:

$$X_N \times (1+E)^{\Delta CT} = K$$

Where X_N is the normalized amount of target according to the reference value and ΔCT is the difference in threshold cycles for target and reference.

Rearranging the expression, becomes:

$$X_N = K \times (1+E)^{-\Delta CT}$$

The last step is to divide X_N for any sample q by the X_N for the calibrator (cb).

$$\frac{X_{N,q}}{X_{N,cb}} = \frac{K \times (1+E)^{-\Delta CT,q}}{K \times (1+E)^{-\Delta CT,cb}} = (1+E)^{-\Delta \Delta CT}$$

Where $\Delta \Delta CT$ is the subtraction of $\Delta CT,q - \Delta CT,cb$

For amplicons smaller than 150 bp and under optimized amplification conditions, E is close to 1.

Therefore the equation can be simplified to: $2^{-\Delta \Delta CT}$.

VITA

NAME: Pedro Uribe Mejía

PERMANENT ADDRESS: Transversal 5. No. 87-87
Bogotá, Colombia, S. A.

EDUCATIONAL BACKGROUND:

DEGREE: Specialist.
MAJOR SUBJECT: Integrated Management of
Environment.
UNIVERSITY: Universidad de los Andes, Bogotá,
Colombia.
DATE: September, 1997.

DEGREE: Bachelor of Science.
MAJOR SUBJECT: Biology.
UNIVERSITY: Universidad de los Andes, Bogotá,
Colombia.
DATE: September, 1992.